CHAPTER 4

4. INVESTIGATING THE EARLY THERMAL BEHAVIOUR OF ROLLER COMPACTED CONCRETE IN LARGE DAMS

4.1. BACKGROUND

In Chapter 3, the specific behaviour occurring in concrete during the hydration temperature development and dissipation cycle in large dams was investigated through referenced literature. In addition, the associated design methodologies traditionally applied for CVC and RCC dams were presented and discussed. Against this background, data from five prototype RCC dams are presented and evaluated in Chapter 4 in an effort to develop a picture of the actual, measured behaviour of the constituent RCC.

4.2. INTRODUCTION

In this Chapter, the author presents and reviews instrumentation data from Wolwedans and Knellpoort Dams in South Africa, Çine Dam in Turkey and Wadi Dayqah Dam in Oman. In addition, some preliminary data collected for the first RCC placed in the dam wall at Changuinola 1 Dam is presented.

As a means to demonstrate the validity of the thermal analysis for Çine Dam and the consequential patterns of temperature dissipation, a comparison is presented of the predicted and measured temperatures in the dam.

Each of the dams addressed and the associated instrumentation installed is described in Chapter 2. The arrangements of the installed instrumentation are illustrated in Chapter 2 and **Appendix C**.

4.3. WOLWEDANS DAM

4.3.1. INSTRUMENTATION DATA

4.3.1.1. General

The network of monitoring instrumentation installed at Wolwedans Dam comprises Long-Base-Strain-Gauge-Temperature-Meters installed across all induced joints, bearing pressure cells at the dam/foundation contact, a number of water and air temperature meters on the dam surface, piezometers in the foundation, seepage measurement weirs in the galleries, pendulums and inverted pendulums in the dam

wall and the foundation and a total of 86 displacement measurement reference points on the dam wall and in the foundation.

For the purposes of reviewing the behaviour of the RCC, the deformation on the induced joints is considered of greatest importance and for that purpose data from the 209 LBSGTMs installed at 4 different elevations (27 + 60 + 80 + 42) must be studied[1 & 2].

4.3.1.2. Typical LBSGTM Data

Temperature and deformation histories for each of the LBSGTMs for the period from installation until the end of 1996 are provided on a CD included with this Thesis. Typical temperature and deformation histories at LBSGTMs on each of the four instrumentation levels are provided for illustration in **Figures 4.1** to **4.8**.

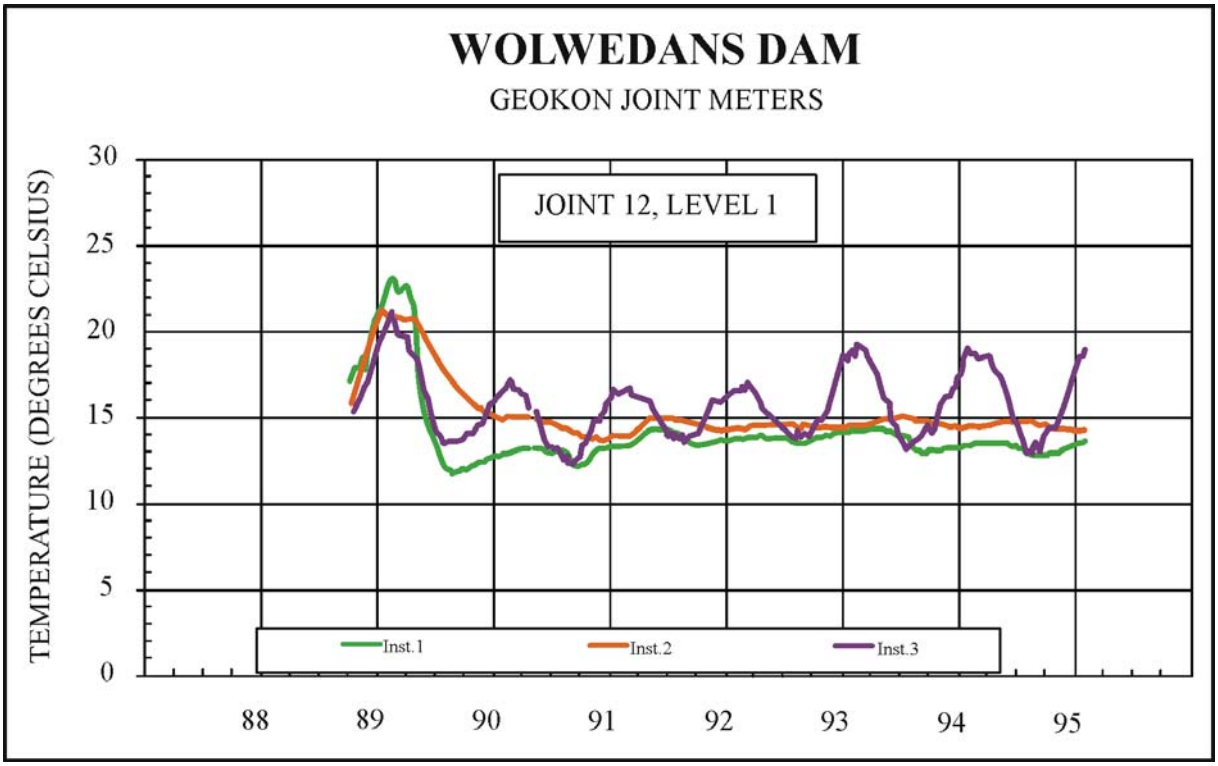

Figure 4.1: Temperatures on LBSGTMs at RL 40.25 m[1 & 2]

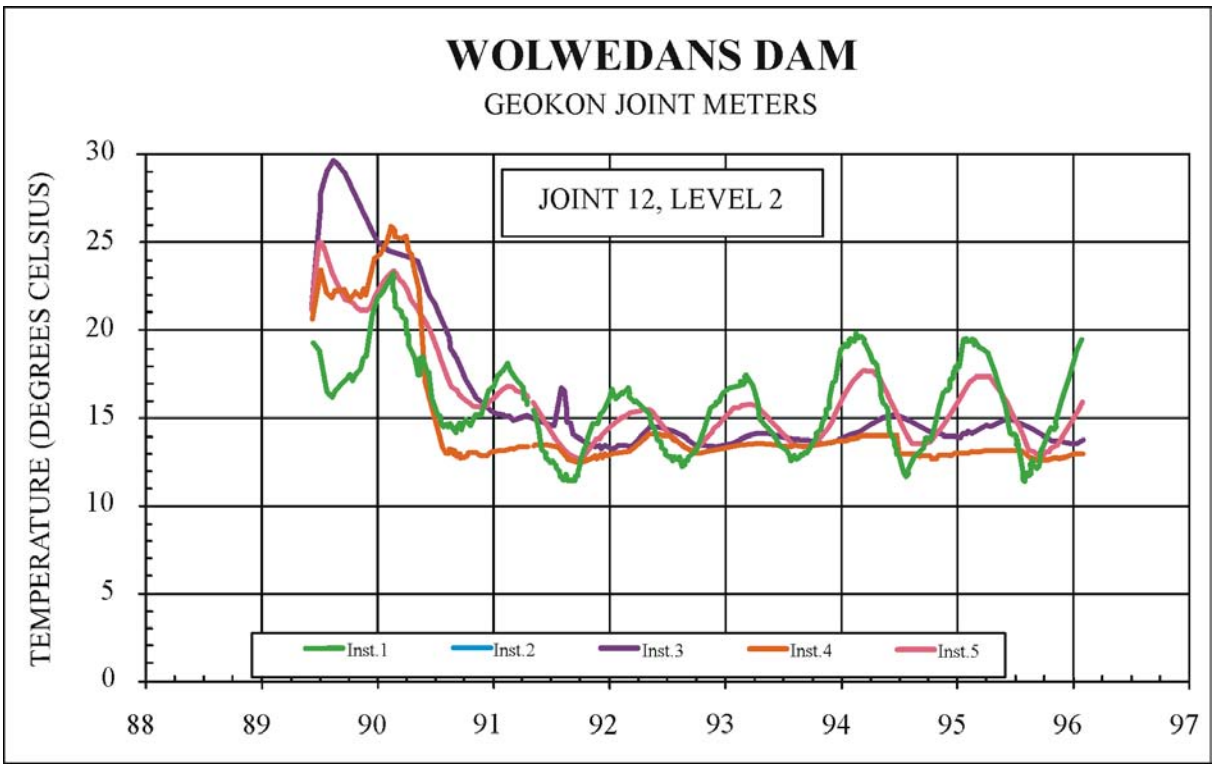

Figure 4.2: Temperatures on LBSGTMs at RL 52.25 m(1 & 2)

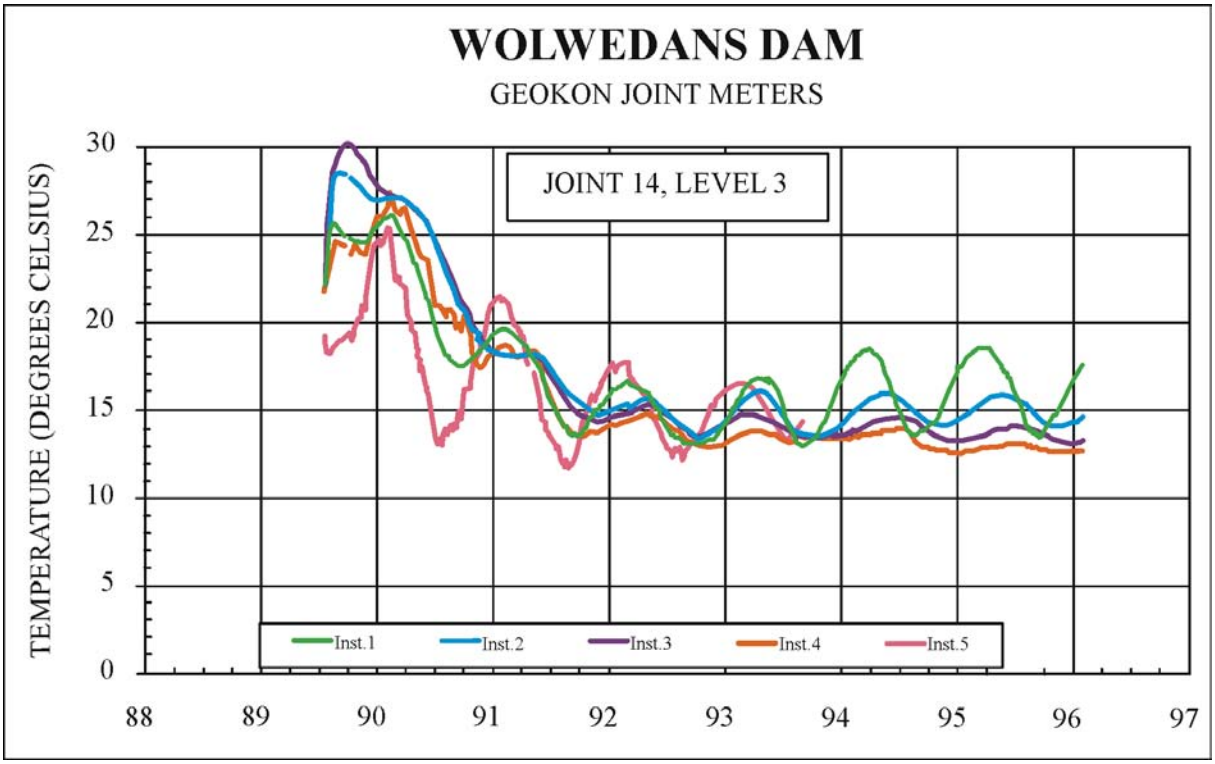

Figure 4.3: Temperatures on LBSGTMs at RL 66.25 m(1 & 2)

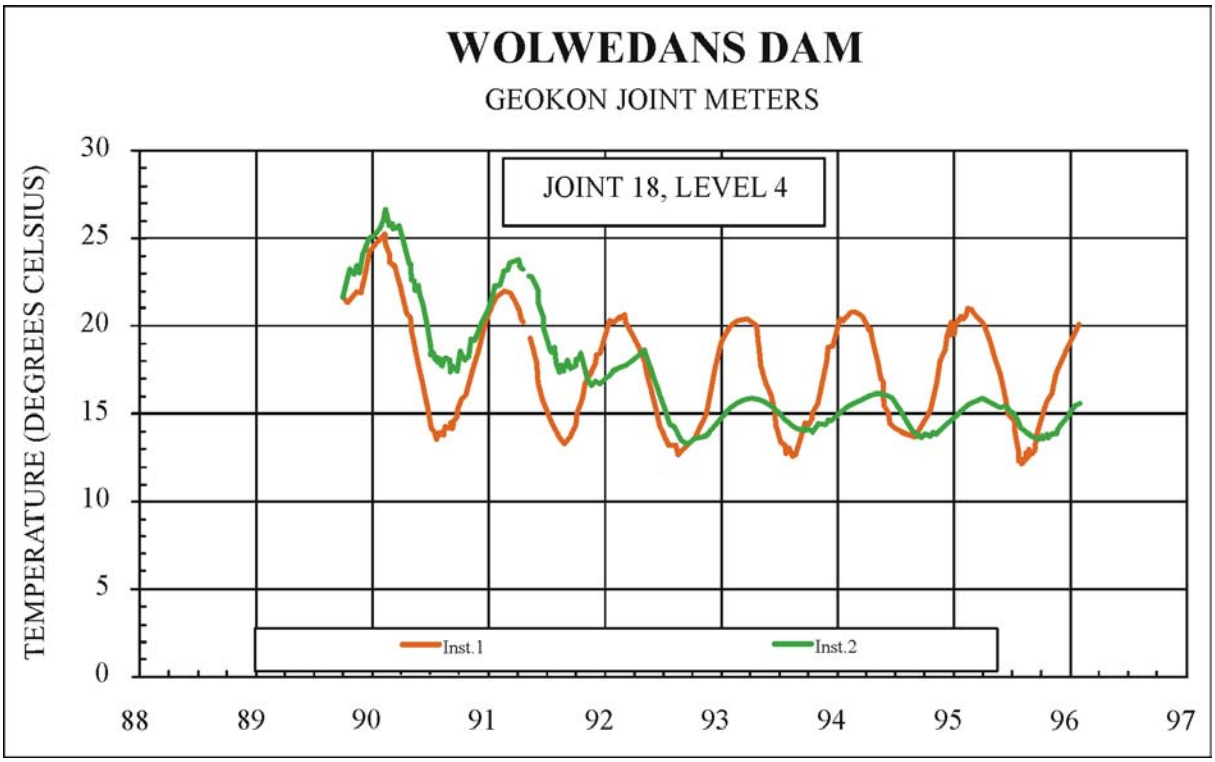

Figure 4.4: Temperatures on LBSGTMs at RL 84.25 m(1 & 2)

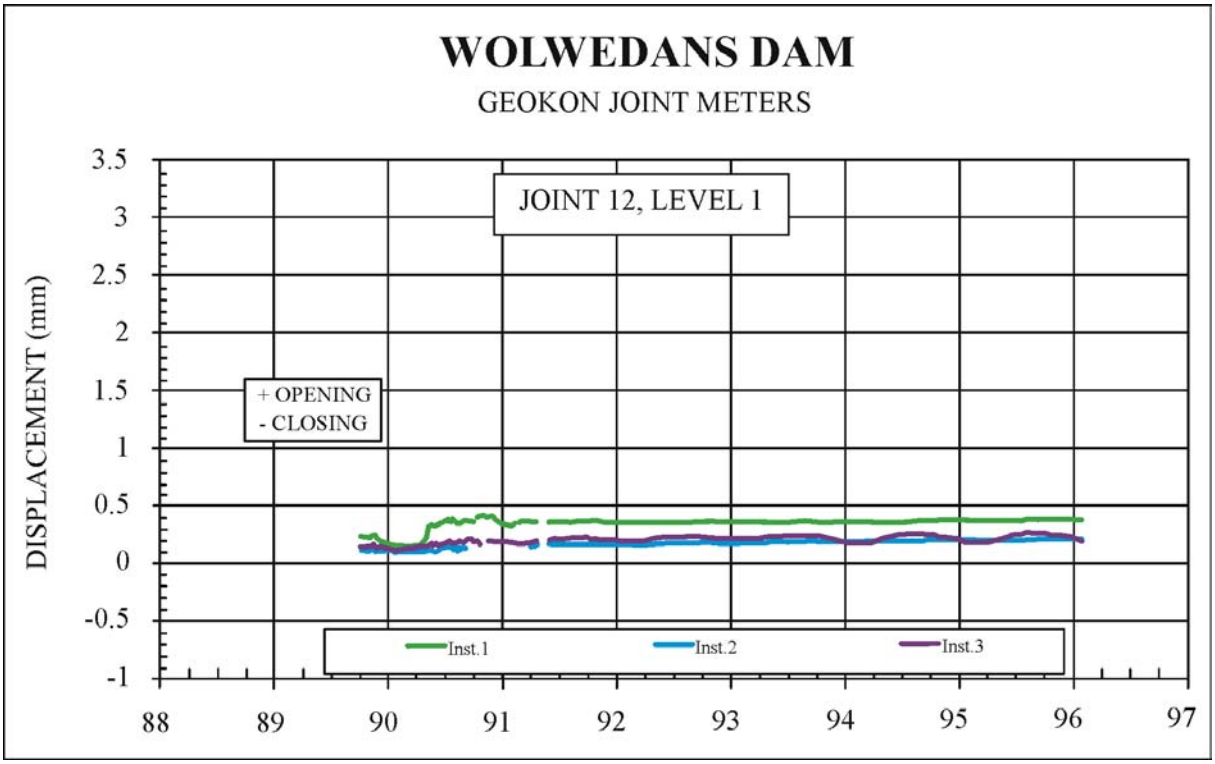

Figure 4.5: Displacement at Joint 12 on LBSGTMs at RL 40.25 m(1 & 2)

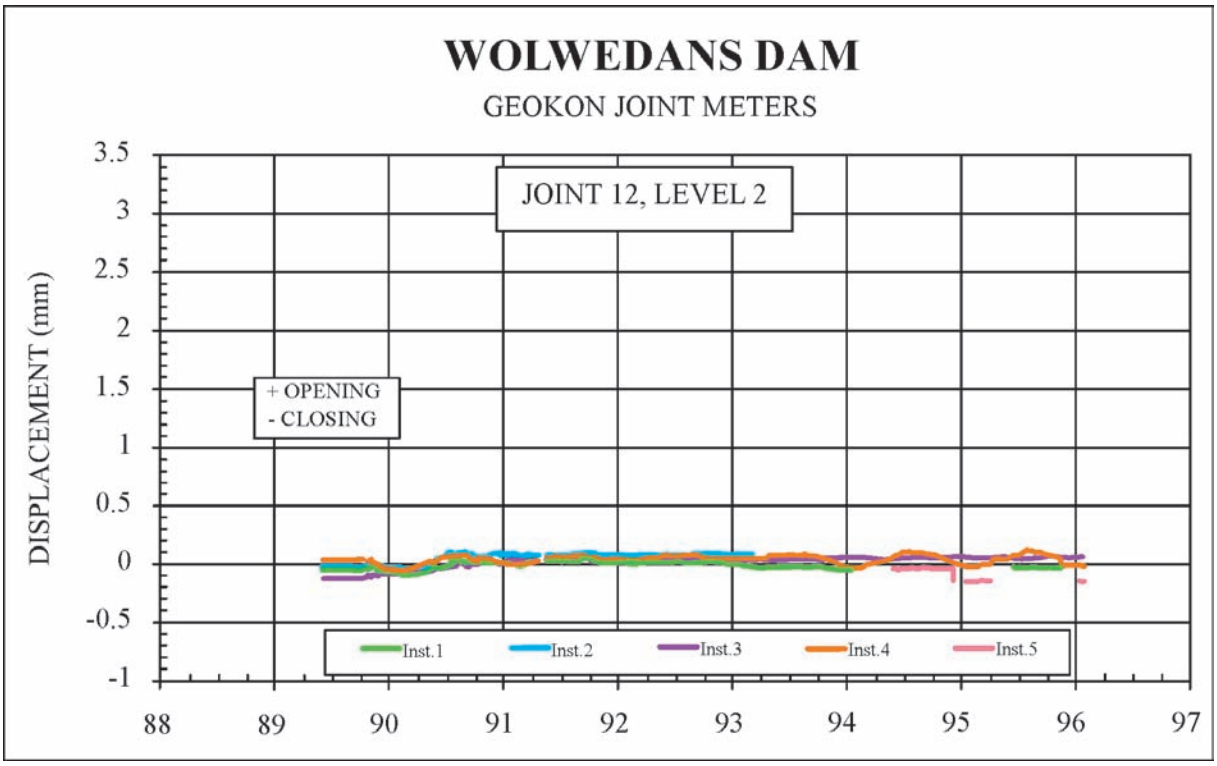

Figure 4.6: Displacement on LBSGTMs at RL 52.25 m(1 & 2)

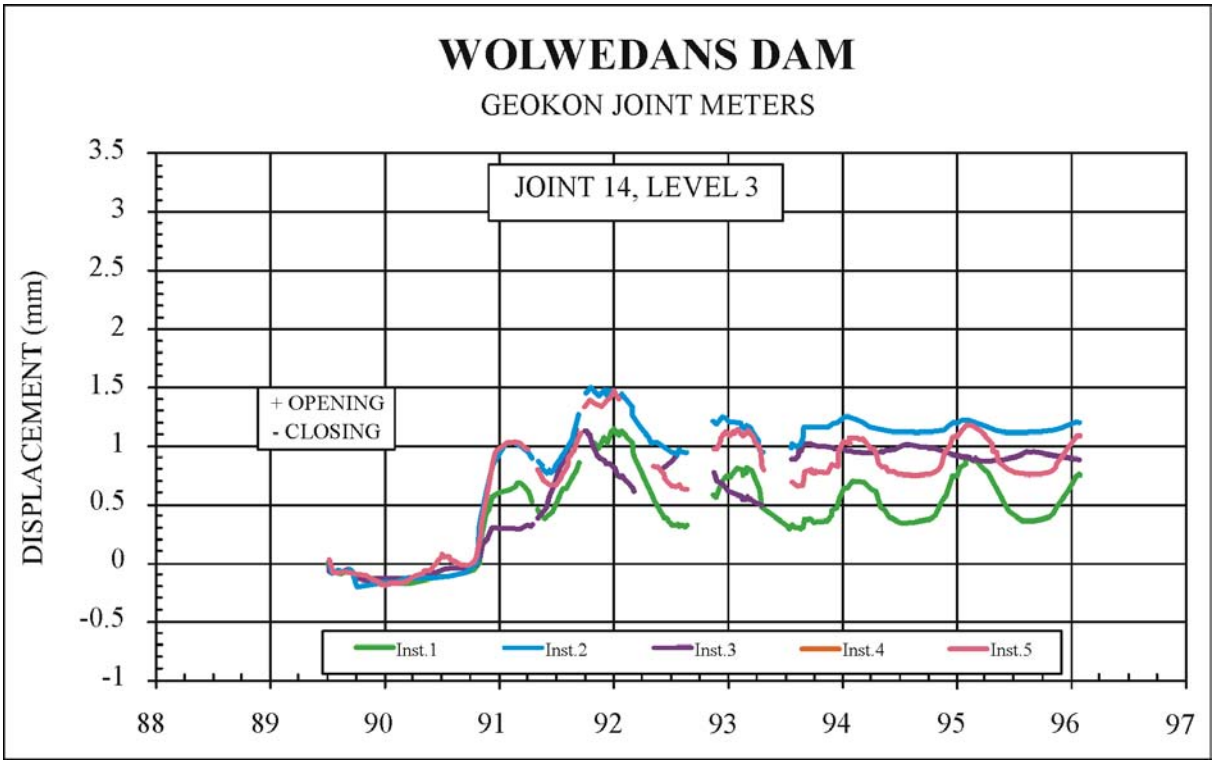

Figure 4.7: Displacement on LBSGTMs at RL 66.25 m(1 & 2)

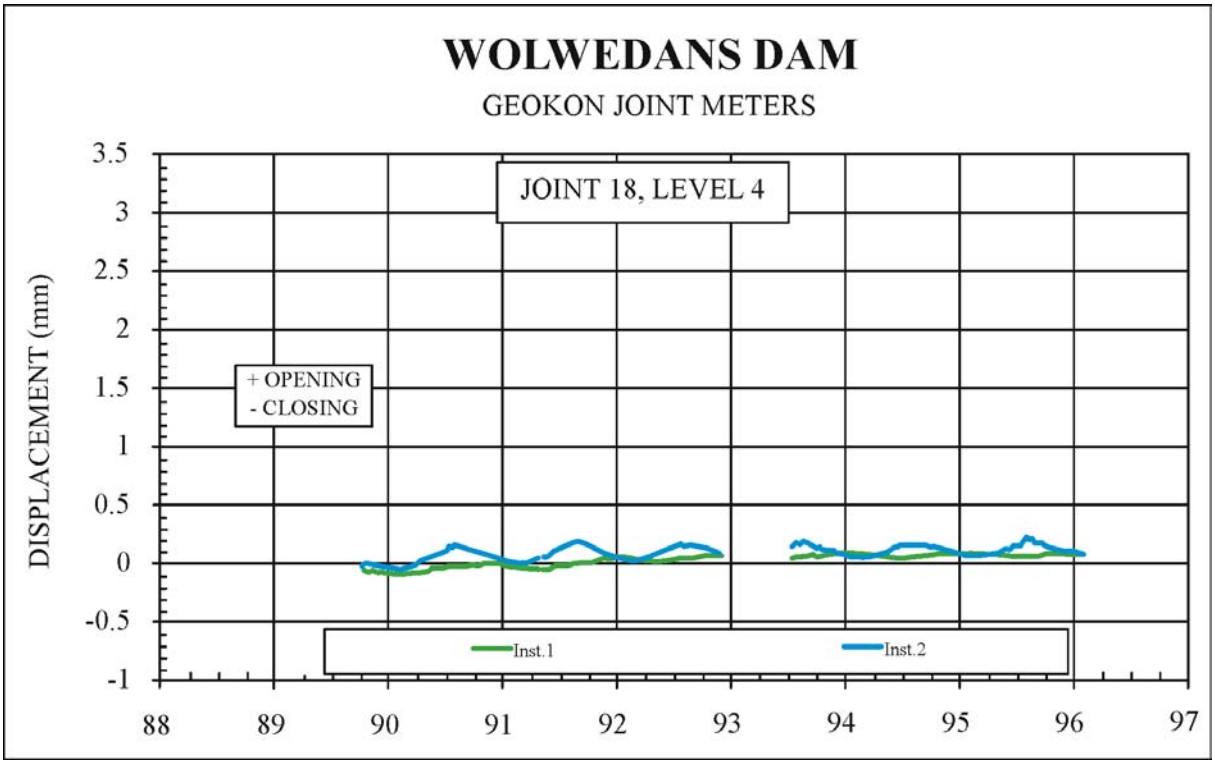

Figure 4.8: Displacement on LBSGTMs at RL 84.25 m(1 & 2)

4.3.1.3. Typical LBSGTM Data Review

The instrumentation levels in Wolwedans dam are numbered from the bottom up and the LBSGTM gauges are numbered from the upstream to the downstream. The various temperature development and dissipation patterns are clearly illustrated, with the core gauges demonstrating the highest rises, as a result of trapped hydration heat, and the smallest long-term seasonal variations and the upstream surface gauges indicating lower seasonal variations than the downstream gauges, as a result of the insulation effect of the reservoir water mass.

Due to the exposure of the first RCC placement to RL 48 m over the period December 1988 to mid May 1989 and the relative proximity of the instruments to the foundation rockmass, it can be seen that the hydration temperature at level RL 40.25 m (Level 1) had essentially fully dissipated by the beginning of 1990. At levels 2 and 3 (RL 52.25 m and RL 66.25 m), it can be seen that the full impact of the hydration heat had only realistically been dissipated during 1992.

It is also significant to note that the only joint to open on the example displacement plots above was Joint No. 14 on Level 3. Bearing in mind that the storage level in the dam had risen to full essentially by late 1992, a situation never consequently existed when the full impact of the loss of hydration heat on the joint opening could be reviewed without the influence of the water load.

Tables 4.1 to **4.4** provide a typical indication of the measured core joint openings during the first winter after the hydration heat had full dissipated (July 1993).

Table 4.1: Core Induced Joint Openings at Level 1 (RL 40.25 m)(1 & 2)

Jt No	11	12	13	14	15	16	17	18	19	Total
Opening (mm)	1.2	0.15	0.45	0.15	0.15	1.6	1.45	0.65	0.1	5.9

In July 1993, the temperature in the core of the dam at RL 40.25 m was approximately 14.5°C, approximately 2°C below the placement temperature, or 8.5°C below the peak hydration temperature. The total joint opening, just 7 m above the foundation, translates into approximately 68 microstrain. Joint 11 is the interface between the RCC and a CVC structure and ignoring this joint would reduce the effective shrinkage across the joints to approximately 50 microstrain. While the levels of residual stress between induced joints and the impact of the foundation restraint cannot be known, the above would suggest some minor creep (approximately 30 microns) occurred in the RCC at this level.

Table 4.2: Core Induced Joint Openings at Level 1 (RL 52.25 m)(1 & 2)

Jt No	9	10	11	12	13	14	15	16	17	18	19	20	Total
Opening (mm)	0.05	0.1	0.9	0	0	1.3	0	0	2.0	0.05	0.75	0	5.15

In July 1993, the temperature in the core of the dam at RL 52.25 m was fractionally below 14°C, approximately 7°C below the placement temperature, or 16°C below the peak hydration temperature. The total joint opening translates into approximately 40 microstrain, suggesting that some closure of the induced joints must have occurred as a result of the water loading, whether, or not any creep of the RCC had occurred.

Table 4.3: Core Induced Joint Openings at Level 1 (RL 66.25 m)(1 & 2)

Jt No	7	8	9	10	11	12	13	14	15	16	17	18	19	20	21	Total
Opening (mm)	0	1.0	0	0	0	0	0	0.95	0	0	1.45	0	0	0	0	3.4

In July 1993, the temperature in the core of the dam at RL 66.25 m was a little below 14°C, approximately 8°C below the placement temperature, or 16°C below the peak hydration temperature. The total joint opening translates into approximately 30 microstrain.

Table 4.4: Upstream Induced Joint Openings at Level 1 (RL 84.25 m)(1 & 2)

Jt No	5	6	7	8	9	10	11	12	13	14	15
Opening (mm)	0	0.15	0	0.2	0	0	0.1	0.08	0.03	0.04	0
Jt No	16	17	18	19	20	21	22	23	24	25	Total
Opening (mm)	0.04	0	0.04	0.1	0.08	0.12	0.11	0.1	2.05	0.08	3.32

* - A LBSGTM was not placed at the centre of the section at RL 84.25 m.

In view of the fact that the gauges at RL 84.25 m were not installed in the centre of the cross section of the dam wall, no real evaluation can be made of the total joint opening, except to state that the variation relate simply to seasonal, surface temperature effects. In this regard, it is particularly pertinent to note that the maximum indicated openings occur during summer on the upstream gauges and during winter on the downstream gauges.

4.3.1.4. LBSGTM Data at RL 66.25 m

In studying the induced joint displacements, the situation at approximately mid-height on the dam (Level No. 3 – RL 66.25 m) is considered to provide the most useful information, as the dam structure at this level is sufficiently broad that temperatures within the core are largely unimpacted by surface effects, while the distance from the foundation is sufficient to minimise the influence of foundation restraint. At this level, which is 33 m above the lowest foundation, the dam wall thickness is approximately 21 m and the core temperature variation over a typical annual cycle is limited to approximately 2°C, while a period of 2 years was required to dissipate the full hydration heat.

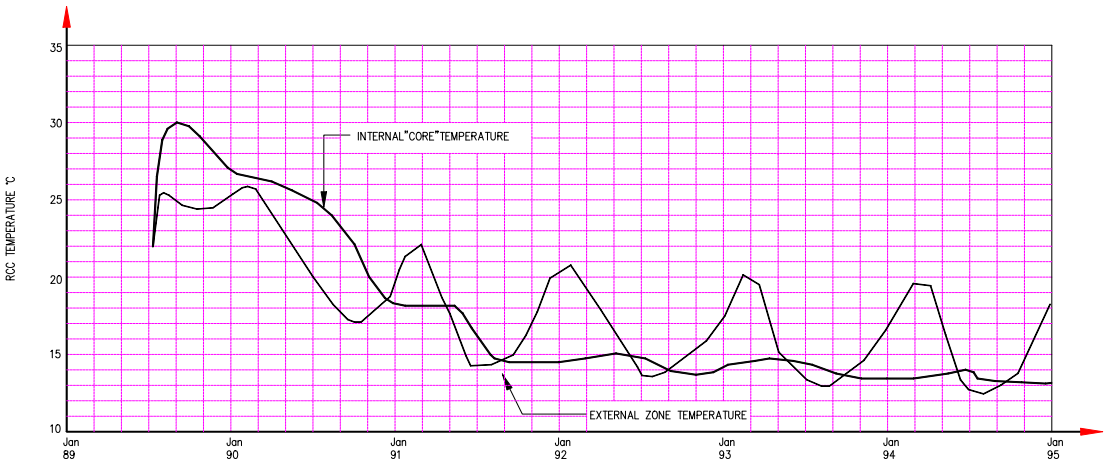

Figure 4.9: Typical RCC Temperature History for Wolwedans Dam[3]

Figure 4.9 illustrates the typical "core" and external RCC temperature history during construction and over the first 5 years after dam completion.

At Instrumentation level No. 3, 16 induced joints were instrumented each with 5 LBSGTMs. With induced joints at 10 m spacings on the upstream face, only three joints indicated any real tension displacement, with the "unopened" joints largely remaining in compression. **Figure 4.10** illustrates the displacement history at a centrally located open joint for a period from placement to five years after dam completion. Whilst this figure indicates a maximum joint tension displacement of approximately 0.8 mm in the internal, or "core" zone, the average maximum winter time joint opening across the full number of joints was approximately 0.28 mm and this was essentially manifested in an average opening of a little under 1.2 mm across three joints (see **Table 4.3**).

Separating the external and internal zones of the dam, the short and long-term thermal insulation at depth within the RCC can clearly be discerned. The hydration heat dissipation and ambient heat absorption within the external zone are equally evident.

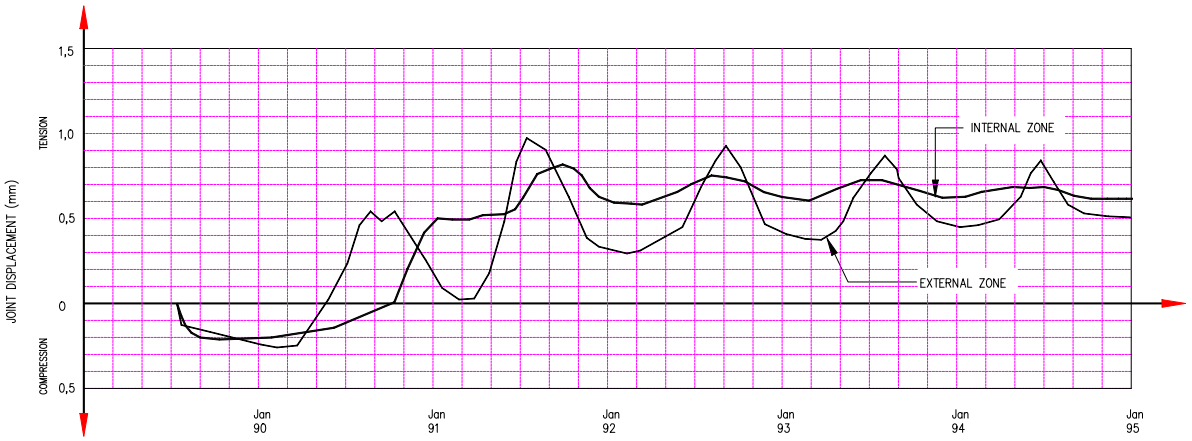

Figure 4.10: Typical Joint Displacement History for Wolwedans Dam[3]

4.3.1.5. Data Review and Analysis for LBSGTMs at RL 66.25 m

The "joint displacements" illustrated on **Figure 4.10** indicate the total displacement experienced between the anchored ends of the 1m long long-base-strain-gauge-temperature-meter. With the induced joint at the centre of these gauges, crack opening width is not measured directly, although when measurable displacements are only registered at (approximately) every third induced joint, the major portion of the indicated displacement in tension obviously represents a crack. It is significant to note that although the tension displacements vary from one induced joint to the next, dependent on which joint actually cracked, the compressions experienced during hydration heat development are substantially constant. Furthermore, the early compression patterns and levels experienced within the internal and external zones are significantly more similar than the tension displacements experienced later. **Figure 4.11** translates the measured internal, or core zone, induced joint displacements (as presented on **Figure 4.10**) into compression and tension strains over the gauge base length of 1m. Over such a gauge base length, a tension strain of 600 microstrain translates into an induced joint opening of 0.6 mm.

It is interesting to note that the compression strain, or joint closure, is apparently capped at approximately 200 microstrain. This could well represent the maximum expansion possible before the geometrical and foundation restraints force all other expansion into direct compressive stress. On the other hand, it could also relate to a susceptibility of the RCC to concentrate initial compression displacements on the induced joints, where installation techniques may result in locally more compressible RCC.

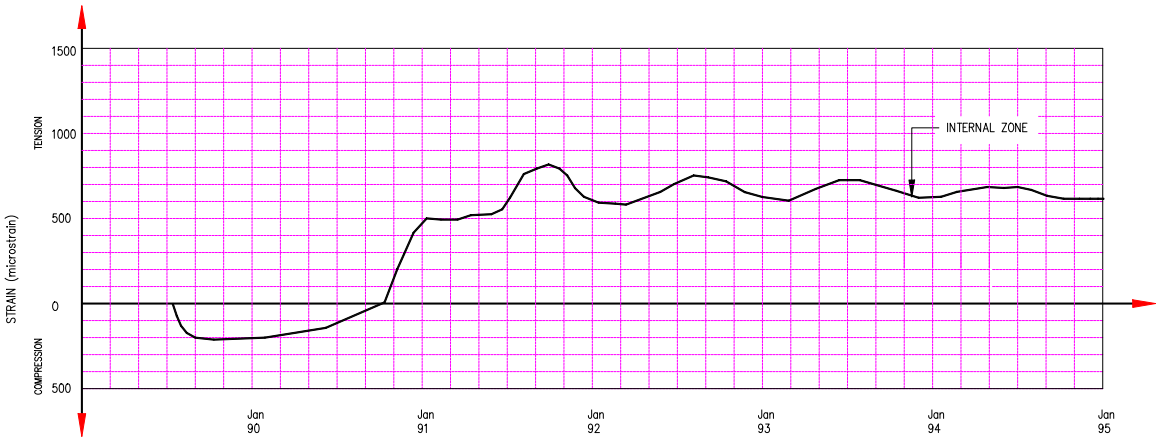

Figure 4.11: Typical Strain History for Induced Joint at which a Crack formed at Wolwedans Dam[3]

Reviewing the strain development at Wolwedans directly against temperature at any particular gauge, it is not possible to determine a direct, or meaningful correlation. Furthermore, significant tension displacements were only observed on three specific joints, effectively equivalent to spacings of approximately 30 m. It is accordingly not realistic to review a single joint in isolation, but it is necessary to observe cumulative displacements and related effects over the total number of joints at each specific instrumentation level.

On the basis of the available instrumentation monitoring data at level No. 3, it can be determined that zero joint displacement is experienced at the point that the dam body cools to a temperature approximately equivalent to the "built-in" placement temperature. In other words, the data suggests that the "zero stress", or natural closure temperature (T3)[4] and the "built-in", or initial placement temperature (T1) are approximately the same. In the absence of any other obvious explanation, this would imply that the hydration temperature rise of approximately 9°C, which developed maximum compression strains of approximately 200 microstrain across the marginally compressible induced joint (see 2.2.5) and possibly significant compressions as a result of strain constraint, seems to have caused no creep in the immature RCC. While this would seem to contradict all expectations of usual concrete behaviour, these indications were the first seeds that grew into the research addressed in this Thesis.

Maximum compression strain within the internal zone of the RCC appears to have been experienced approximately 3 months after placement, with this level of compression strain being maintained for a further 6 months, even though the temperature drops approximately 3°C over this latter period. This particular

phenomenon suggests some creep in the RCC during this period of temperature drop, or inelastic behaviour of the RCC, or physical constraint against expansion for the last 3°C of hydration temperature rise. The last hypothesis is considered the most likely and a 3°C temperature rise would incur a strain of 30 microstrain for a coefficient of thermal expansion of perhaps 10 x 10^{-6}/°C. For a green RCC deformation modulus of perhaps 15 GPa, at 7 days age, such a strain would relate to a 450 kPa compression stress.

For the instrumentation on level No. 3 (RL 66.25 m) at Wolwedans, the "built in" placement temperature (T1) was approximately 22 – 22.5°C, the maximum hydration temperature (T2) approximately 30°C and the lowest final winter temperature (T4) approximately 14°C. At the lowest temperature, the total cumulative openings on the joints, within the centre of the wall, amounted to approximately 3.4 mm, which translates into a direct strain of approximately 30 microstrain (3.4 mm/137 m). Overall associated tension is more difficult to determine, as records exist only for the strain across 1 m long gauges at each of the joints, which are approximately 10 m apart. There is no direct recording of the residual tension levels remaining between joints and across blocks where cracking did not occur. With approximately only every third crack joint actually opening to form a crack, the residual strain within the closed joints, at the coldest winter temperature, varied between 100 microstrain compression and 100 microstrain tension. Whilst this might appear to represent the situation of an average residual strain of 0, it is safer to assume a figure of perhaps 20 microstrain for related analysis. This strain would translate into a residual tension of the order of 300 kPa, for an elastic modulus of 15 GPa.

For a total continuous wall length of 137 m, at the level of the instruments in question, the total shrinkage strain associated with a structural temperature drop of approximately 8.5°C (22.5 – 14) accordingly might be approximately 50 microstrain. Such a strain infers an RCC coefficient of thermal expansion of approximately 6 x 10^{-6} strain per °C, which is lower than the value of 10 to 12 x 10^{-6}/°C, which might more usually be anticipated for a concrete comprising quartzitic aggregates.

The discrepancy in the apparent coefficient of thermal expansion could be a result of underestimated residual tensions within the uncracked RCC, a lower actual effective structural temperature drop, an actual lower coefficient of thermal expansion, creep of the RCC in tension, or a combination these factors. It must also be borne in mind that the dam wall structure was under full water load for most of the period of measurement and the structural closure of the joints under water load should also be considered. Whatever the case may be, the fact is that the deleterious effect of post hydration temperature drop on the structure of the arch wall was significantly less than theoretically predicted.

4.4. KNELLPOORT DAM

4.4.1. INSTRUMENTATION RESULTS

Unlike Wolwedans Dam, Knellpoort[1 & 2] was constructed largely during a particularly cold winter, with built-in temperatures frequently below 15°C. With a similar RCC mix to Wolwedans, compression strain experienced during hydration heat development again peaked at approximately 200 microstrain, or 0.2 mm displacement.

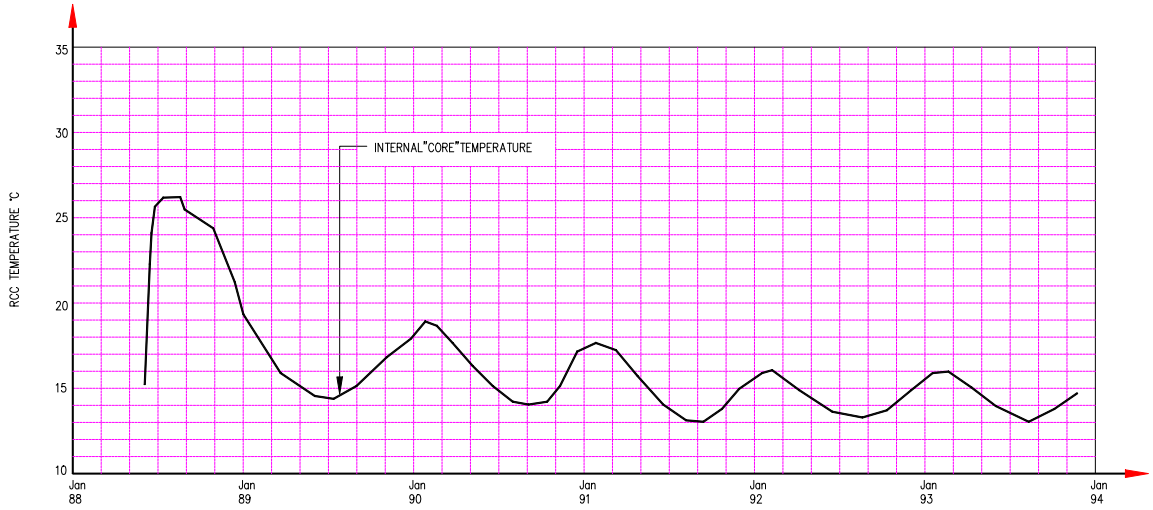

Figure 4.12: Typical RCC Temperature History for Knellpoort Dam[3]

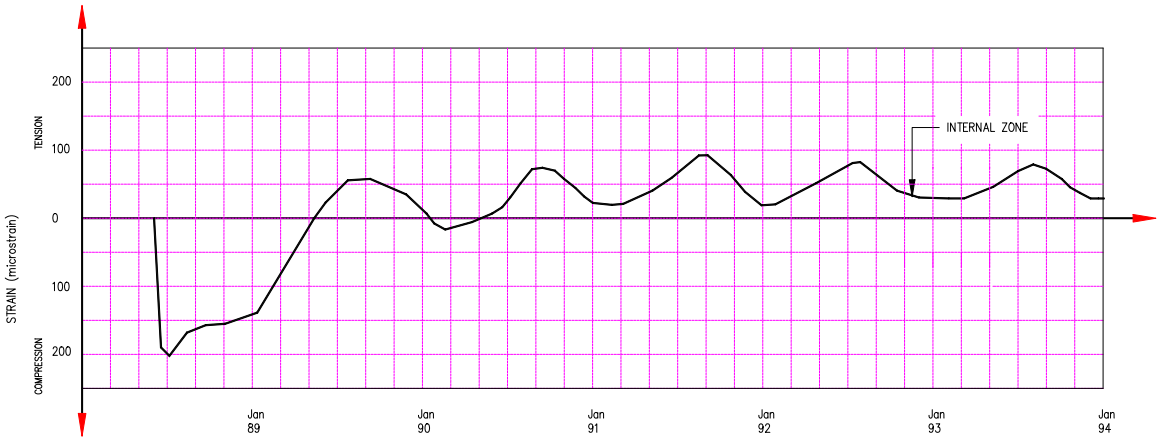

Figure 4.13: Typical RCC Strain History for Knellpoort Dam[3]

4.4.1.1. Data Review and Analysis

In general, the Knellpoort joint displacement and strain results demonstrated a very similar pattern to those for Wolwedans, although a specific difference can be seen in

the low tension strains experienced as a result of the final internal equilibrium temperatures being only fractionally above the placement temperature. Again, within the general variability of the measured data from joint to joint, the placement (T1) and "zero stress temperature" (T3) can be seen to be approximately the same, confirming the lack of creep under the early thermal compressions. Interestingly, the corresponding occurrence of a compression strain peak in conjunction with the temperature peak at Knellpoort suggests that the argument for compression strain being limited by constraint, while compression stress continues to increase, is invalid in this instance. On the other hand, a good elastic correlation of strain and temperature is more clearly evident at Knellpoort. Studying **Figures 4.12** and **4.13**, the proportional relationship between temperature and strain is clearly demonstrated, with an 11°C hydration temperature rise developing a compressive strain of approximately 200 microstrain, while long-term seasonal temperature variations of approximately 3°C give rise to strain variations of approximately 55 microstrain. From these figures, a uniform coefficient of thermal expansion of 1.8 x10^{-5}/°C (55/3 x 10^{-6} = 200/11 x 10^{-6} = 1.8 x 10^{-5}) can be calculated and while this figure is rather high, it is further confirmation of the minimal influence of creep and the apparent elastic behaviour of the RCC body under internal temperature variations. It is considered most likely that the apparent coefficient of thermal expansion is exaggerated as a consequence of the concentration of movements on the induced joints, where a weakness in the body of the RCC is effectively created.

The smaller proportions of Knellpoort (59 000 m^3) compared to Wolwedans (200 000 m^3) imply reduced thermal insulation at the core, with temperatures varying by 3°C seasonally at the instruments indicated for the former dam and only 1.5°C at the latter. The data for Knellpoort was measured at level No. 4, 37m up the 50 m high structure, where cover is limited to approximately 4 m.

4.5. ÇINE DAM

4.5.1. GENERAL

The data evaluation for Çine Dam is subsequently presented in two part; the first part describing the first review of data from Çine Dam in 2007 and the second evaluating data at three levels at the beginning of 2009.

4.5.2. BACKGROUND

Instruments were installed at three elevations; 147.50 mASL in October 2005, 184.25 mASL in November 2007 and 208.50 mASL in November 2008 respectively. A final set of instruments was installed at elevation 232 mASL in November 2009[5].

Plate 4.1: January 2005 – El 147.50 mASL

The Çine instrumentation is comprehensive and focuses on the measurement of strain and temperature, with one set of instruments measuring displacement across each of the induced joints, parallel to the dam axis, and another measuring strain perpendicular to the axis of the dam.

A comprehensive thermal analysis was completed for Çine Dam, with the initial 2005 exercise being supplemented with an evaluation of a possible continuous placement of the top 55 m of the structure in 2008. The placement of the RCC for Çine Dam will be completed during 2010 and the dam has been constructed in a series of 6 winter-season placements, which started in 2004/2005.

With placement initiated in October/November each year, a total of approximately 300 000 m^3 was placed by the following March/April. Thereafter, the structure was left exposed until the following winter placement season. The purpose of the thermal analysis was to model the development and dissipation of the hydration heat and to establish whether the proposed winter-season RCC placement schedule and approach might result in the development of any deleterious stresses at any stage. On the basis of the critical temperature patterns identified, stress analyses were completed in order to isolate and evaluate the consequential maximum tensions developed.

Plate 4.2: April 2007 – El 187 mASL

Plate 4.3: April 2008 – El 208.25 mASL

While the thermal analyses demonstrated that the temperatures within Çine Dam will only reach an equilibrium condition in approximately 50 years after completion of the dam, the winter placement approach further implies that the induced joints are unlikely to open for a long time, if at all. Consequently, it will be many years still before the performance of the dam structure in its cooling cycle can realistically be evaluated and accordingly only the short-term "heated" performance of the dam structure can be investigated at this stage.

4.5.3. INSTRUMENTATION LAYOUTS

The arrangements of the installed instrumentation at Çine Dam are described in Chapter 2. **Figures C5** to **C7** in **Appendix C** provide a basic illustration of how and where the strain gauges and the LBSGTMs were arranged on each of the instrumentation levels for which monitoring data was available by the end of 2008.

4.5.4. INSTRUMENTATION DATA EVALUATION 2007

4.5.4.1. General

Instrumentation was installed in the dam at elevation 147.5 mASL during October 2005 and this is being read and monitored on an ongoing basis[5]. A comprehensive thermal analysis, simulating the anticipated construction sequence, was completed for the dam before RCC placement was initiated and the related actual temperature readings are regularly compared with the predictions of the model.

For the purposes of this work, the strain measurements from the LBSGTMs (termed SGT gauges at Çine Dam), located across the induced joints, and from strain gauges (termed SGA gauges at Çine Dam), orientated in a perpendicular direction to the dam axis, are evaluated. At the level of the installed instruments, the dam section measures almost 115 m in width and accordingly, the internal instruments are well insulated from surface effects.

4.5.4.2. Instrumentation Results

The evaluation presented herein was completed in early February 2007, analysing instrumentation reading records of some 16 months. Both the SGT and SGA gauges measure temperature and demonstrate a hydration temperature rise of the order of 12 to 14°C, with the internal core temperature remaining at around 25°C, while the temperature closer to the surface had dropped during winter 2006 by up to 3°C.

In evaluating the instrumentation readings, it is important to take cogniscance of the installation timing, processes and procedures and the subsequent RCC placement timing. At Çine Dam, RCC is placed annually during winter, between October/November and March/April. The instruments evaluated as part of this work were installed during October 2005 on the surface of a 14 m deep block of RCC placed during the previous winter. The gauges were subsequently covered by the winter 2005/06 RCC placement, which commenced on the 11th of November 2005. A depth of approximately 18 m of RCC was placed during this winter season.

Accordingly, the gauge readings presented document the behaviour of the winter 2005/06 RCC placement.

The general patterns discernable from the strain measuring instrumentation readings to date at Çine Dam are distinct and in accordance with expectations.

The SGA strain gauges demonstrate a total maximum thermal expansion strain of the order of 120 microstrain for a hydration temperature rise of approximately 14°C, which translates into an equivalent RCC coefficient of thermal expansion of 8.4 x 10^{-6}/°C. The magnitudes of both the temperatures and the strains are as expected and predicted.

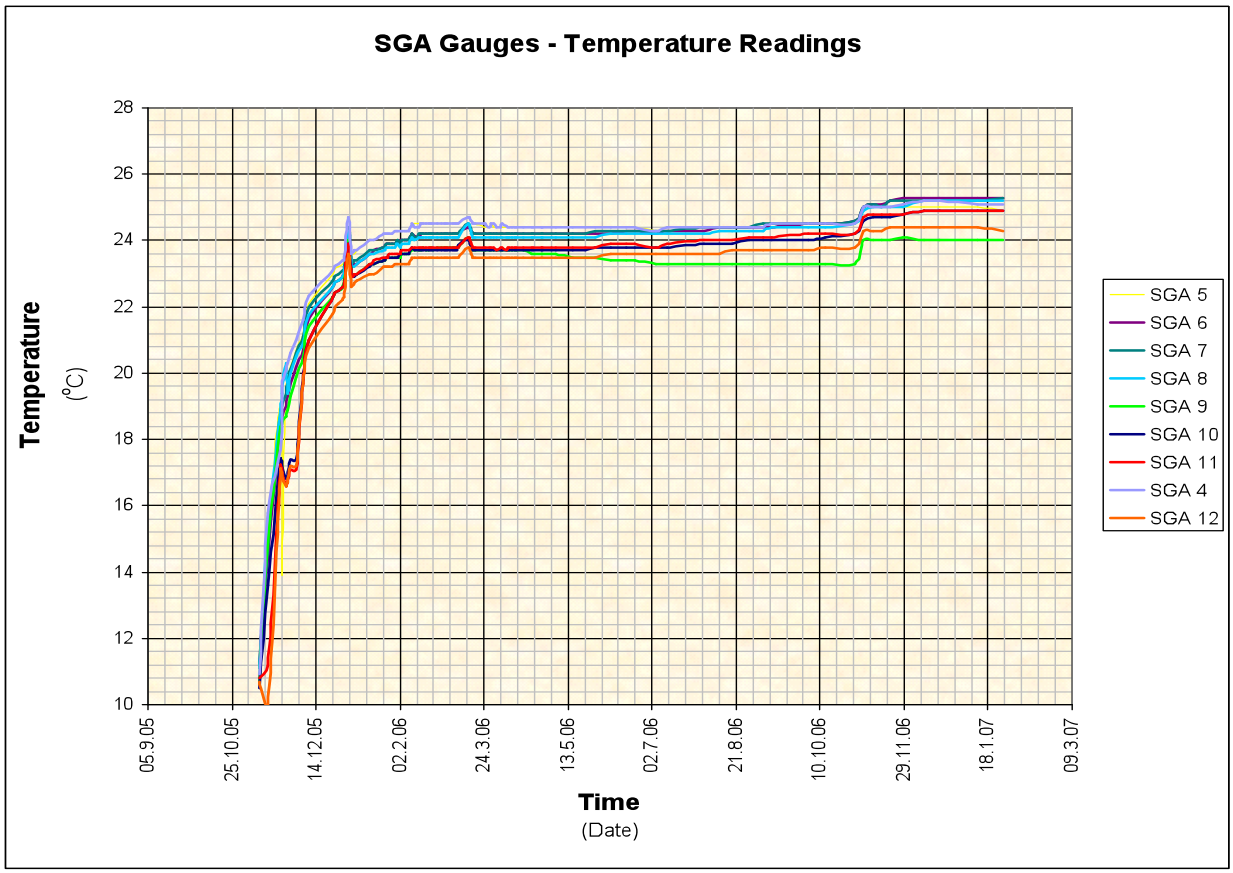

Figure 4.14: Typical RCC Temperature History for Çine Dam(5)

It is considered quite surprising that a direct and apparently linear expansion of the RCC with a temperature rise of 14°C should have been evident less than 20 m above the foundation level, within the core of a dam with a base length exceeding 100 m. It would have rather been expected that internal restraint would have caused most of the associated thermal expansion to have been constrained.

The SGA gauges further demonstrate clearly a strain relaxation (**Figure 4.15**), over the period between 3 and 7 months after the start of RCC placement. While the temperature measured on these gauges remained relatively constant until a further

slight increase was indicated at the start of the winter 2006/07 RCC placement, the total strain relaxation indicated was of the order of 15 microstrain, or 12.5%.

The SGT gauges (**Figure 4.16**) illustrate a relatively rapid increase in temperature over the first two weeks, which slows slightly over the following month and distinctly over the subsequent two and a half months. Approximately 4 months after initiation of the winter 2005/06 RCC placement, the instruments indicate that the maximum temperature has been reached.

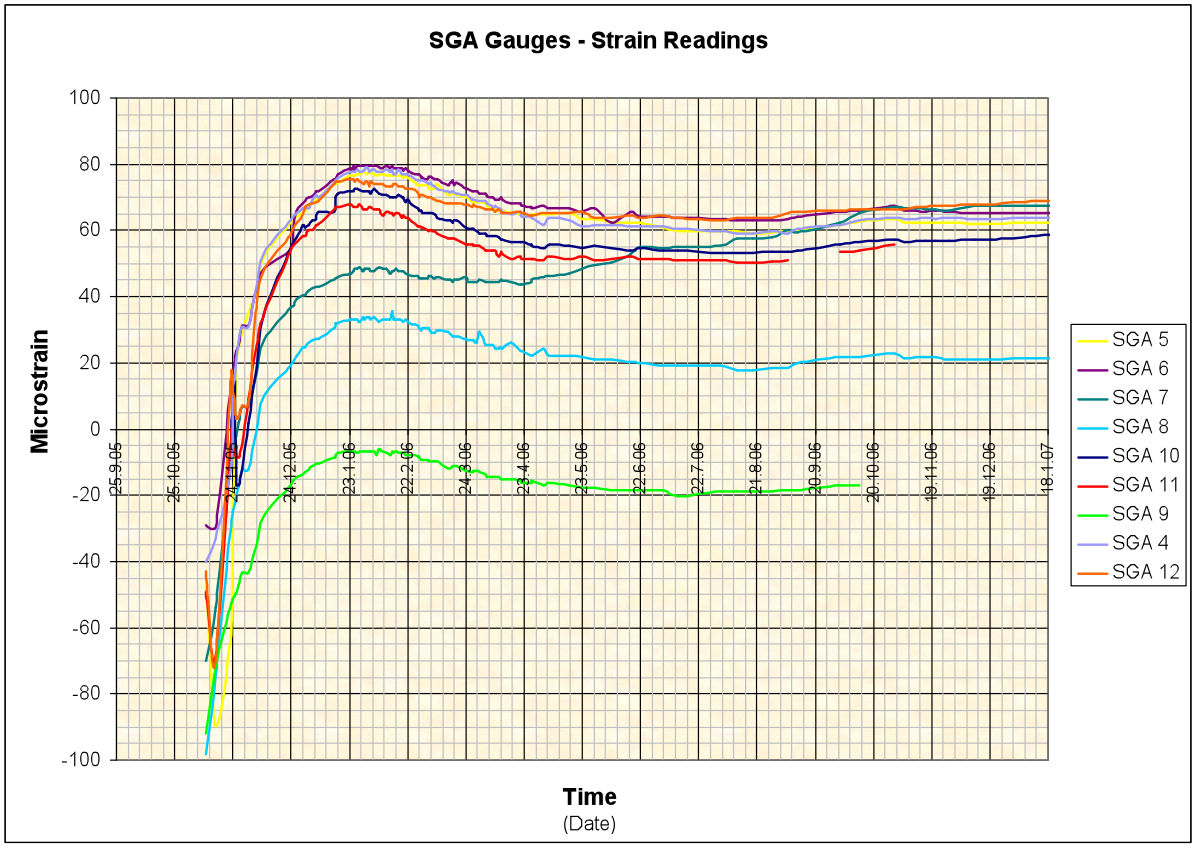

Figure 4.15: Typical Strain History for SGA Instruments[5]

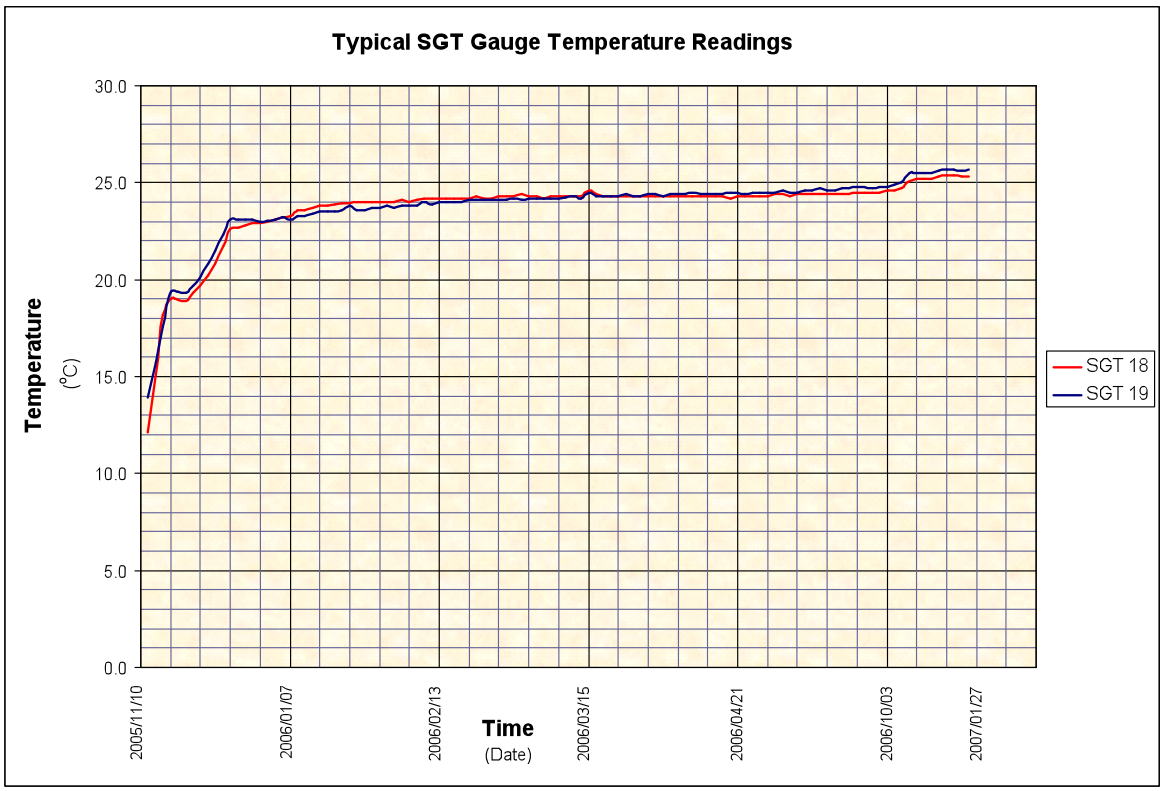

Figure 4.16: Typical Temperature History for SGT Instruments[5]

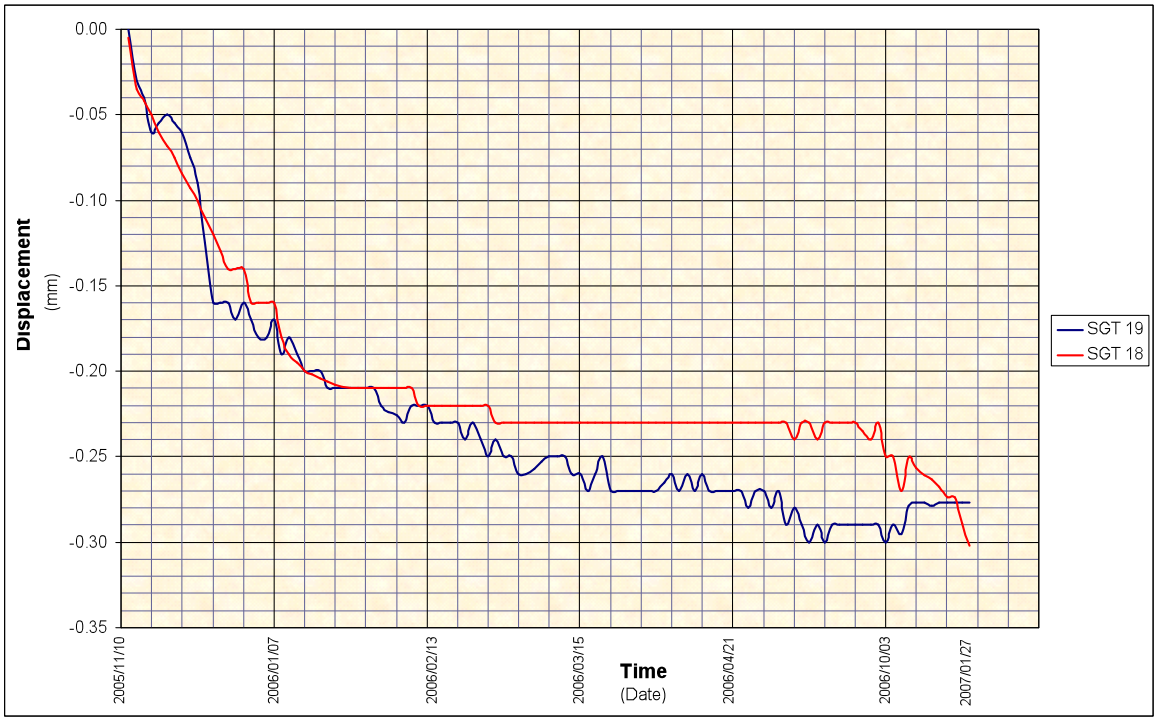

Figure 4.17: Typical Joint Deformation History for SGT Instruments[5]

In relation to strain, the SGT gauges demonstrate compression displacements (**Figure 4.17**) that increase linearly over the first two months after installation followed by an additional 2 months of displacement increasing at a reduced rate. Thereafter, the displacements remain essentially constant. The displacement behaviour of the RCC measured on the gauges can accordingly be seen to follow directly the hydration temperature development. Typical maximum compression displacements vary between 0.11 and 0.50 mm, with an average of approximately 0.28 mm, which translates to 280 microstrain over a gauge length of 1000 mm.

4.5.4.3. Interpretation of Instrumentation Results

Three specific issues come to light and require consideration in respect of the apparent RCC behaviour patterns demonstrated through the Çine Dam instrumentation to date. These can be summarised as follows:

- While the SGA gauges demonstrate expansion strain directly related to the hydration temperature development, they indicate a subsequent relaxation of strain of the order of 15 microstrain over a period of approximately 4 months after the hydration peak temperature is reached and maintained.
- Once the strain relaxation apparent on the SGA gauges has occurred, a constant level of strain is subsequently maintained. Similarly, at maximum strain on the SGT gauges, no change in strain is evident that could signal the occurrence of creep.
- The SGT gauges experience compression strains, which develop with increasing hydration temperature and are maintained without relaxation. The indicated compression displacements suggest some compressibility of the induced joint (see 2.2.5).

It is considered most likely that the strain relaxation indicated on the SGA gauges reflects creep, developed as a consequence of the different behaviour of the RCC materials structure under thermal expansion compared to restrained compression. While this 15 microstrain shrinkage would imply that the RCC, which is generally experiencing compression stresses while its temperature is elevated by hydration heat, will start to experience tension at a temperature of a little less than 2°C above the "built in" temperature, as the hydration heat is gradually dissipated. It should be noted that the lignite fly ash used at Çine Dam is a relatively low grade material, which may play some part in the evident behaviour.

It was initially considered anomalous that compression strains of 250 to 280 microstrain should be indicated on the SGT gauges for a typical hydration temperature rise of 14°C. While lower strains could be anticipated in the direction of the dam axis, as the body of the wall is restrained within the foundation, expansion, as opposed to contraction would be anticipated, corresponding with the expanded materials volume associated with increased temperature.

The evident contraction across the LBSGTMs can, however, be explained by the fact that the meters are located on the induced joint, immediately above a crack director (which are installed in every 4th layer). The method of construction of these induced joints effectively causes them to act, to a minor extent, as compressible expansion joints, as discussed in Chapter 2. While the process of roller compaction results in the development of horizontal restraining stress within the RCC, this stress is broken as the induced joint faces are opened to facilitate the insertion of the de-bonding plate. On completion of the induced joint construction, some capacity to absorb expansion of the adjacent RCC is developed. This is also considered to be the reason for the scatter of the applicable compression strain values evident on the SGT gauges, when compared with the strains indicated on the SGA gauges.

As the temperature in the dam rises during the process of hydration, the resultant restrained expansion will cause compression across the dam wall structure between abutments. With more ability to accommodate contraction across the induced joint than in the remainder of the RCC, a disproportionate part of the thermal expansion of the RCC will be taken up in contraction across the induced joint, while the balance will be experienced as compression in the RCC. Ignoring autogenous shrinkage, a 14°C temperature increase would give rise to a strain of approximately 120 microstrain, as indicated on the SGA gauges. At 1.5 to 2 months age, the long-term RCC deformation modulus might be 10 to 12 GPa, suggesting a restrained compression stress of a little over 1 MPa.

The thermal analyses for Çine Dam indicated that the temperature at the location of the particular instruments addressed in this work will stabilise at around 18.5°C, approximately 50 years after construction completion. In view of the fact that the "built in" temperature for the internal instruments in this installation was between 12 and 14°C, it is accordingly quite possible that tension will never be experienced across the induced joints within this section of the dam wall, as the equilibrium temperature is higher than the natural closure temperature, even allowing for a 2°C increase consequential to shrinkage and creep, or a possible 1°C seasonal variation within the body of the dam wall.

4.5.5. INSTRUMENTATION DATA EVALUATION 2009

4.5.5.1. General

While the top level of instrumentation for Çine Dam had not been installed at the time the present review was undertaken, the value of the instrumentation evaluation undertaken was compromised by the fact that the readout unit started developing inconsistencies during 2007. The consequential problems really serve to demonstrate the critical importance of building redundancy into dam monitoring instrumentation systems. The evaluations in this Chapter were made on the basis of instrumentation measurements from date of installation until the end of 2008.

4.5.5.2. Instrumentation Measurements

Figures 4.18 to **4.33** illustrate the typical temperature and strain/displacement measurements recorded at Elevations 147.50, 185.25 and 208.50 mASL respectively[3, 5 & 7]. The pattern of results indicated at the specific chainages selected was essentially repeated at all of the other induced joints and while the data presented is by no means comprehensive, it is fully representative of the measurements made and the behaviour apparent throughout.

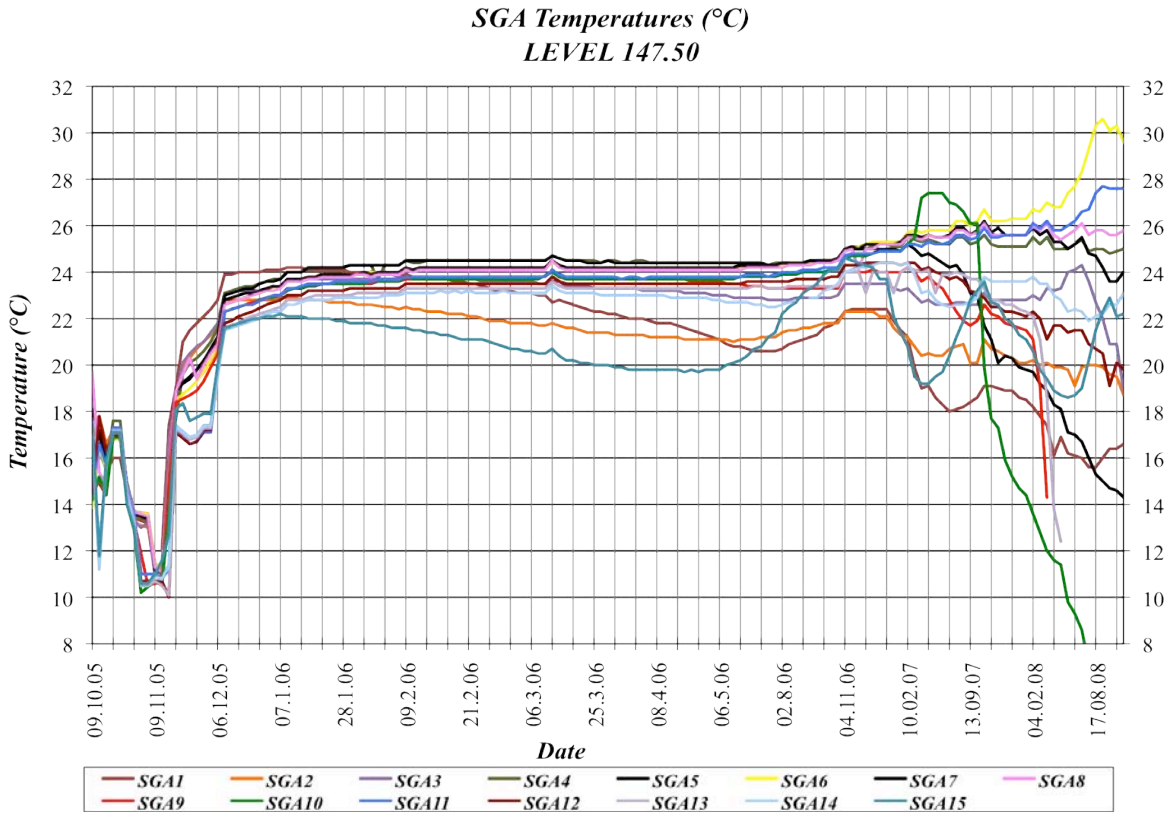

Figure 4.18: Temperature on Strain Gauges (SGA) at El 147.5 m - Ch 127 m[5]

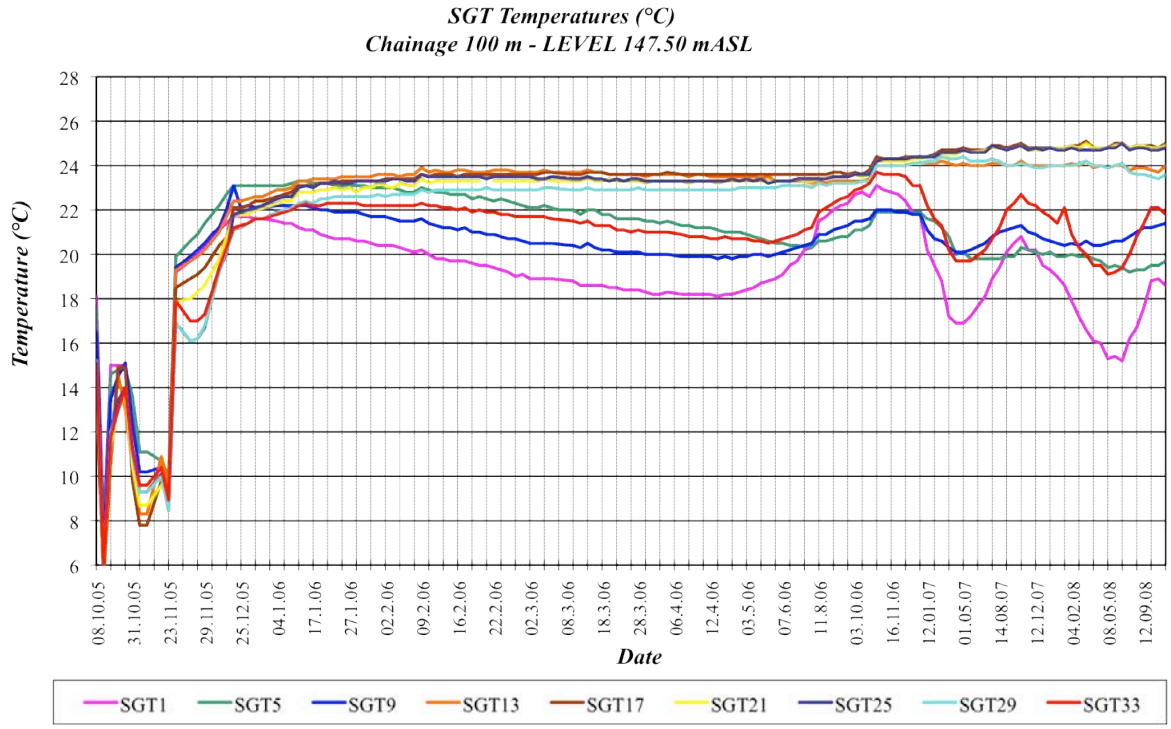

Figure 4.19: Temperature on LBSGTMs (SGT) at El 147.5 m – Ch 100 m[5]

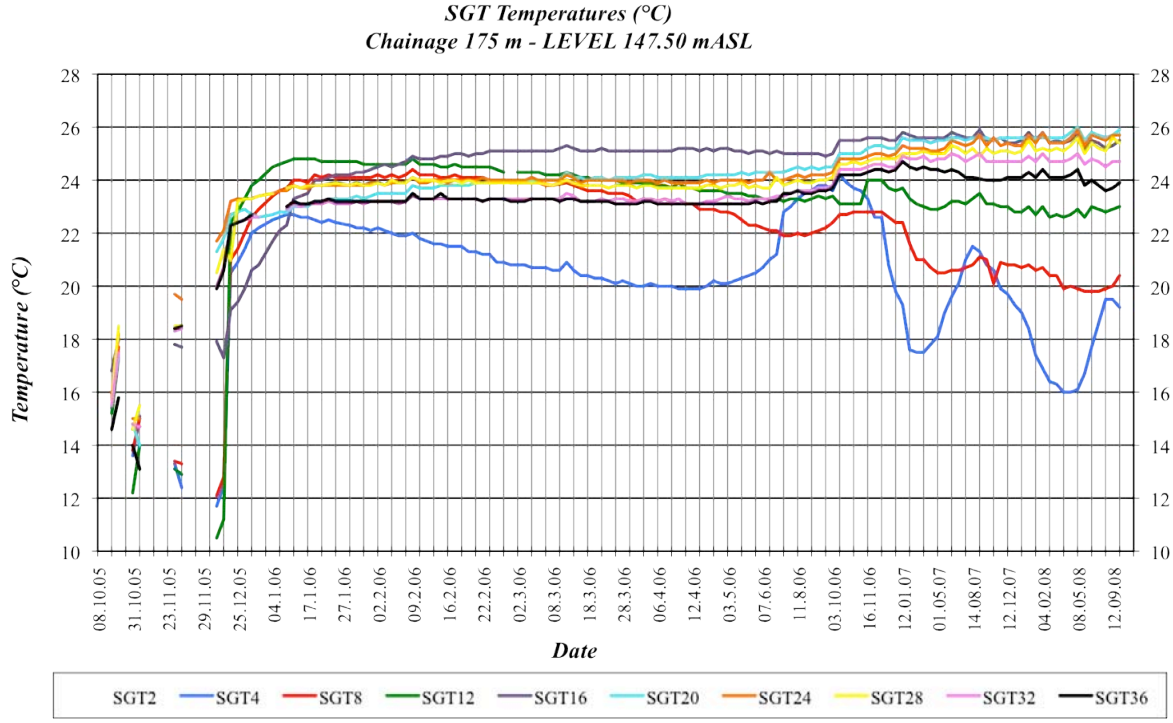

Figure 4.20: Temperature on LBSGTMs (SGT) at El 147.5 m - Ch 175 m[5]

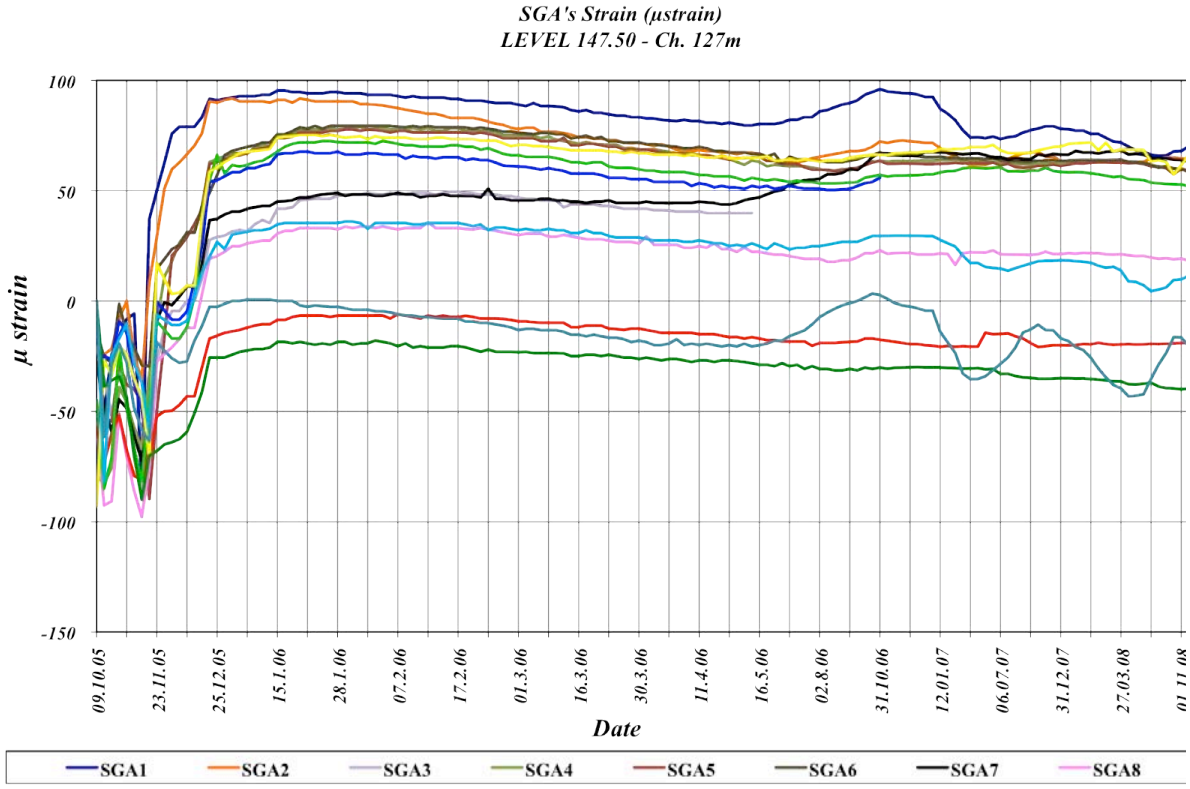

Figure 4.21: Strain on Strain Gauges (SGA) at El 147.5 m - Ch 127 m[5]

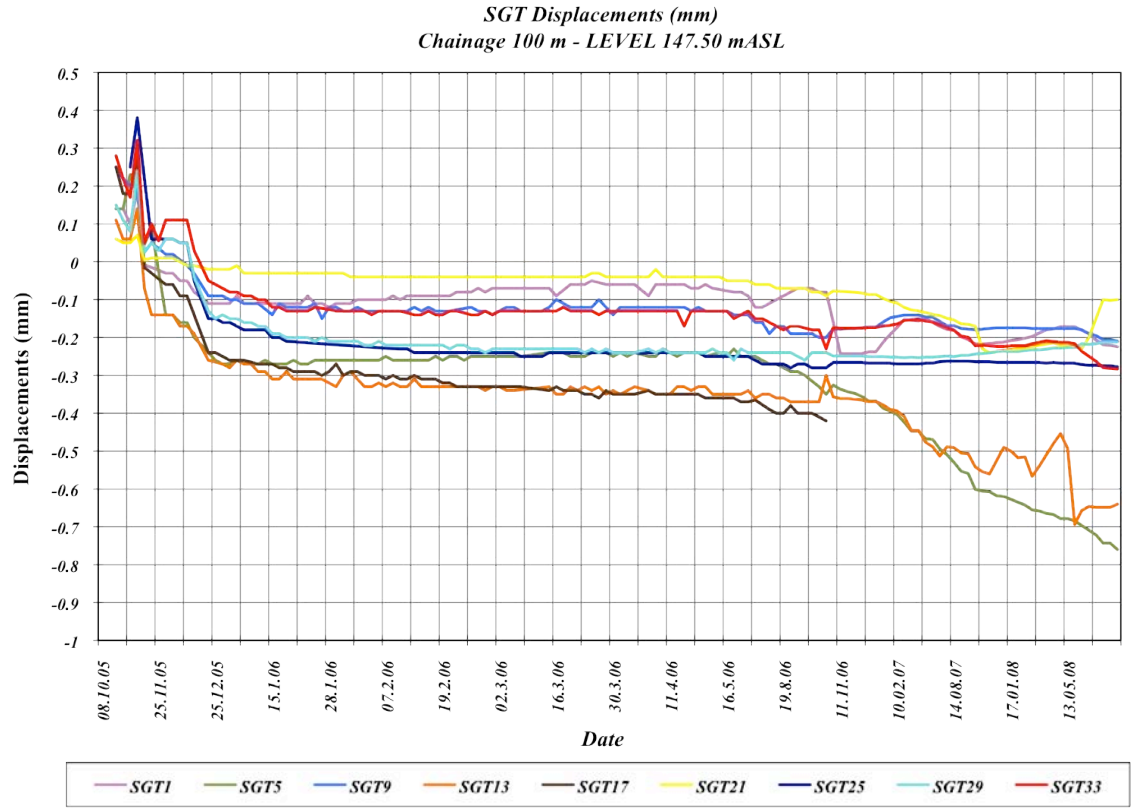

Figure 4.22: Displacements on LBSGTMs (SGT) at El 147.5 m - Ch 100 m[5]

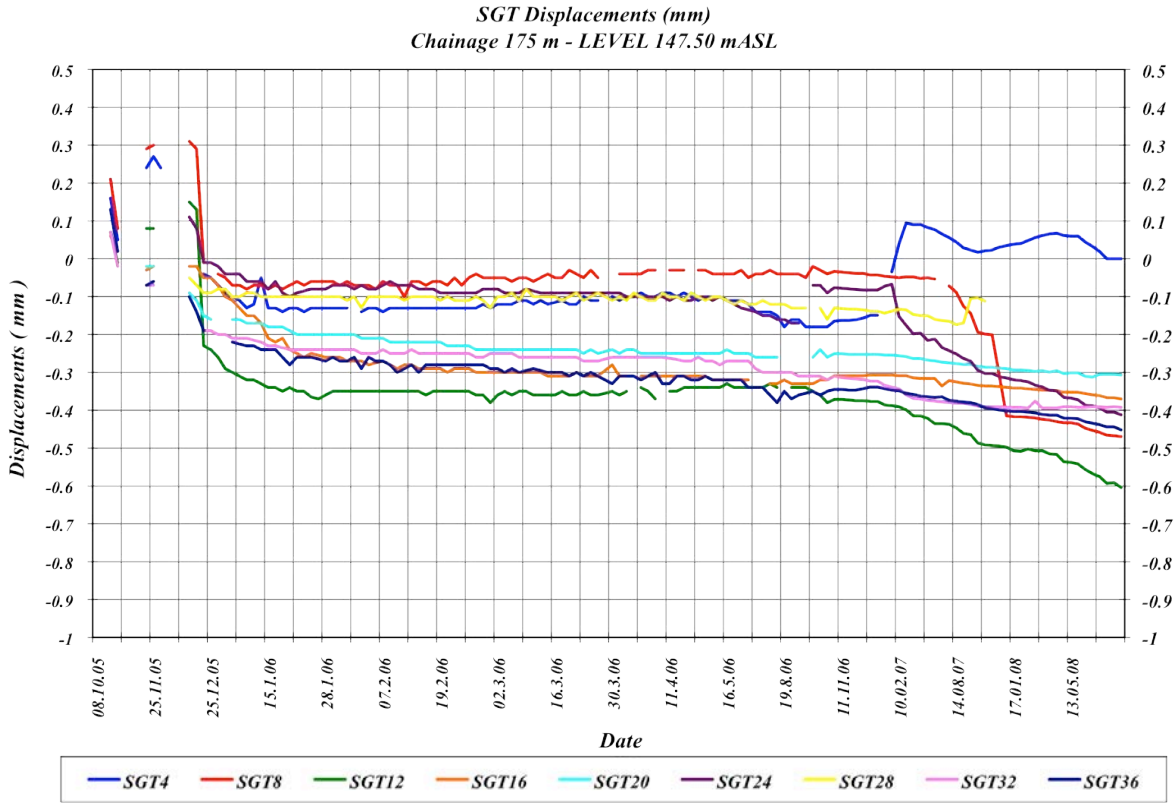

Figure 4.23: Displacements on LBSGTMs (SGT) at El 147.5 m – Ch 175 m[5]

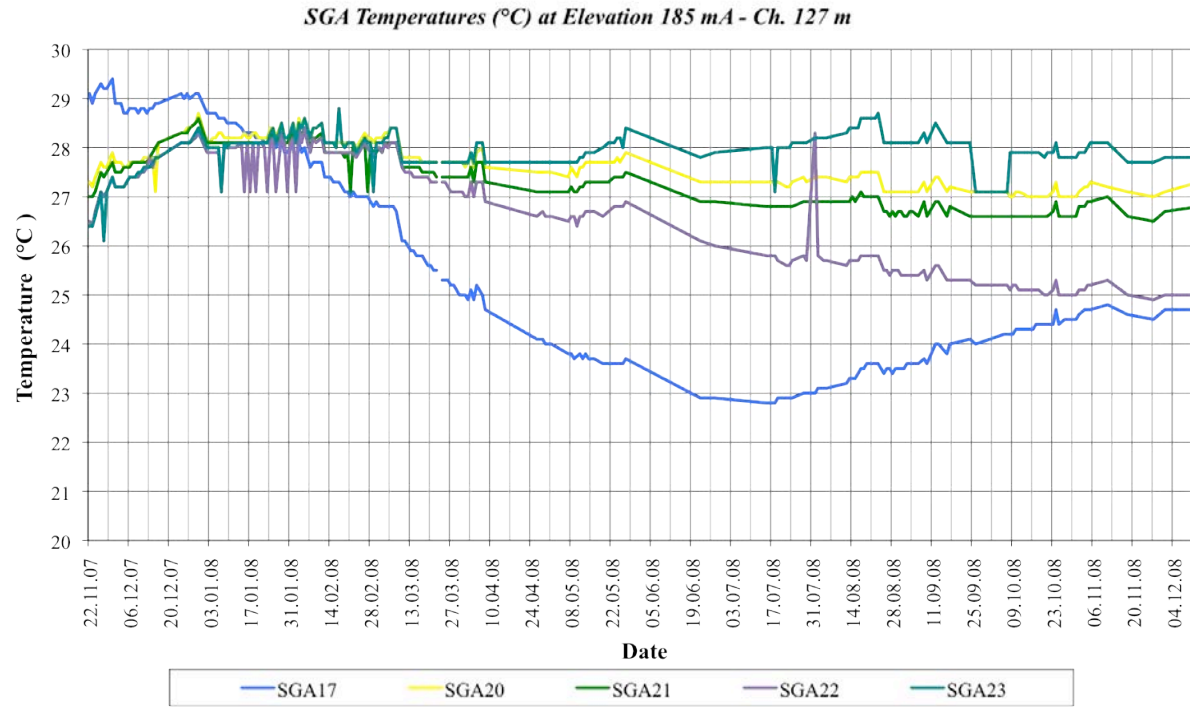

Figure 4.24: Temperature on Strain Gauges (SGA) at El 185 m - Ch 127 m[5]

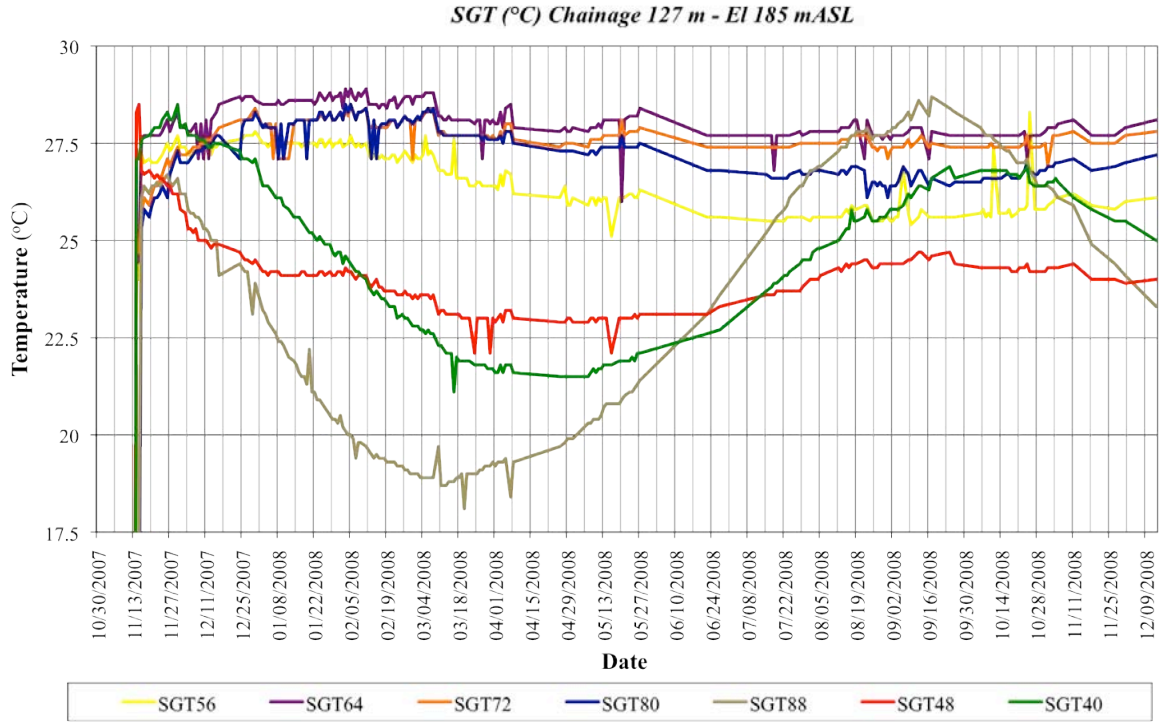

Figure 4.25: Temperatures on LBSGTMs (SGT) at El 185 m – Ch 127 m[5]

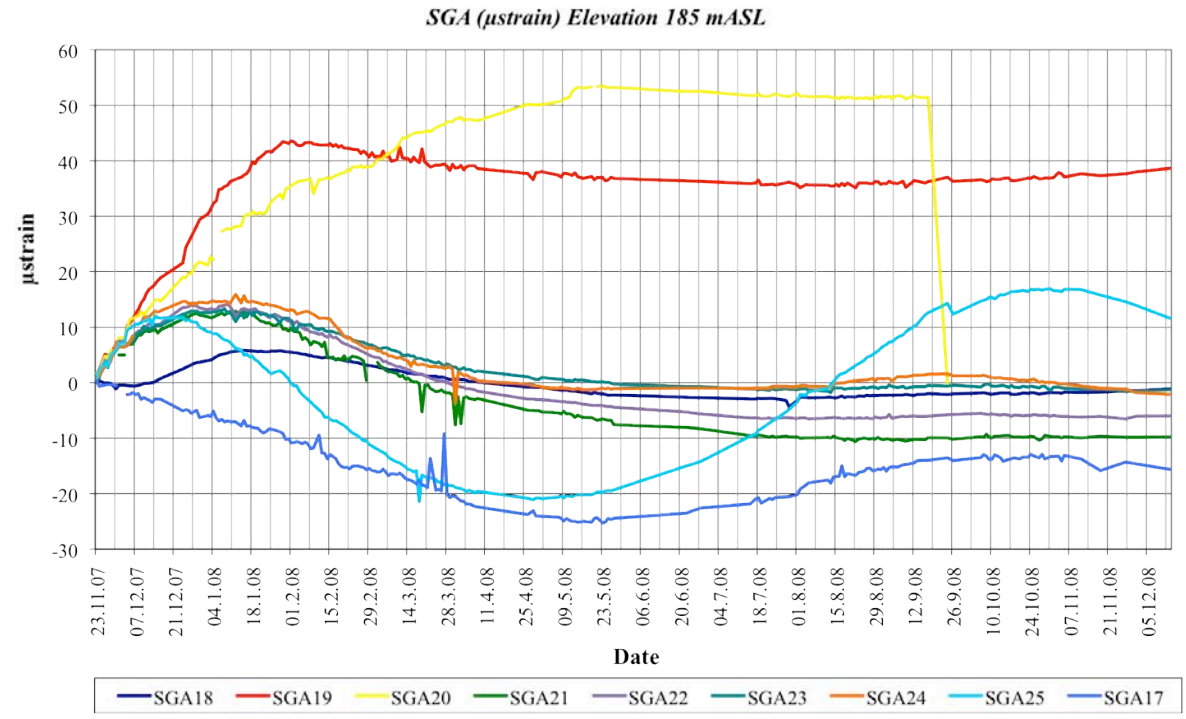

Figure 4.26: Strain on Strain Gauges (SGA) at El 185 m - Ch 127 m[5]

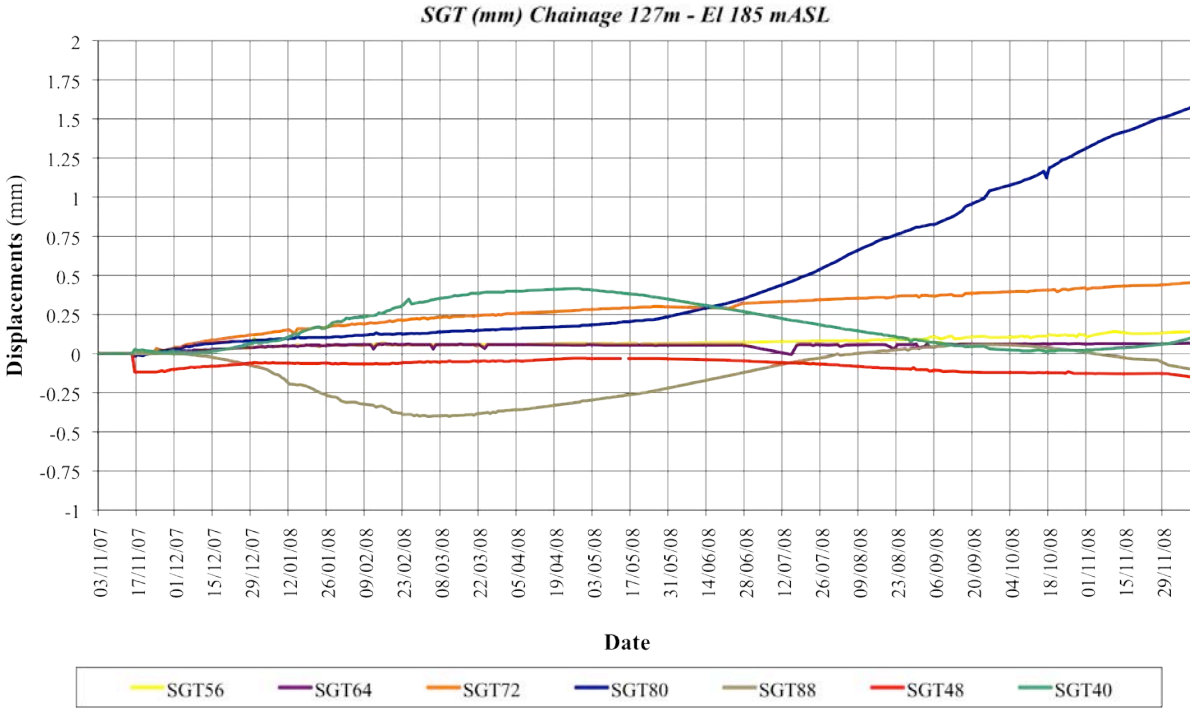

Figure 4.27: Displacements on LBSGTMs (SGT) at El 185 m – Ch 127 m[5]

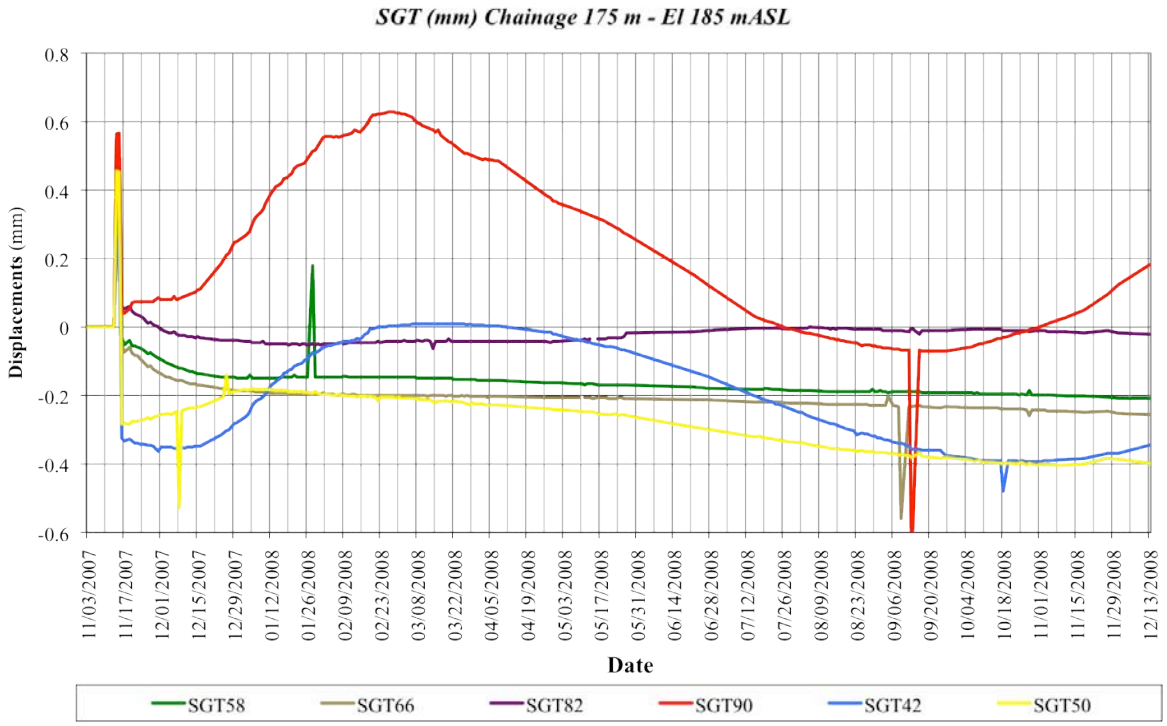

Figure 4.28: Displacements on LBSGTMs (SGT) at El 185 m – Ch 175 m[5]

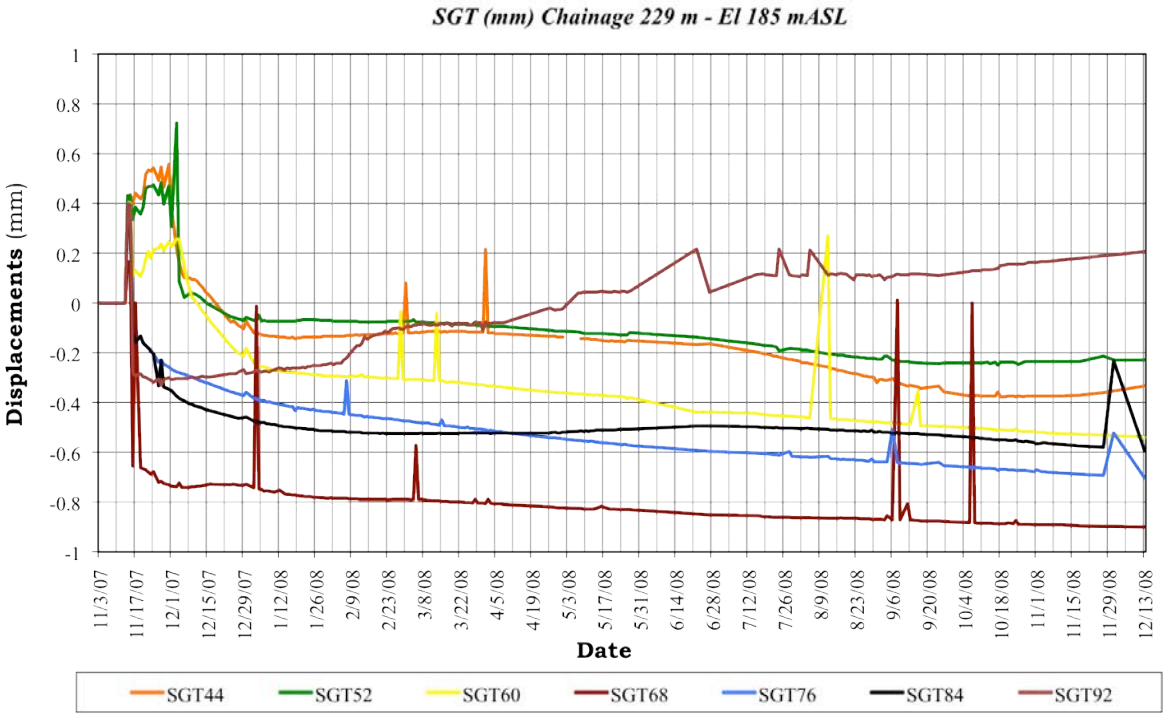

Figure 4.29: Displacements on LBSGTMs (SGT) at El 185 m – Ch 229 m[5]

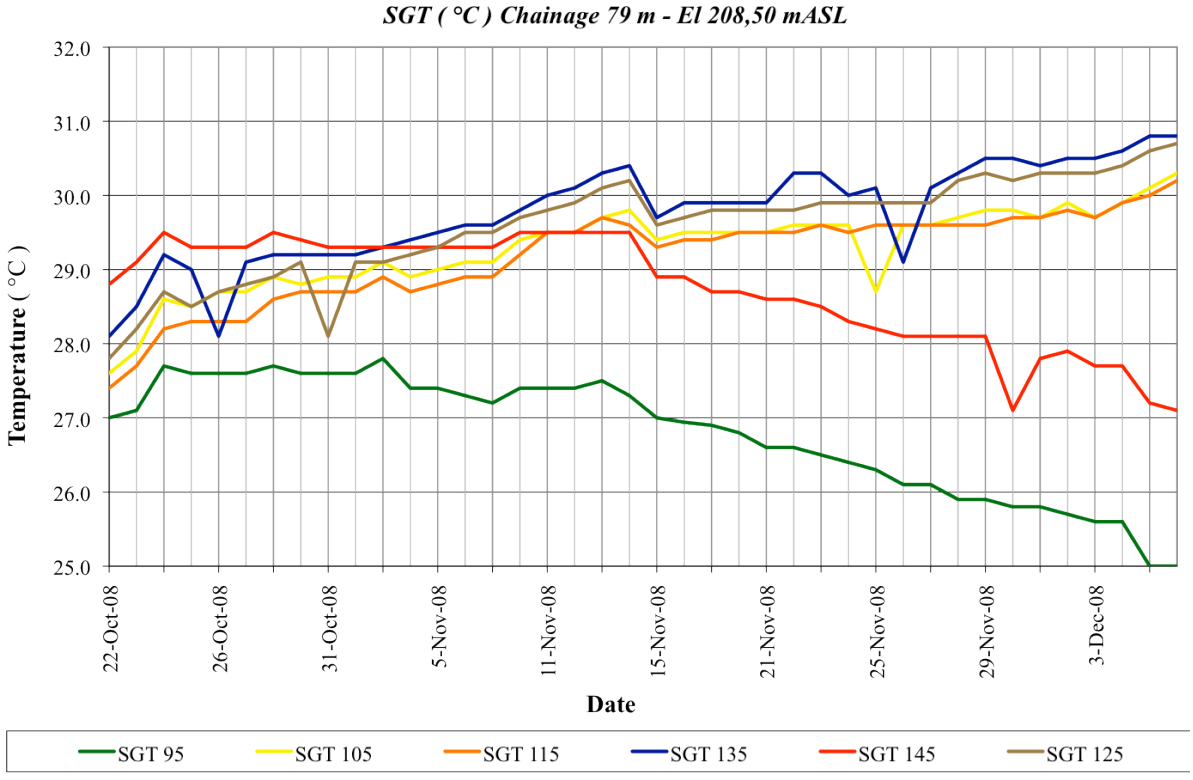

Figure 4.30: Temperatures on LBSGTMs (SGT) at El 208 m – Ch 79 m[5]

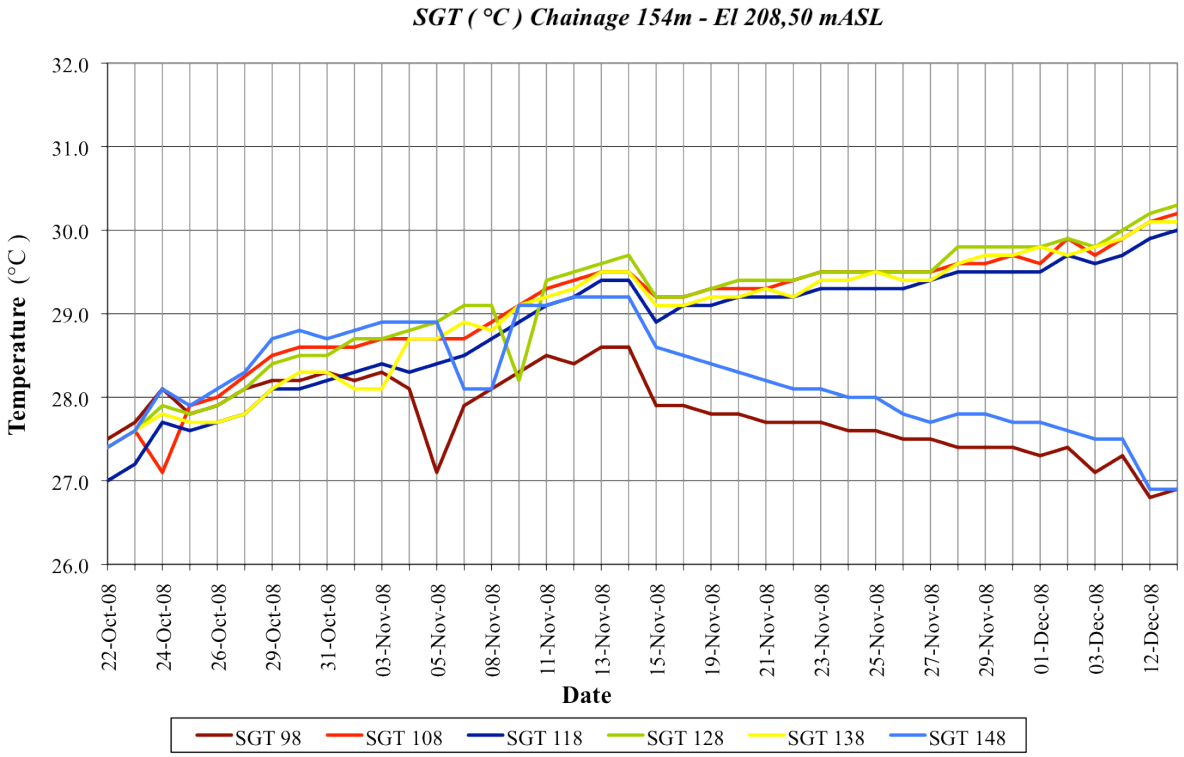

Figure 4.31: Temperatures on LBSGTMs (SGT) at El 208 m – Ch 154 m[5]

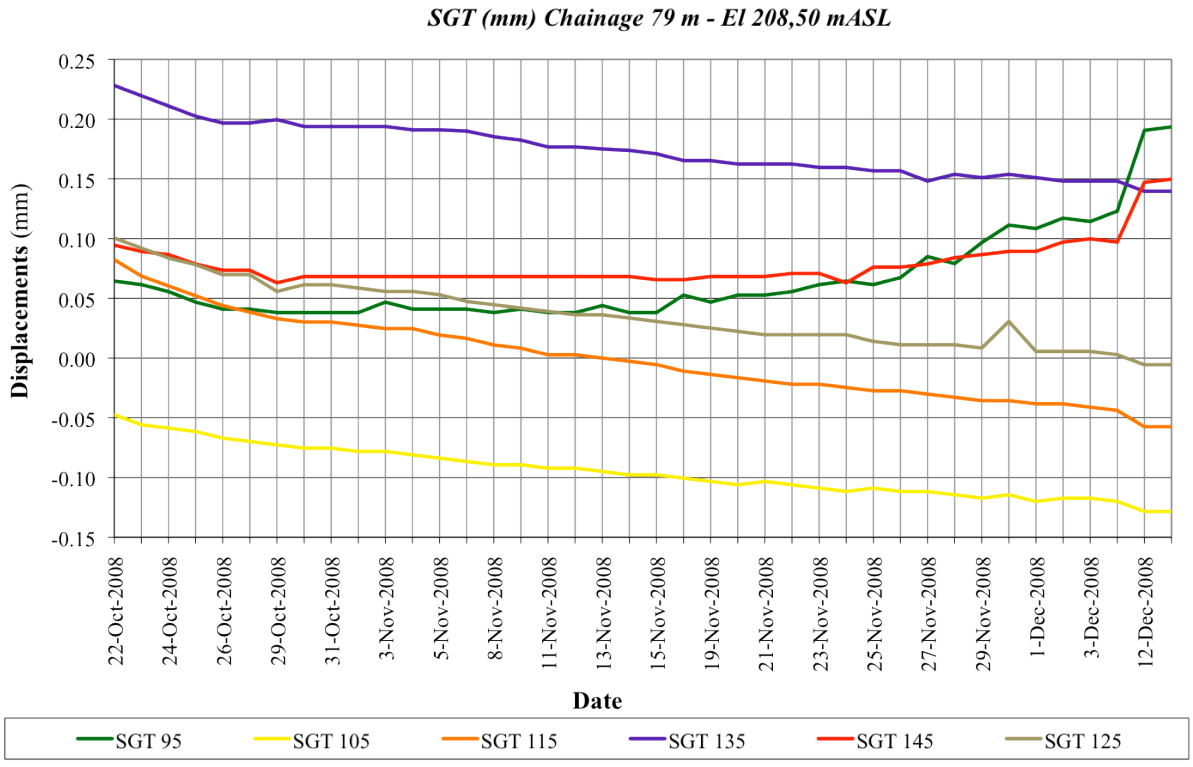

Figure 4.32: Displacements on LBSGTMs (SGT) at El 208 m – Ch 79 m[5]

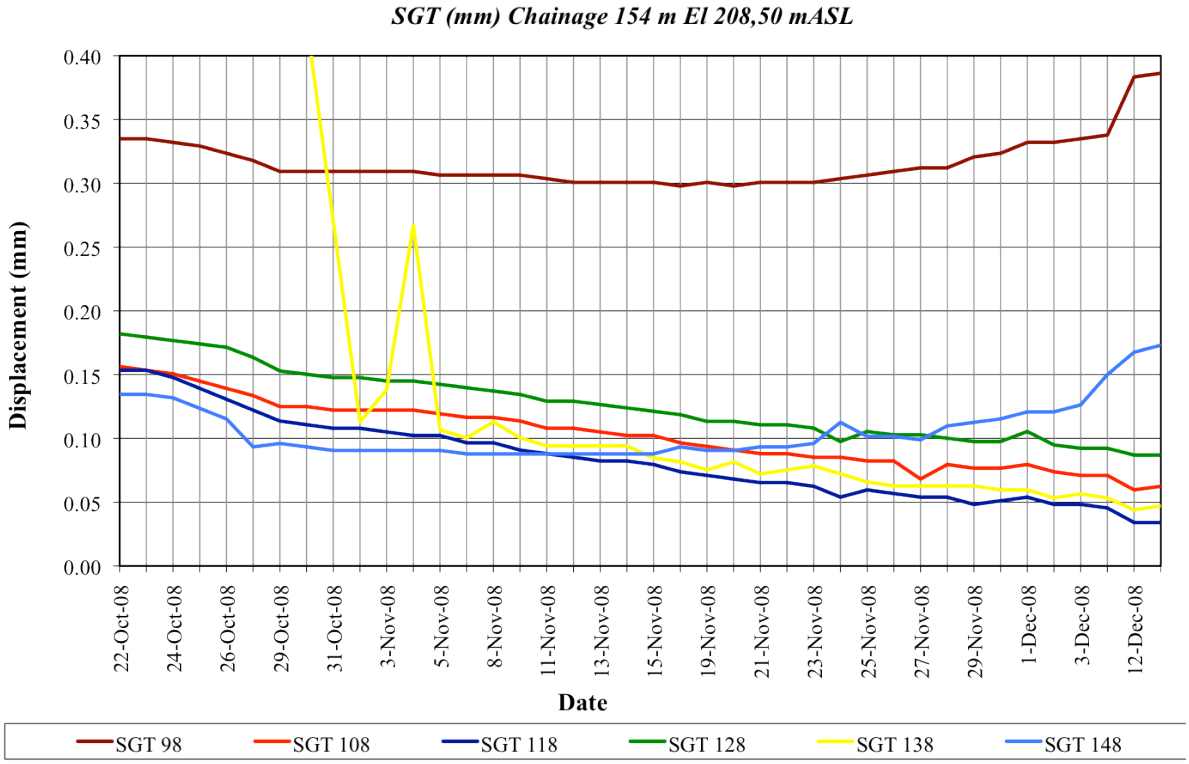

Figure 4.33: Displacements on LBSGTMs (SGT) at El 208 m – Ch 154 m[5]

4.5.6. DISCUSSION OF INSTRUMENTATION DATA FINDINGS

4.5.6.1. General

Before attempting to determine patterns of behaviour within the data available, it is considered important to highlight a number of general comments in relation to the observed data. Firstly, it is clear that a number of errors are present within all data sets and these can be seen in the odd, random and obviously incorrect data point, or "outlier". Secondly, the impact of the faulty instrumentation readout unit can be seen in some strange and, in some cases, contradictory data as early as the beginning of 2007. Thirdly, the occasional inconsistency between the listed location of a specific instrument and the associated temperature measurements suggest that certain of the instrument cables were incorrectly labelled.

As a consequence of the above and the nature of such measurement within a dam structure, the available data is of greatest use in illustrating patterns of behaviour, particularly where consistent patterns are demonstrated. The data available demonstrates clearly that the temperatures within the core zone of the dam structure at the lower elevations have remained fairly constant, at their hydration peak, with no apparent dissipation by the end of 2008. The closer the instrument to the surface, the more dissipation that is evident and correspondingly, the greater the influence of external ambient temperature variations.

Indications from the coffer dam and theoretical calculations suggested that a hydration heat of approximately 12°C should be applicable for Çine Dam and the measurements on the main dam wall have confirmed this figure to be quite realistic. In general, the SGA and SGT temperature measurements indicated a high degree of correlation.

Laboratory testing at the Middle Eastern Technical University (METU)[7] indicated an average instantaneous E modulus of approximately 25 GPa for the Çine Dam RCC. Under a sustained compressive stress of 5.5 MPa, the test cylinders subsequently indicated a creep of approximately 110 microstrain over a period of approximately 60 days. Including the creep, the total strain consequently indicates an E modulus of 16.67 GPa, which corresponds to a sustained E modulus equivalent to 2/3 of the instantaneous value, which is in line with typical expectations[10]. Due to the inelastic properties of concrete, increased deformation under a sustained load, compared to an instantaneous load, is manifested as creep that is gradually reversed on release of the load. For this reason, an effective E modulus under sustained loading equivalent to 2/3 of the instantaneous value is usually assumed. On the basis of the above calculation, it would appear that the creep measured in the METU laboratory accordingly relates only to the reversible phenomenon associated with the response of concrete under sustained loading. The METU testing further confirmed the instrumentation observations that drying shrinkage of the RCC was minimal.

4.5.6.2. Issues Related to Specific Elevations

The instrumentation installed at El 147.50 mASL is the most comprehensive and offers the best and most consistent data. At Elevations 147.50 & 208.25 mASL, the LBSGTMs were not effectively zeroed at installation and accordingly, it is not always straightforward to develop a clear picture of the total displacements caused by thermal effects.

The RCC of the layer in which the instrumentation was installed at El 147.50 mASL indicated a placement/built-in temperature ranging between 10 and 16°C, with an average of the order of 13°C. The maximum temperature reached in the core RCC varied between approximately 24 and 26°C. At El 147.50 mASL, the two gauges on the upstream side of the gallery, the gauge immediately downstream of the gallery and the gauge closest downstream face indicated “surface” temperature behaviour, while the remainder reflected “core” temperature behaviour.

The instruments at El 208.25 mASL had only been installed for around 2 months by the end of 2008, when the data was forwarded for interpretation, and accordingly, the data from these instruments is of little value in respect of the study addressed in this chapter. While the external two gauges at the lower elevations seem to represent “surface” and intermediate temperature behaviour, only the single, outer gauges at El 208.25 mASL reflect “surface” behaviour.

4.5.6.3. SGA Meters

General

Strain gauges orientated perpendicular to the dam axis were only installed on the lower two levels of instrumentation at Çine Dam. In view of the fact that these instruments are not influenced by crack directors, they tend to indicate greater quantitative consistency.

Elevation 147.50 mASL

As a consequence of the apparent problems with the instrumentation readout unit, it is not realistically possible to make any meaningful, or quantitative analysis of the strain variations with rising and falling temperature in the surface zones of the RCC at El 147.50 mASL once this zone reached its long-term equilibrium cycle. However, the behaviour of the RCC in the core zones is very clear, at least until the temperature rise around 1 year after placement. For the first three to four weeks after installation, the strain gauges appear to have experienced some minor contraction. Thereafter, the RCC expands. Examining, the temperatures confirms that the initial contraction occurred before the instruments were covered with RCC. While this resulted in divergent zero values across the gauges, it is clearly evident that total strain increases of between 62 and 155 microstrain occurred as a consequence of the hydration heat development.

As this strain was a thermal swelling, it can be observed that the peak values were recorded at 1/3 and 2/3 points across the dam section. The maximum strain increased from the upstream surface to the 1/3 point, decreased slightly to the middle of the section, increased to the 2/3 point and decreased to the downstream surface, as illustrated in **Figure 4.34**.

The average strain across the section, as measured on the SGA gauges, was approximately 105 microstrain. This can be compared with a figure of approximately 85 microstrain, which would have been anticipated for a temperature increase of 12°C and a coefficient of thermal expansion of 7.1 x 10^{-6}/°C. The fact that the measured expansion exceeds that predicted probably relates to a lack of accuracy in the tested thermal expansion coefficient, but more importantly it confirms that the early expansion occurred in a very elastic manner, with no apparent losses to creep, despite the immature nature of the RCC at the time. The strain values measured suggests that the RCC might have an initial coefficient of thermal expansion of approximately 8.75 x 10^{-6}/°C. A second possible origin of the unexpectedly high expansion is that this occurs due to constraint in the perpendicular direction. However, it did not prove possible to verify this hypothesis through analysis.

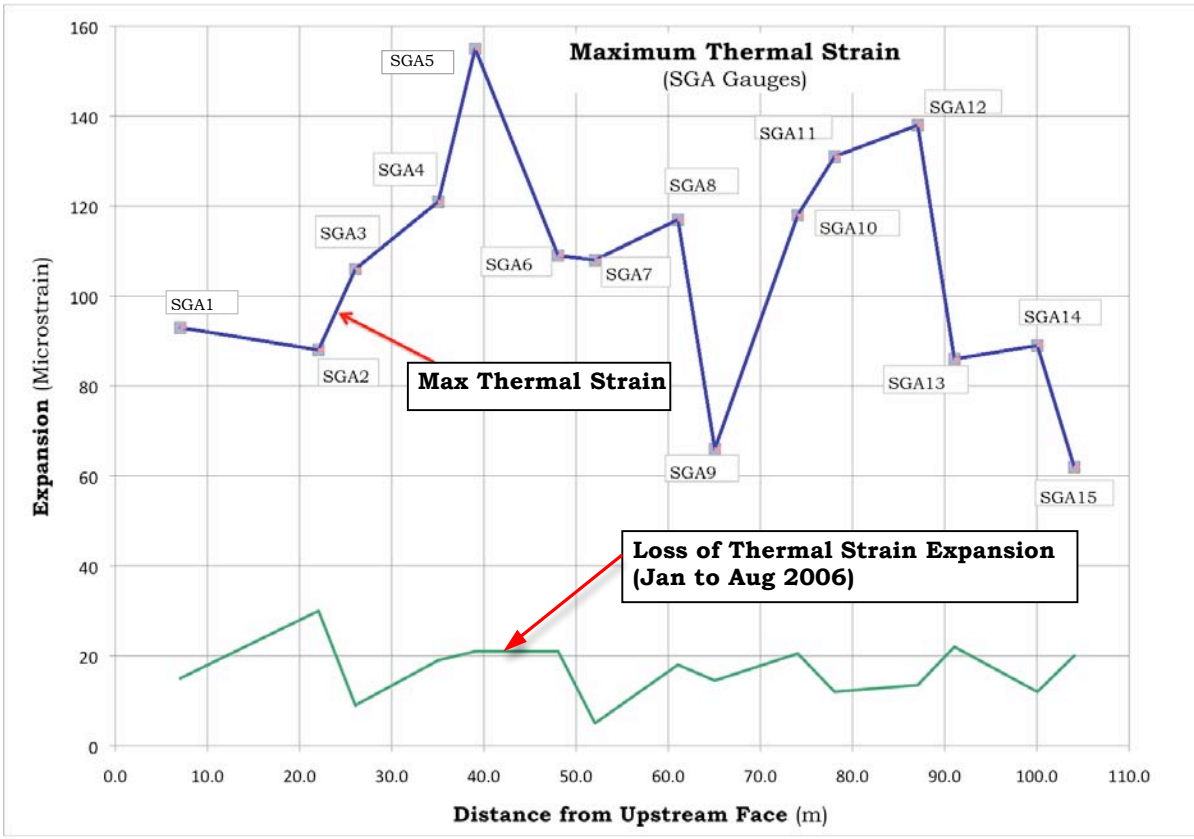

Figure 4.34: Strain Distribution Across Cross Section Measured on SGA Gauges

During the subsequent 7 to 8 months, a gradual relaxation in the expansion strain is evident on all gauges apart from SGA 7, which is located at the centre of the section. The average strain relaxation experienced over this period within the zone where the temperature remains constant is approximately 16 microstrain (or 15%). When the section starts to experience an increase in temperature again, towards the end of 2006, an average expansion of approximately 7 microstrain is experienced for an average temperature increase marginally exceeding 1°C. To all intents and purposes, it appears that no further strain relaxation is experienced after mid 2008. For the same coefficient of thermal expansion that was demonstrated during hydration heating, an expansion of slightly in excess of 9 microstrain would be anticipated, so it remains possible that approximately 2 microstrain (or 25%) has been lost to creep. On the other hand, the latter expansion corresponds accurately with the coefficient of thermal expansion measured in laboratory testing[7] (7.1 x 10^{-6}/°C), without any losses to creep. By the same token, the initial hydration expansion, less the loss for apparent creep, approximately corresponds to a net expansion at a coefficient of thermal expansion of 7.4 x 10^{-6}/°C (89 microstrain/12°C), which is again approximately equivalent to the average laboratory figure.

In summary, the data for the SGA strain gauge instrumentation installed at El 147.50 mASL appear to be demonstrating that a total creep/drying shrinkage of less than 20 microstrain (or approximately 15% of the total expansion developed as a result of hydration heat) occurred at Çine Dam over a period of 2 to 3 years, where unrestrained expansion was allowed to occur, perpendicular to the axis of the dam. The 200 microstrain autogenous and creep shrinkage traditionally assumed definitely did not occur at Çine Dam and, even if the measured strain relaxation was a consequence of autogenous shrinkage and/or creep, the reality is less than $1/10^{th}$ of the figure traditionally assumed. The fact that thermal expansion was evident in a situation where internal restraint would be expected to be dominant, however, was considered quite surprising and a strong indication of the different behaviour of high-paste RCC compared to CVC.

Elevation 185.00 mASL

At El 185.00 mASL, some anomalies exist in respect of data from some of the SGA gauges. For example, the temperature data from SGA24 makes no sense and yet the strain readings for the same instrument are quite believable. While the origin of these problems is unclear, additional care must be applied in all consequential interpretations.

The RCC placement above El 185 mASL started on 15/16 November 2007, but strain measurement on the SGA gauges was only initiated approximately 1 week later, when a substantial amount of the hydration heat would have already developed. Gauges SGA17, 21, 22, 23, 24 & 25, however, provided data that is significantly useful. All gauges were zeroed for strain approximately 7 days after RCC placement and accordingly it is apparent that the expansion due to the first period of hydration heat development was not measured, or is not recorded in the available data. While this implies that it is not possible to compare the actual and the anticipated coefficient of thermal expansion, the instruments that indicated temperatures remaining at the peak hydration level until the end of 2008 demonstrated an expansion strain development of around 10 microstrain, which was dissipated over the following four to five months. Thereafter, no further creep/shrinkage was apparent. In gauge SGA23, where a net temperature drop of around 1.3°C was experienced, the expansion strain was dissipated earlier and a further 10 microstrain in tension was developed, as would be expected for a linear shrinkage at a coefficient of thermal expansion of approximately 7×10^{-6}/°C. Gauge SGA22 indicated an additional shrinkage of approximately 5 microstrain, despite an apparent temperature drop of 3°C, although such a temperature drop is viewed with suspicion at a gauge within the core zone of the dam cross-section.

While the temperature reading function of gauge SGA25 (close to downstream surface) seems to have failed very early on, the strain readings indicate a seasonal strain variation of just under 40 microstrain, which makes some sense compared to

an anticipated temperature variation range of the order of 6°C. Gauge SGA17 (close to upstream surface) indicates a seasonal strain variation of approximately 13 microstrain after an apparent creep/shrinkage of approximately 12 microstrain. This corresponds to a temperature variation range of 1.9°C, indicating a linear-elastic response for a coefficient of thermal expansion of approximately 7 x 10^{-6}/°C.

4.5.6.4. SGT Meters

Elevation 147.50 mASL

At El 147.50 mASL, the joint closure measured across the LBSGTMs apparently generally peaked at 0.40 mm at maximum hydration temperature. Over an instrument length of 1 m, this represents a strain of 400 microstrain. For a hydration temperature rise of 11°C, this would translate directly into a thermal expansion coefficient of approximately 36 x 10^{-6}/°C, which is obviously rather improbable. Furthermore, while the effects of the increase in temperature during 2008 are evident, the problem with the instrumentation readout unit cloud any real quantitative analysis. However, the fact that a 1°C temperature rise might result in compression across the induced joints of the typical order of 0.02 to 0.04 mm again suggests relatively linear-elastic behaviour.

Should the RCC of Çine Dam have behaved in the traditionally assumed manner, shrinkage/creep of approximately 200 microstrain should have exceeded the temperature expansion of approximately 78 microstrain (11°C x 7.1 x 10^{-6}/°C) by 122 microstrain. The net shrinkage should have caused a tensile stress of approximately 1.8 MPa, which should have consequently exceeded the tensile strength of the weakened induced joints, which are spaced at 27 m centres, and translated into an opening of approximately 3.3 mm in width. Instead, a joint closure of approximately 0.4 mm has been maintained since the peak temperature was reached, which increased with increasing temperature.

The behaviour recorded suggests, again, that the RCC of Çine Dam cannot be behaving in a manner at all like that traditionally assumed. While no evidence of shrinkage, or creep can be determined on the SGT meter readings, should any in fact be evident, it can only be of an order of magnitude different to that which might traditionally be assumed.

Elevation 185.00 mASL

At El 185 mASL, the temperature data is apparently consistent in demonstrating a hydration temperature rise of the order of 12°C. Interpretation of the displacements on the SGT gauges, however, is less straightforward, with some anomalous and contradictory readings.

The SGT gauges at Chainage 127 m indicate some strange behaviour. SGTs 72 and 80 suggest that a significant crack is developing towards the downstream of the

section, but SGT 88 (closest to the downstream face) indicates exactly the opposite. SGT 40 (closest to the upstream face) indicates a crack of 0.4 mm width that opens with dropping temperature, while SGT 88 indicates a joint closure of the same order, while experiencing a greater temperature drop. It is accordingly considered that a sufficient level of confidence cannot be placed in this data and that any attempt at interpretation would consequently not be of any value.

While inconsistent zero readings complicate the interpretation of the data from the SGT gauges at Chainage 175 m, the "core" instruments indicate compression strain that follows the temperature pattern and is apparently maintained without creep. The upstream surface gauge SGT42 indicates a change in strain of 400 microstrain for a temperature change of approximately 6°C, superficially suggesting a coefficient of thermal expansion of 67 x 10^{-6}/°C, while the adjacent gauge, SGT50, indicates a strain change of 200 microstrain for a temperature variation of approximately 3°C, superficially suggesting a coefficient of thermal expansion of the same order. The gauge closest to the downstream face suggests that a crack of 0.6 mm opened when the temperature dropped by approximately 8°C, while the crack closes and indicates a compression strain of approximately 55 microstrain for a temperature increase of 12°C above minimum, or approximately 4°C above maximum hydration temperature.

At Chainage 229 m, the SGT gauges indicate substantially more consistent behaviour and behaviour more similar to the gauges at El 147.50 mASL. Again, it is difficult to isolate a realistic zero value for the displacements due to an apparent break in RCC placement at this specific chainage. However, in the core zone the slow increase of temperature throughout 2008 is reflected in continuously increasing compression strain. For a temperature increase of perhaps 0.5°C over this period, the strain at gauges 60, 68 & 76 increases by approximately 100 microstrain. The reason for this last behaviour is not completely clear, but it is perhaps indicative of some creep compression across the induced joint.

Elevation 208.50 mASL

At El 208.5 mASL, neither temperature, or strain/displacement seem to have been measured from first placement of the RCC layer above and accordingly a fully comprehensive analysis of the data at this elevation is again not possible. Evaluating the concrete placement data, it would appear that the built-in (placement) temperature for the SGT gauges was approximately 22°C. Seven weeks after placement, the temperature in the core zone was steadily rising, at approximately 30 – 31°C. Referring to temperature measurements at the lower levels suggests that the indicated temperatures should rise a further 1 to 2°C before reaching their peak. The only conclusions that can be drawn from the SGT instrumentation at El 208.5 mASL is that for fairly linear rise in "core" temperatures at just under 1°C in a month, SGT compression strain increased at a

rate of approximately 30 microstrain/month. Conversely, in the "surface" zones indicated tension movements in a fairly linear manner, suggesting coefficients of thermal expansion of between 18 and 50 x 10^{-6}/°C. All expansions and contractions as a consequence of temperature changes, when measured across the induced joints, were greater than would have been anticipated within a simple block of RCC and while no indication of any shrinkage, or creep was evident, the apparent effective action of the induced joints as an expansion joint compromises any ability to make any real quantitative evaluations.

4.5.7. EVALUATION FINDINGS

4.5.7.1. Reliability & Consistency

Although quantitative interpretation of instrumentation installed in a dam is notoriously problematic, where considered reliable, the data analysed in this case at Çine Dam demonstrates a consistent pattern of behaviour. This consistency and its corroboration of the behaviour patterns observed at Wolwedans and Knellpoort Dams, further serve to confirm a high level of reliability in respect of interpretation. The fact that the METU testing on Çine RCC cores[7] did not demonstrate creep, beyond that which differentiates the behaviour of concrete under an instantaneous and a sustained load, and indicated minimal drying shrinkage, further increases the perceived reliability of the interpretations of the instrumentation data.

4.5.7.2. Value of Results

While the behaviour observed on the instrumentation at Çine Dam confirms in principle the findings at Wolwedans and Knellpoort Dams, the Çine records are particularly useful in providing strain measurement perpendicular to the dam axis and the related linear thermal expansion under conditions of significant internal restraint is considered one of the most important observations in respect of the Çine RCC behaviour.

The fact that unrestrained expansion occurred in the RCC under a temperature rise is quite surprising. In a block of over 100 m in length and less than 20 m in height, it would have been assumed that most of the thermal expansion due to the hydration temperature rise would have been constrained by foundation and internal restraint. As will be discussed in Chapter 6, it is hypothesised that it is the cause of this very effect that is the origin of the difference in the early behaviour of high-paste RCC, compared to CVC.

All other measurement at Çine Dam recorded displacement across induced joints, parallel to the dam axis, measuring the dam behaviour in compression, as a consequence of restrained thermal expansion.

Unfortunately, insufficient time has passed to determine the final behaviour of the Çine RCC across the induced joints at their final equilibrium temperature, after all the hydration heat has dissipated. As a consequence of the applicable thickness of the section, it will in fact be several decades before cooling to the equilibrium temperature cycle will be achieved at the base of the dam and due to winter-season RCC placement, cracking will almost certainly not occur on all of the induced joints in this location.

4.5.8. CONCLUSIONS

4.5.8.1. General

Despite problems with the instrumentation readout unit, some incorrect cable labelling and some apparently conflicting data, the instrumentation confirms the early thermal RCC behaviour at Çine Dam to comply with the indications from Wolwedans and Knellpoort Dams and correspondingly to suggest lower shrinkage/creep that would be traditionally assumed.

Undoubtedly some creep relaxation was experienced when unrestrained thermal expansion of RCC occurred at Çine Dam. However, this was more than an order of magnitude less than would be expected according to the traditionally accepted materials models. Furthermore, the net expansion recorded after creep relaxation corresponds with the coefficient of thermal expansion indicated for the Çine Dam RCC in laboratory testing.

Accordingly, it is apparent that the behaviour recorded at Çine Dam so far confirms the findings indicated for Wolwedans and Knellpoort Dams.

4.5.8.2. Summary

The data recorded at Çine Dam provides a different, and yet confirmatory, slant on the apparent early behaviour of RCC. While the Çine Dam RCC was similar to that used at Wolwedans and Knellpoort, it was also quite different in using a low-grade fly ash and a lower total cementitious materials content.

4.5.9. ÇINE DAM THERMAL ANALYSIS

4.5.9.1. Background

In reviewing the instrumentation data recorded at Çine Dam, it is considered of value to demonstrate briefly the indications developed through a Thermal analysis for the dam and the consequential accuracy with which the measured temperature development and dissipation were predicted. A more comprehensive Thermal analysis is presented for Changuinola 1 Dam in Chapter 5, where the methodology

and modelling are described in some detail, and the thermal analysis for Çine Dam addressed in this Chapter is presented simply to demonstrate the correlation of modelling results with actual measurement.

4.5.9.2. Introduction

The Çine Dam thermal modelling was undertaken in mid 2005[8 & 9], after the first season of RCC placement had seen the dam constructed from its lowest foundation level of EL 128.5 mASL to EL 147.5 mASL. Thereafter, it was initially assumed that the construction would proceed at a slightly more rapid rate than that finally realised.

Compared to reality, the temperatures built into the model for Çine Dam were on the higher side, taking a conservative view to ensure that the related consequences of thermal gradients were not under-estimated. However, as a consequence, the measured maximum temperatures were generally lower than those modelled, particularly at EL 147.50 mASL.

4.5.9.3. Çine Dam RCC Materials Properties

For the Thermal Analysis of Çine Dam, various important thermal properties for the RCC were determined by laboratory testing at the Middle Eastern Technical University (METU)[7]. The following average values for the important indicated properties were determined:

Coefficient of Thermal Expansion	7.10 x 10^{-6} strain/°C
Elastic Modulus under 5.5 MPa	24.7 GPa
Creep under 5.5 MPa for 1500 hours	110 microstrain
Drying Shrinkage	< 25 microstrain

4.5.9.4. Comparative Analysis Results

The Çine Dam thermal modelling indicated that a period of approximately 50 years would elapse before the effects of the trapped heat of hydration would be fully dissipated. The most immediate effects, however, that could be seen to occur within the first few years of placement was a complete absence of temperature drop within the core of the structure and a movement of heat downwards that caused a rise in temperature at EL 147.5 mASL, for example, of around 1°C by October 2008. While both these effects were observed in the measurements on the prototype, the temperature increase was essentially from 24°C to 25°C on the prototype, compared to 26°C to 27°C on the model, as illustrated on **Figures 4.35** and **4.36**.

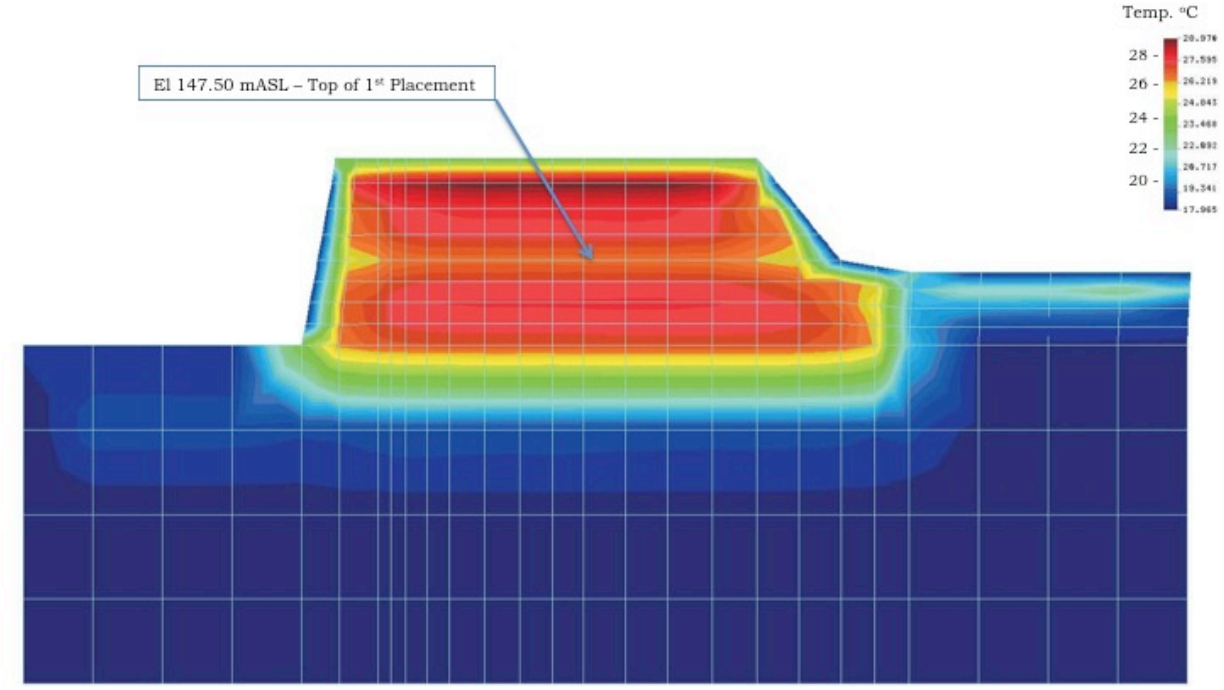

Figure 4.35: Çine Dam Thermal Analysis Temperature Plot – October 2006(9)

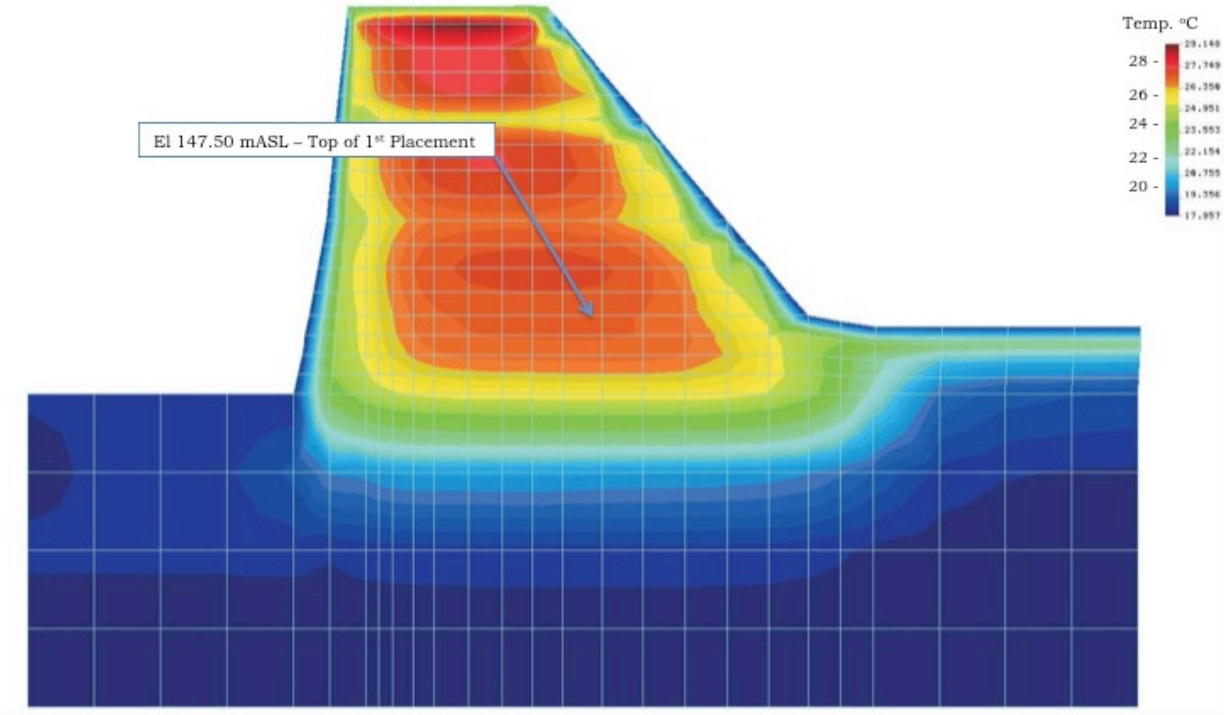

Figure 4.36: Çine Dam Thermal Analysis Temperature Plot – October 2008(9)

At Elevation 185.25 mASL, the modelling predicted a temperature of approximately 26.5°C in October 2008, while the actual measurements reflected temperatures ranging from 25.5 to 27.5°C.

4.6. WADI DAYQAH DAM

4.6.1. GENERAL

The general arrangements of Wadi Dayqah Dam and the layout of the instrumentation installed are described in Chapter 2. In this Chapter, the early thermal behaviour of the RCC structure is evaluated through an analysis of the temperature and induced joint strain/displacement data from placement to March 2009.

4.6.2. INSTRUMENTATION

Due to a relatively restrictive budget and the simplicity of the dam structure, the thermal monitoring instrumentation for Wadi Dayqah Dam was relatively simple, comprising air temperature, water temperature and arrays of concrete temperature meters (termed RTD gauges) at five elevations (El 109.80, 125.00, 140.00 & 155.00 mASL) on two cross sections[11]. In addition, Long-Base-Strain-Gauge-Temperature-Meters (LBSGTMs – sometimes abbreviated to LBSG) were installed across all of the induced joints, approximately in the centre of the cross section at two elevations. The LBSGTMs at elevation EL 135 mASL were installed in mid August 2008 and those at elevation EL 150 mASL were installed in mid October 2008[12].

Figure 4.37 illustrates the basic layout of the important thermal behaviour monitoring instrumentation. The LBSGTMs at EL 135 mASL are located in the centre of the section, at approximately 15 m from the up- and downstream faces, while the LBSGTMs at EL 150 mASL are located at approximately 12 m from either face.

Plate 4.4: Early RCC Placement

4.6.3. IMPORTANT CONSIDERATIONS

In the case of Wadi Dayqah Dam and the interpretation of the installed instrumentation, a number of specific factors of influence must be given careful consideration, as follows:

- The RCC was generally cooled to approximately 24 to 26°C for placement[13], a temperature well below that of the ambient environment;
- The LBSGTMs were installed in the top of a layer, which was approximately at ambient/ maximum hydration temperature, having been exposed to intense solar radiation for 5 to 6 days when the new RCC was placed above;
- Joint inducers were placed in every second layer of RCC, giving rise to a particularly low effective tensile strength across the induced joints;

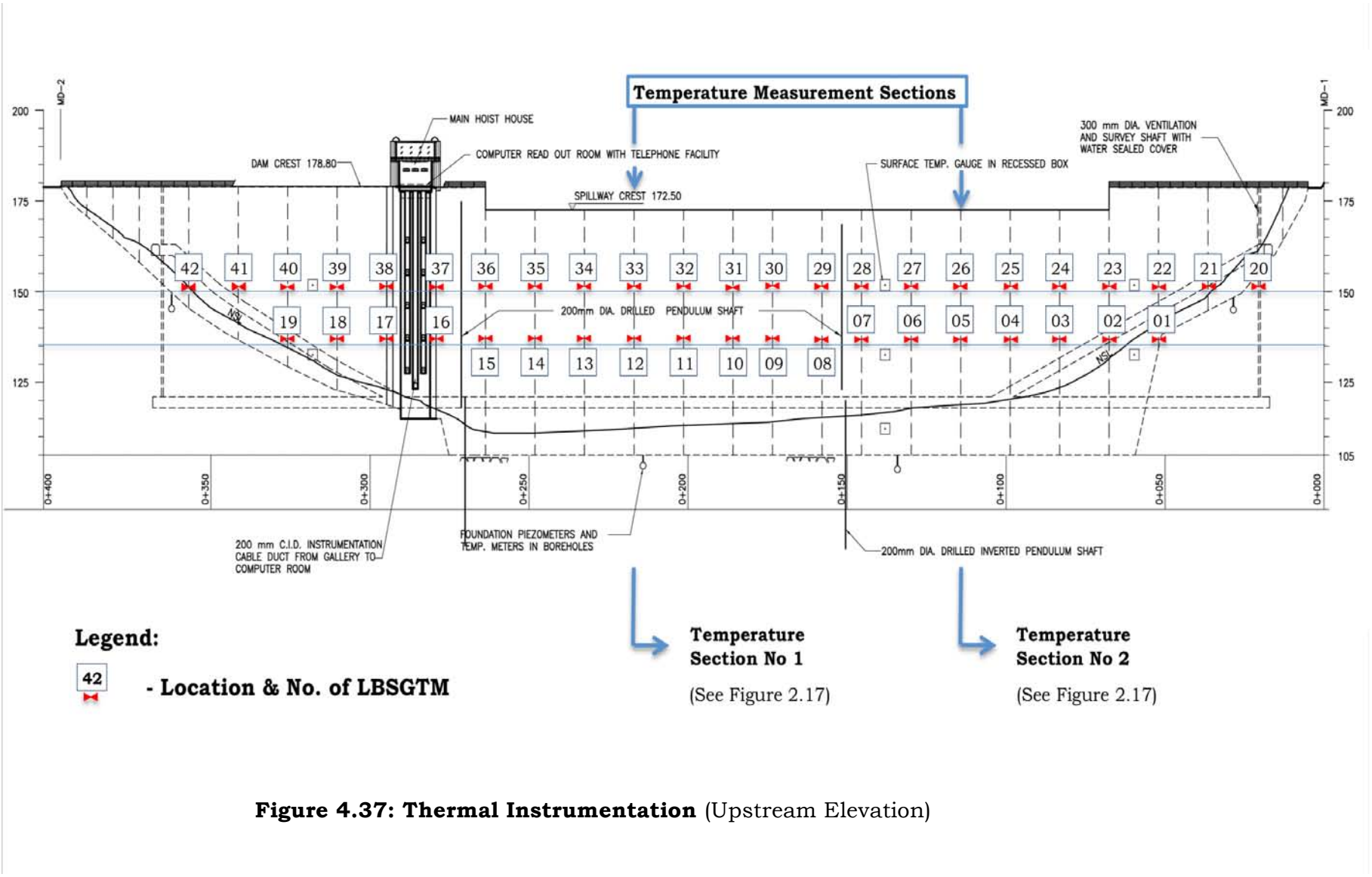

Figure 4.37: Thermal Instrumentation (Upstream Elevation)

- The RCC mix had a low cementitious materials content;
- The RCC mix contained a ground limestone filler material;
- The RCC mix contained crushed natural limestone as part of the sand fraction;
- The RCC mix contained a large proportion of fines;
- The RCC contained a sand/aggregate ratio of 0.44; and
- The aggregates comprised a partially crushed colluvial gravel, which was probably not of the highest quality.

Over the main period of placement between August and October 2008, the daytime ambient temperatures on site typically ranged between 30 and 40°C. From mid October, the ambient temperatures started dropping, indicating a minimum in mid to late January.

As a consequence of the above, several apparently strange behaviour patterns were observed.

When the RCC into which a LBSGTM was installed was particularly warm, the "zero" temperature of the gauge was substantially higher than that of the artificially cooled RCC placed immediately above. By the same token, the RCC immediately around the gauge had experienced expansion stress in the process of its temperature gain from placement. As a consequence, a complex and localised temperature/stress environment was developed. While the gauge was inserted into

Plate 4.5: Wadi Dayqah Dam – May 2009

RCC that had already been heated by the environment and hydration heat, the cooler temperature of the RCC placed above caused the temperature of the gauge and its surrounding concrete to cool rapidly by a few degrees. Thereafter, the hydration heat development in the RCC above started raising the temperature of the concrete around the gauge. As the increasing temperature created expansion/swelling stresses in the newly placed RCC above, the RCC below would have experienced shear stresses, as it effectively acted as a partial restraint against expansion for the RCC above.

This process gave rise to a very different pattern of early behaviour compared to a situation where a gauge was embedded in RCC at a similar temperature to that of the new RCC placed above. In the latter case, the rapid hydration temperature rise caused the gauge, located above a joint inducer, to contract. On the graphs of LBSGTM data for Wadi Dayqah, the above phenomena caused patterns at the different gauges that apparently contradicted each other significantly, with one set of gauges indicating rapid expansion that gradually slowed and another indicating rapid contraction that gradually slowed and in some cases subsequently reversed to expansion.

4.6.4. RCC MIX, MATERIALS & PROPERTIES

As described in Chapter 2, two RCC mixes were specified for Wadi Dayqah Dam; a 15 and a 12 MPa mix. The former mix was specified for the upstream impermeable zone and the toe zone of higher stress. The latter mix was specified for the bulk, core zones in which all of the LBSGTMs were installed.

The Wadi Dayqah Dam RCC mix was unusual in that it was a “high-paste” RCC that contained only 112 kg/m^3 of cement combined with 48 kg/m^3 of ground limestone filler, in the case of the Zone 2, 12 MPa mix. Furthermore, the crushed sand was blended with 34% crushed limestone. The resultant RCC mix contained over 13% fines and over 26% of the RCC material was finer than 1.2 mm. The mix further indicated a rather high sand content, with a sand/aggregate ratio of 0.44. Treating the ground limestone as a non-cementitious filler, the Zone 1 and 2 RCCs indicated w/c ratios of 1.02 and 1.11, respectively.

On the basis of an extensive programme of core extraction and testing, the in-situ properties listed in **Table 4.5** were determined for the two RCC mixes[13].

Table 4.5: Average RCC Properties measured on Cores (90 days age)[13]

Parameter		**RCC**	
		15 MPa (Zone 1)	**12 MPa** (Zone 2)
Compressive Strength (MPa)	90 days	15.3	14.2
	365 days	20.3	17.0
Tensile Strength (MPa) - 90 days		1.10	0.81
Permeability (m/s)		3.1×10^{-11}	4×10^{-8}
Direct Shear Strength (MPa)		1.80	1.16
Modulus of Elasticity (GPa) – 365 days		23.5	20.8
Poisson's ratio		0.15	0.1
In-situ Measured Density (kg/m^3)		2420	2428
Vebe Time (seconds)		14 - 15	12 - 13

4.6.5. TEMPERATURE DATA

4.6.5.1. Heat of Hydration

Theoretical calculations for the adiabatic heat of hydration, based on the anticipated cement and aggregate characteristics, indicated an anticipated temperature rise of 13.5°C for the Zone 1 RCC and 12.5°C for the Zone 2 RCC, respectively. The temperature data recorded within the dam would suggest that these figures over-estimate the actual situation by up to 2°C, suggesting that the Omani cement used was probably a relatively low heat material.

4.6.5.2. Measured Temperatures

The RCC temperatures were measured using resistance thermal detectors (RTDs) at four separate elevations on two different cross-sections on the dam wall, as illustrated on **Figure 4.37**. **Figures 4.38** to **4.43** illustrate the temperatures recorded to March 2009 on each of these levels, at both cross-sections.

In **Figure 4.38**, a significant delay between the installation of the temperature meters at Sections 1 and 2 can clearly be seen. Furthermore, the placement temperature was evidently substantially higher at the latter section.

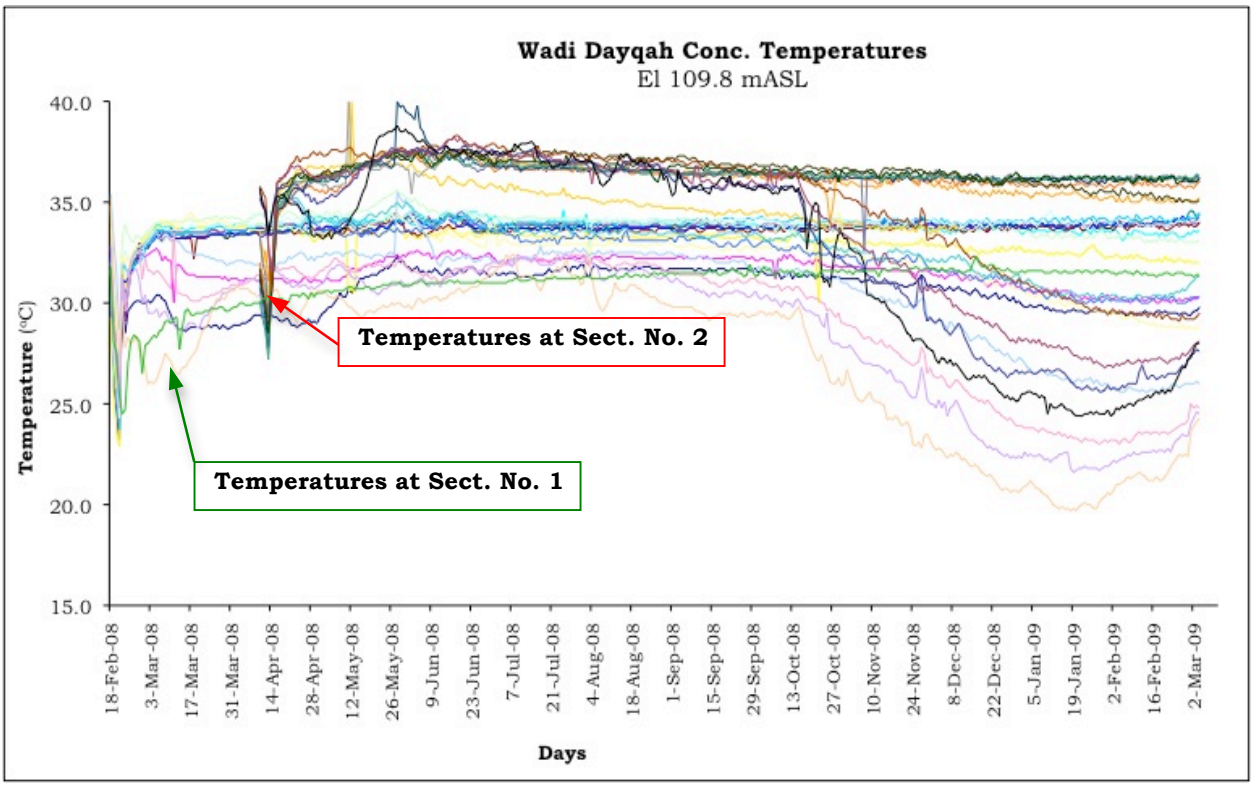

Figure 4.38: Temperatures Measured on RTD Gauges at EL 109.8 mASL(12)

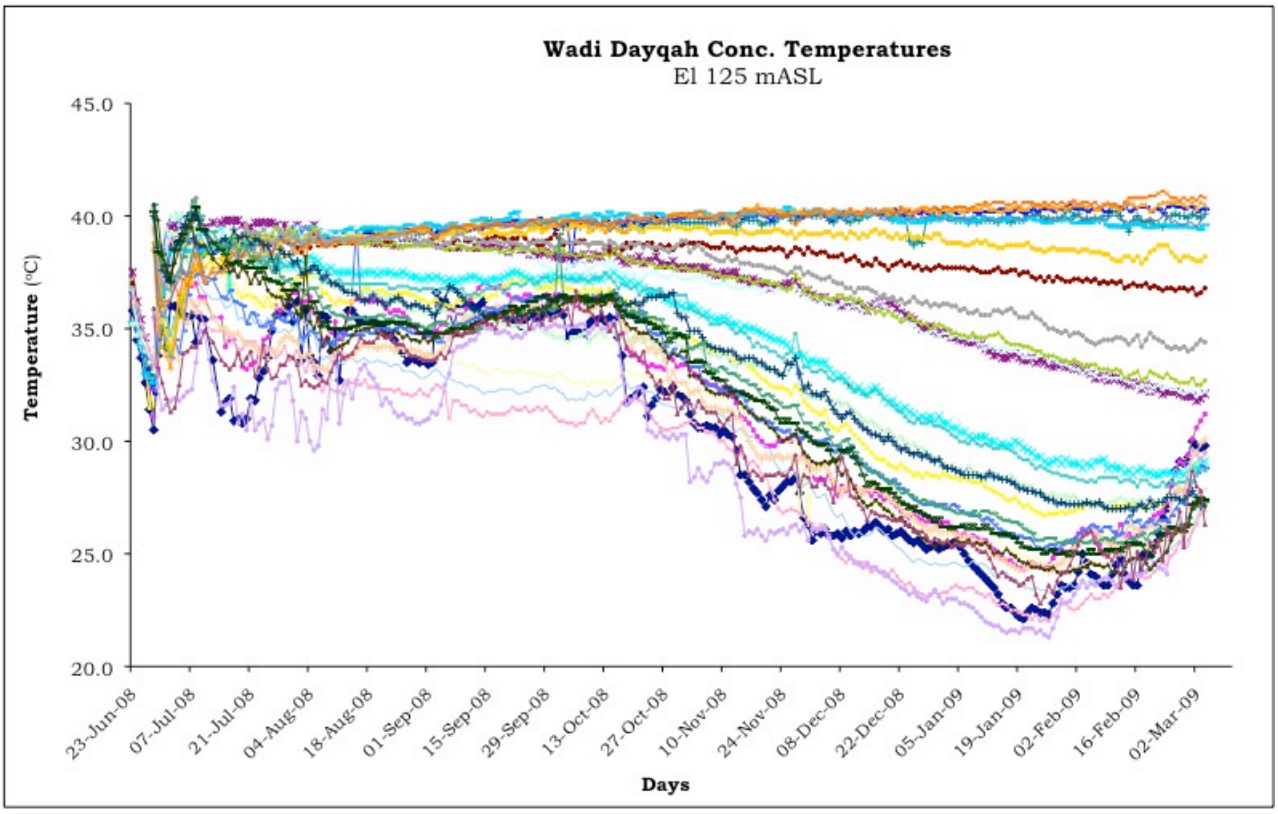

Figure 4.39: Temperatures Measured on RTD Gauges at EL 125 mASL(12)

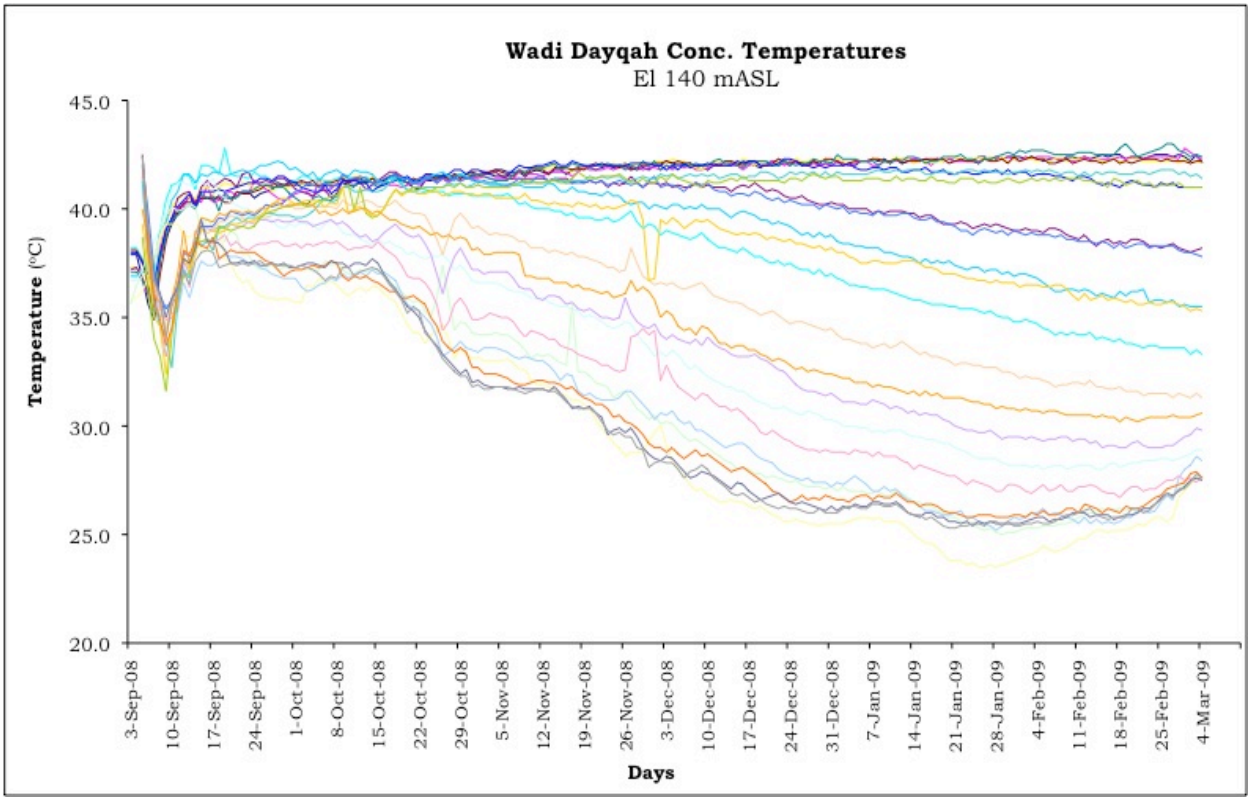

Figure 4.40: Temperatures Measured on RTD Gauges at EL 140 mASL(12)

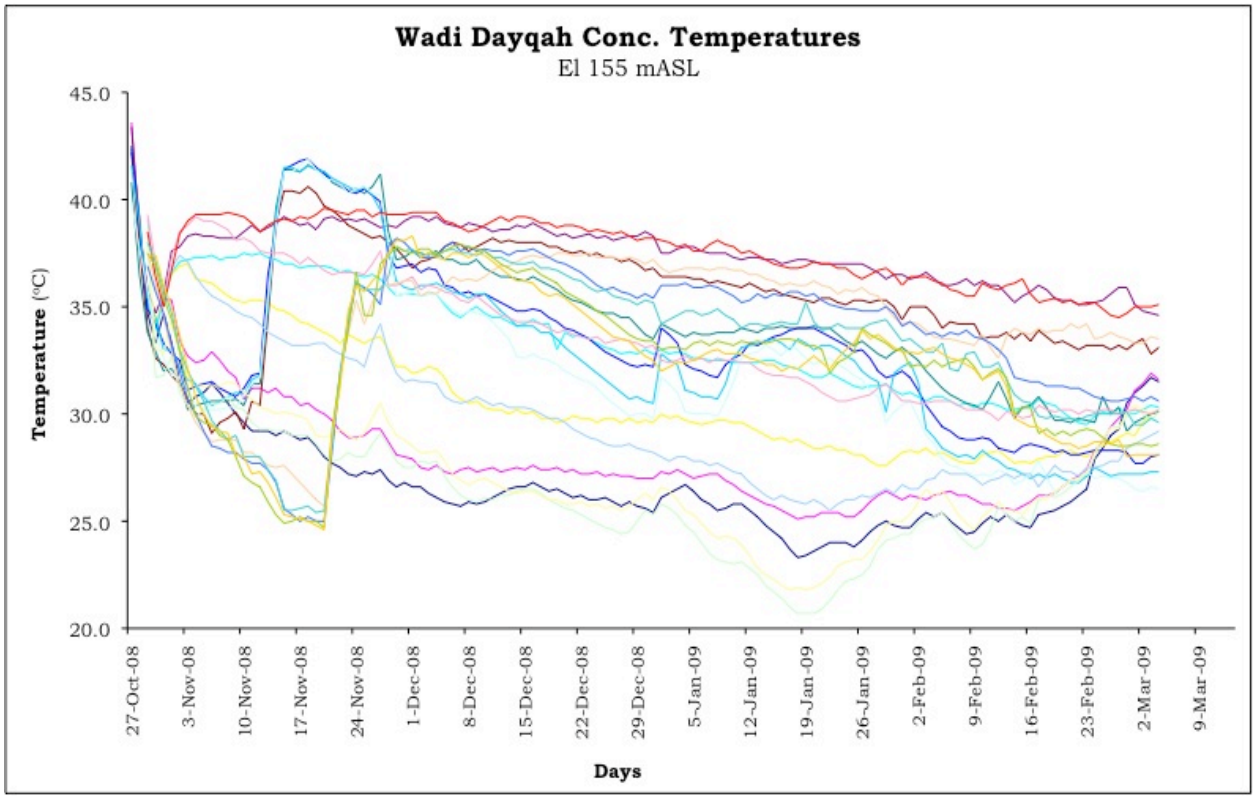

Figure 4.41: Temperatures Measured on RTD Gauges at EL 155 mASL(12)

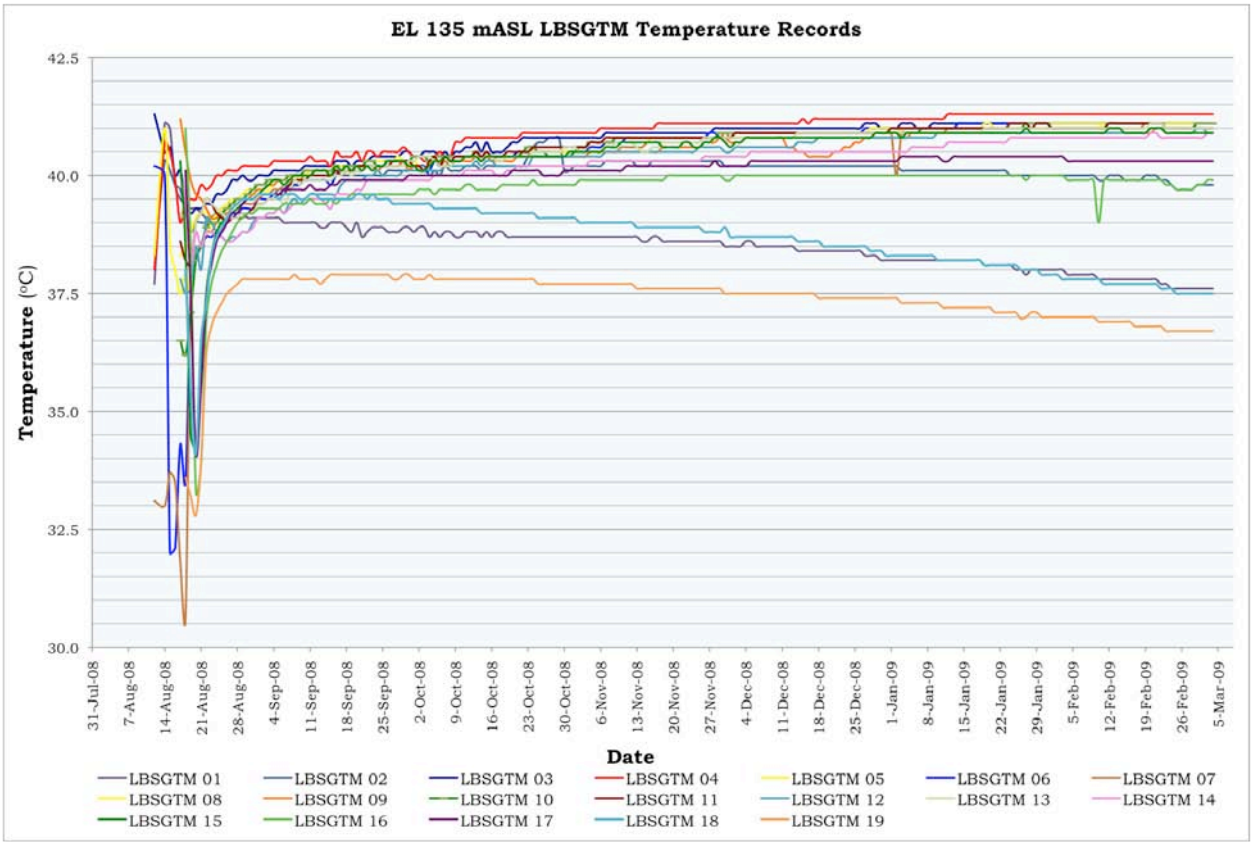

Figure 4.45: Temperatures on LBSGTM Gauges at EL 135 mASL(12)

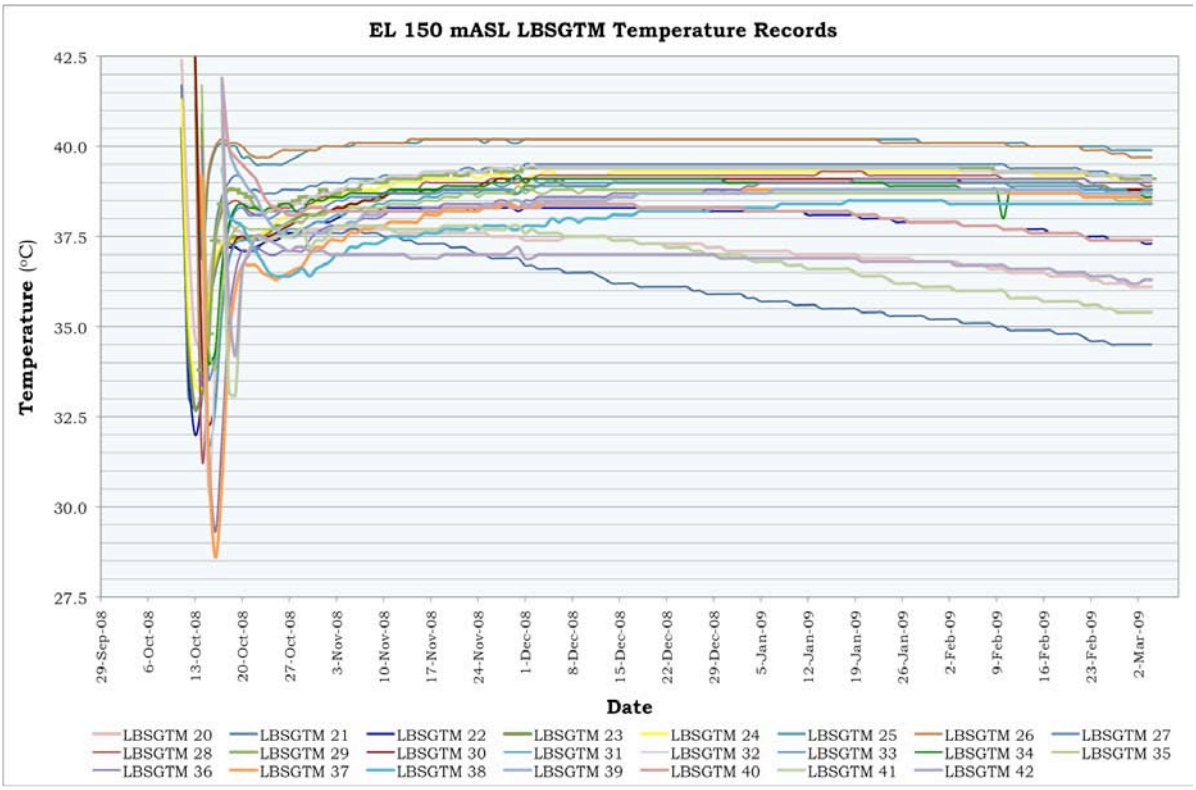

Figure 4.43: Temperatures on LBSGTM Gauges at EL 150 mASL(12)

4.6.5.3. Discussion of Temperature Patterns

The observed temperature patterns are generally consistent with expectations. Where the section is relatively wide, temperatures are either maintained at their hydration peak, or were still climbing slowly in March 2009. Where the section is thinner, closer to the faces and close to the foundation, the temperatures had started to drop from peak. Close to the dam faces, the hydration heat had already been dissipated and the temperature was observed to follow the external ambient patterns.

At El 109.8 mASL, the temperature gauges (RTDs) placed in the core zone of the dam on the first instrumentation section, where the foundation level is deeper, can be seen to be indicating a continuing rise in temperature. On the second section, where the temperature gauges (RTDs) are located only a few metres above the foundation, the opposite trend can be perceived, with the temperatures gradually dropping as a result of the proximity of the cooler foundation rockmass. At El 125 mASL and El 140 mASL, on the other hand, the temperature of all core zone RTDs can be seen again to be slowly rising. At El 155 mASL, not only is the section substantially narrower, but all of the RTDs are essentially in the surface zone and, unsurprisingly, it can be seen that the temperatures are quickly influenced by the cooler external ambient conditions.

On the LBSGTMs, the temperature patterns are similarly in accordance with expectations, with the core temperatures at the lower elevation continuing to rise slowly, except where close to a cooler foundation. At El 150 mASL, the thinner section can be seen in the fact that the temperatures appear to have peaked and were starting to drop by March 2009. Again, on either abutment, the influence of the proximity to the foundation could clearly be determined, with the temperatures generally becoming more depressed with time, the closer to the cooler rockmass.

Two specific peculiarities, however, could be determined from the recorded temperature data. Firstly, the placement of significantly cooled RCC could be determined in the initial drop in temperature measured on all of the installed instruments. Secondly, the apparent hydration temperature rise, after this initial drop, never exceeded 10°C and was quite often significantly less.

4.6.6. LBSGTM Deformation Readings

4.6.6.1. General

Deformations were recorded on LBSGTMs across each of the joints at two elevations, as described earlier. All of these instruments proved to be reliable, although oscillations of the readings of as much as 0.1 mm were frequently observed. Whereas the deformation patterns generally evident were quite different from those observed on other dams addressed in this study, Wadi Dayqah is the

only dam investigated for which the RCC was significantly artificially cooled well below ambient temperature for placement, while it is also the only lean RCC considered in this investigation.

4.6.6.2. LBSGTM Behaviour at El 135 mASL

The deformations measured on the LBGTMs at El 135 mASL from installation to March 2009 are illustrated on **Figure 4.44**. The same deformations are presented again, but separated into the gauges close to the abutment on **Figure 4.45** and those remote from the abutment on **Figure 4.46**.

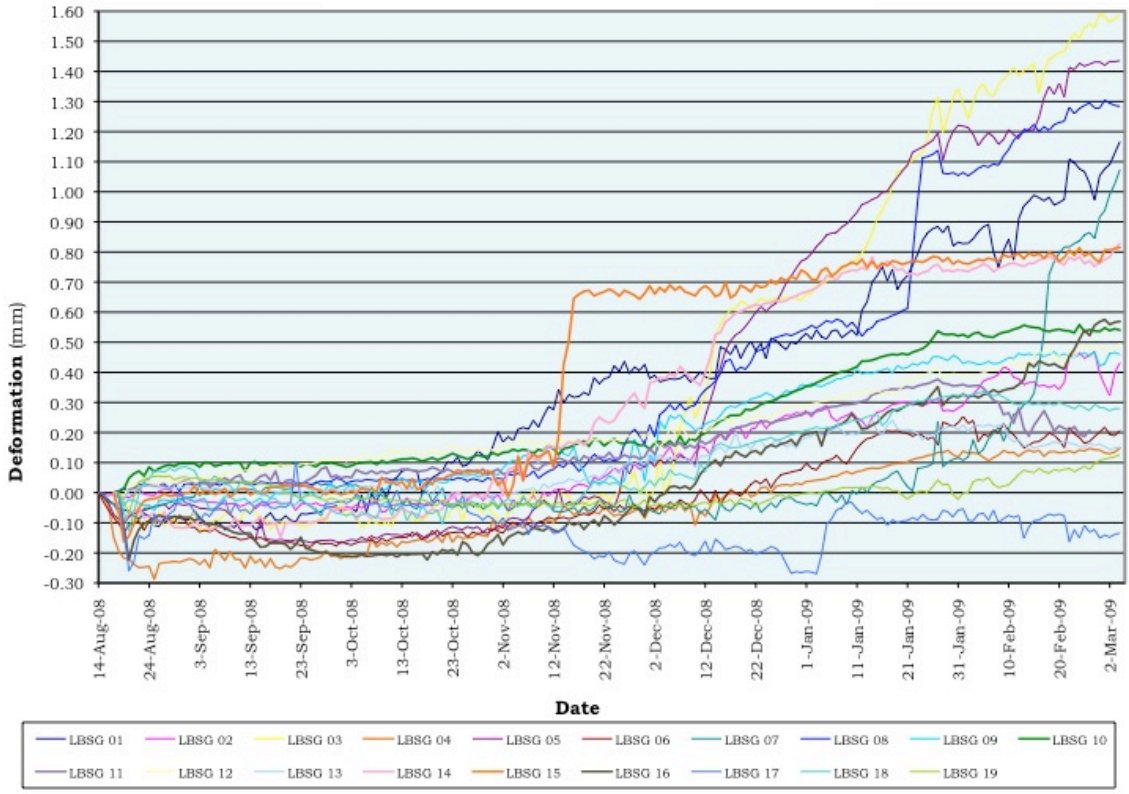

Figure 4.44: LBSGTM Deformation Measurement at EL 135 mASL(12)

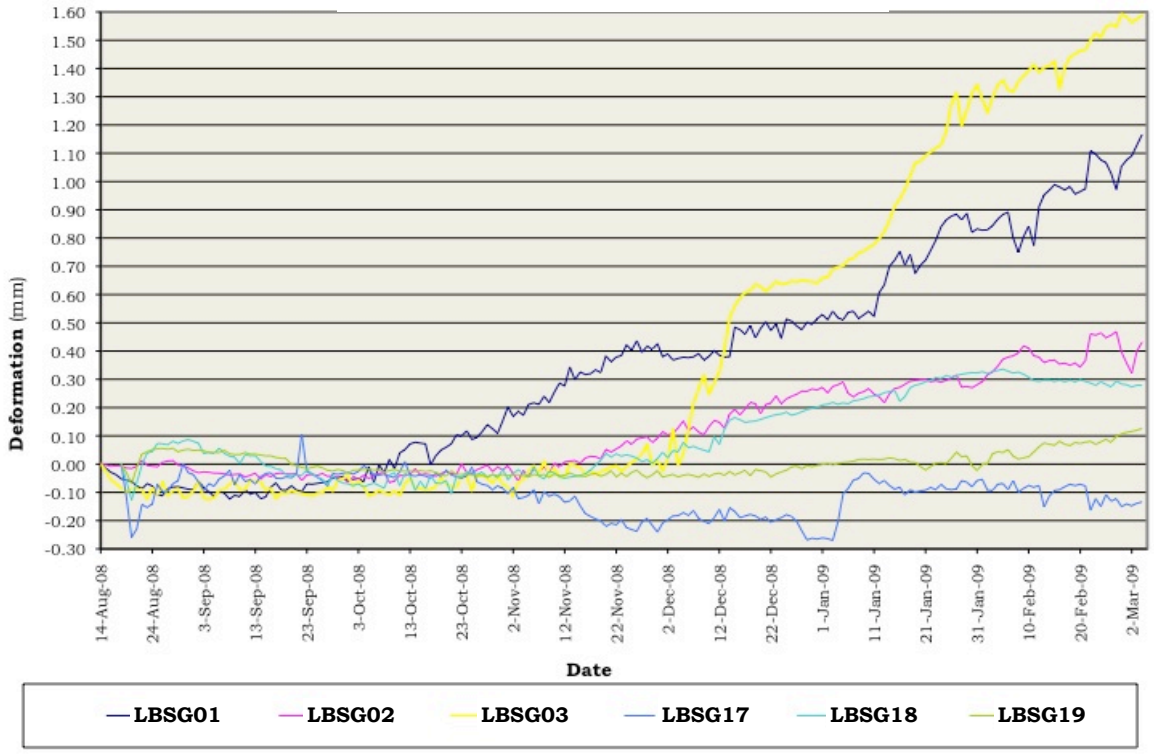

Figure 4.45: LBSGTM Deformations at EL 135 mASL Closer to Abutments(12)

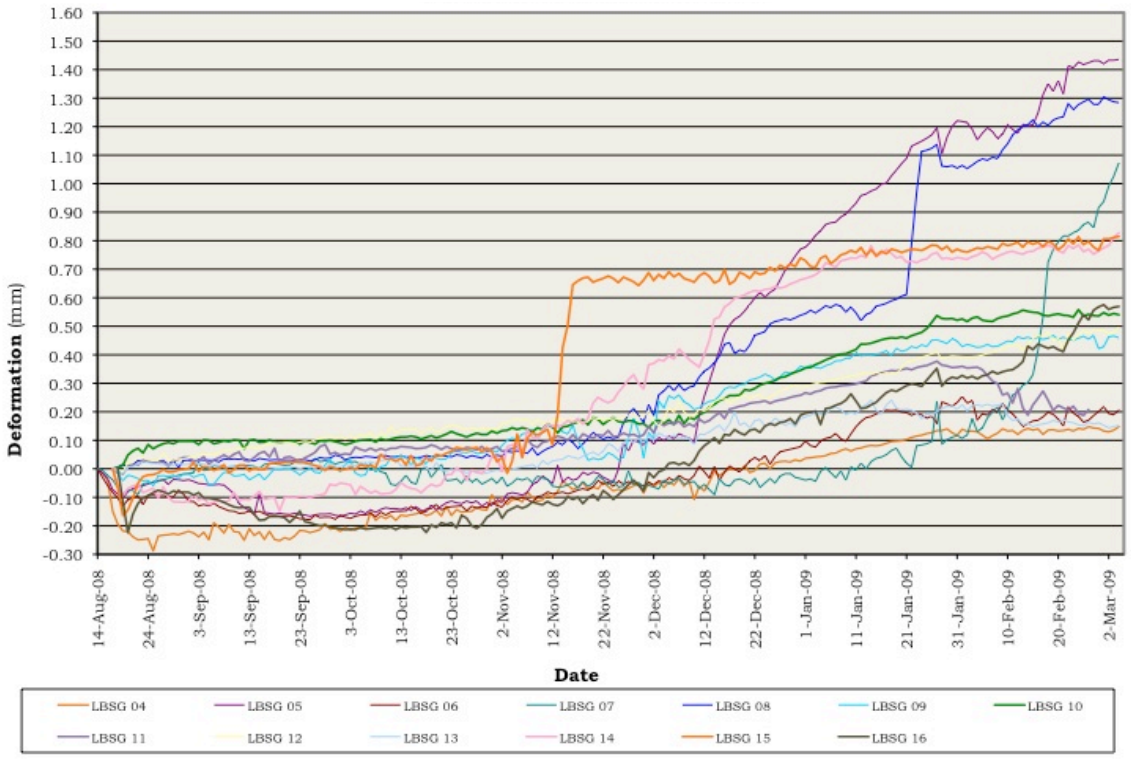

Figure 4.46: LBSGTM Deformations at EL 135 mASL Remote from Abutments(12)

At El 135 mASL, the temperature of the core LBSGTMs (LBSG gauges) was generally still rising very slowly by March 2009. The exceptions were the gauges at either end, closest to the abutments, where temperatures had fallen by as much as 2°C.

The most significant issue in respect of the LBSGTMs installed at El 135 mASL is the fact that it is not possible to determine distinctive and predictable patterns that are repeated. The gauges on the abutments at the right side of the dam (LBSG 01, 02 & 03 on Figure 4.45) indicated significant expansion/cracking, still increasing in March 2009, while the gauges on the left abutments indicated little, or no expansion at all (LBSG 17, 18 & 19 on Figure 4.45).

Certain of the LBSGTMs indicated very obvious cracking, while others demonstrated the steady development of strain. Of the 19 gauges installed at El 135 mASL, 16 indicated a very distinct levelling-off of the expansion strain by March 2009, while the remaining 3 (1 centrally located & 2 on the abutments) indicated continued expansion. Over December 2008 and January 2009 the majority of the gauges indicated fairly linear expansion at approximately the same rate.

The measured total maximum expansion across all the gauges sums to 11.5 mm.

4.6.6.3. LBSGTM Behaviour at El 150 mASL

The deformations measured on the LBGTMs at El 150 mASL from installation to March 2009 are illustrated on **Figure 4.47**. The same deformations are presented on the following two figures, with the gauges close to the abutment on **Figure 4.48** and those remote from the abutment on **Figure 4.49**.

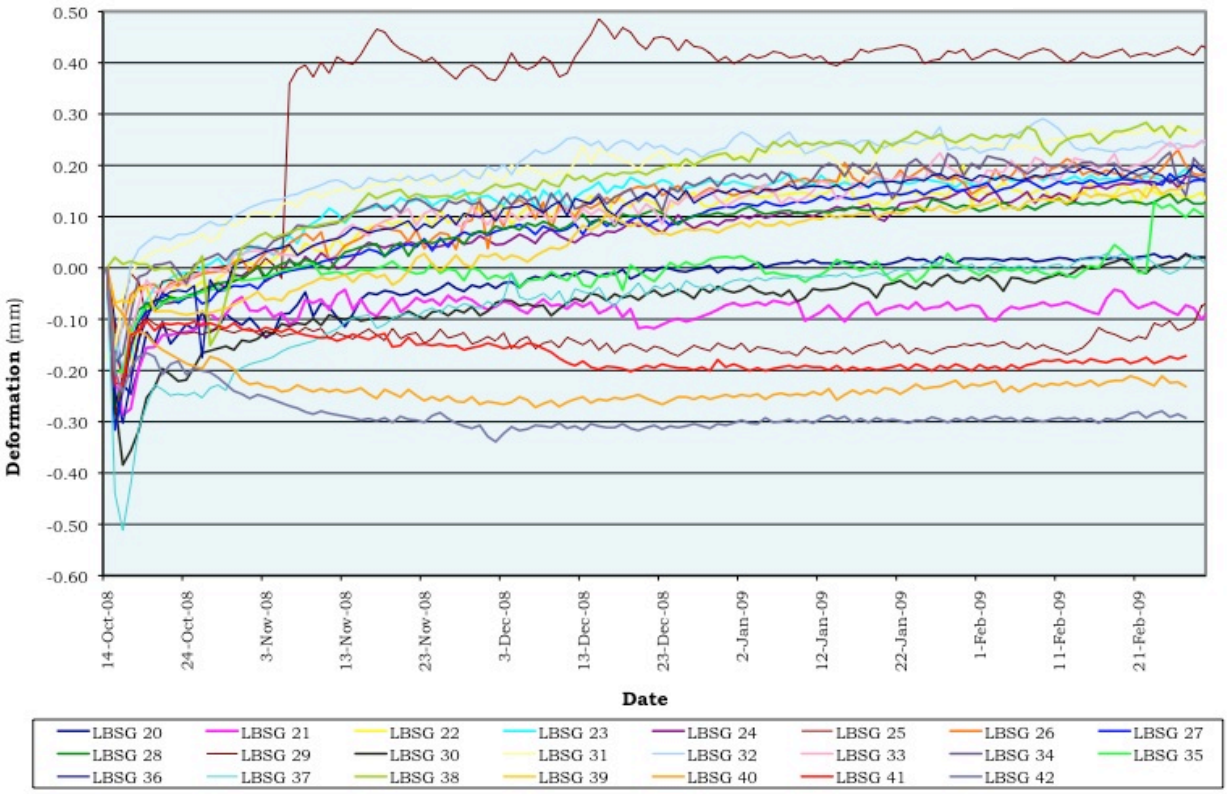

Figure 4.47: LBSGTM Deformations Measurement at EL 150 mASL(12)

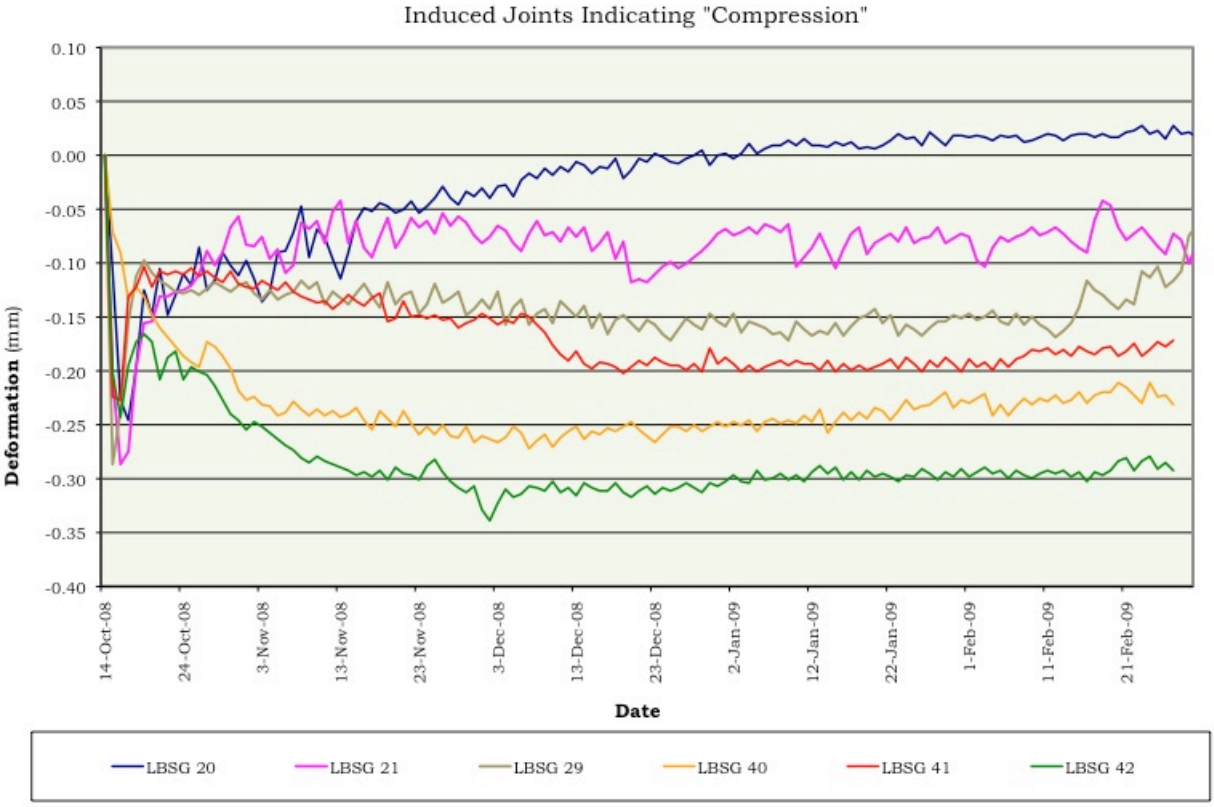

Figure 4.48: LBSGTM Deformations at EL 150 mASL Closer to Abutments(12)

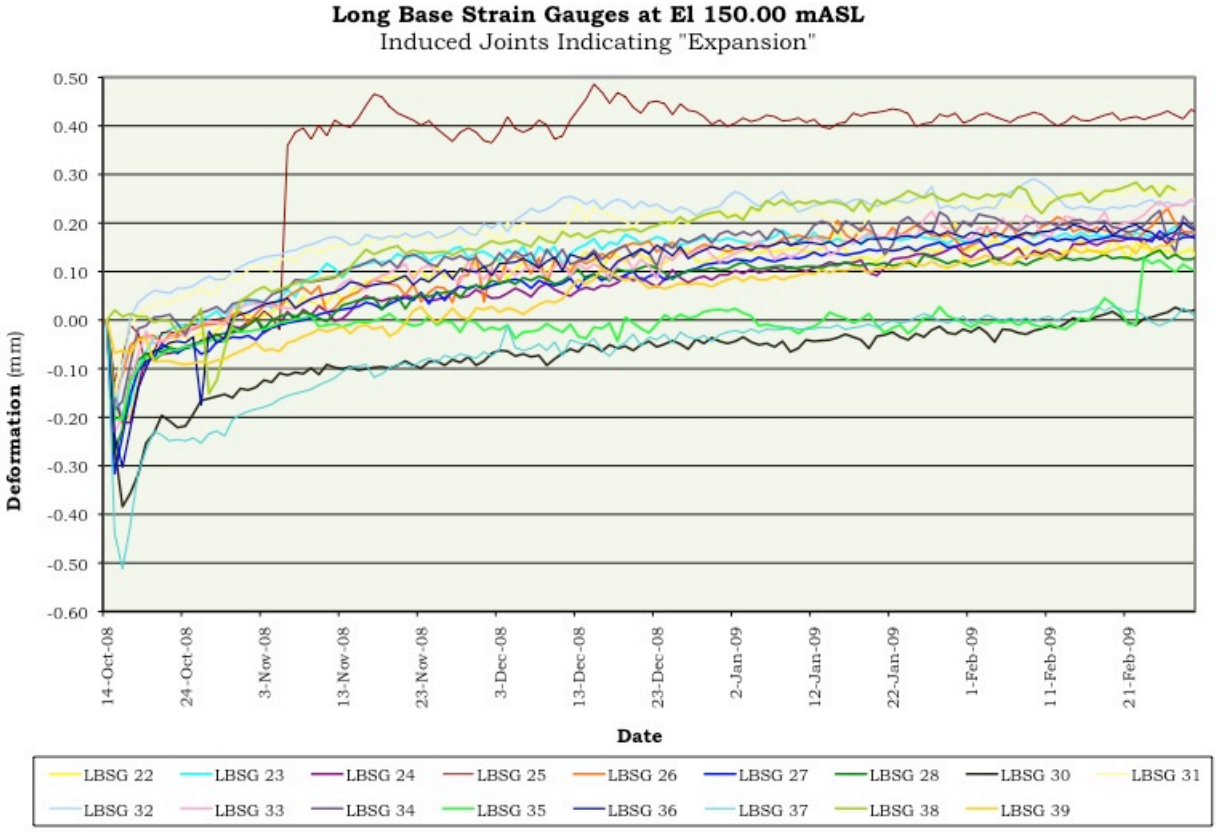

Figure 4.49: LBSGTM Deformations at EL 150 mASL Remote from Abutments(12)

The LBGTMs at El 150 mASL indicate a pattern of compression where close to the abutments and expansion away from the abutment rockmass. Similarly to the gauges at El 135 mASL, a pattern of greater compression/joint closure is evident on the gauges on the left abutment (LBSG 40, 41 & 42 on Figure 4.48), while a greater tendency towards expansion/joint opening can be discerned on the right abutment (LBSG 20 & 21 on Figure 4.48). While this situation might seem difficult to understand, it is important to take note that although the majority of the gauges, and the top of the previous RCC layer, were exposed to severe solar radiation for a period of 5 to 6 days before the cooler RCC was placed on top, four gauges at El 150 mASL were in fact installed immediately before new RCC placement. **Figure 4.50** illustrates the deformation histories for these gauges.

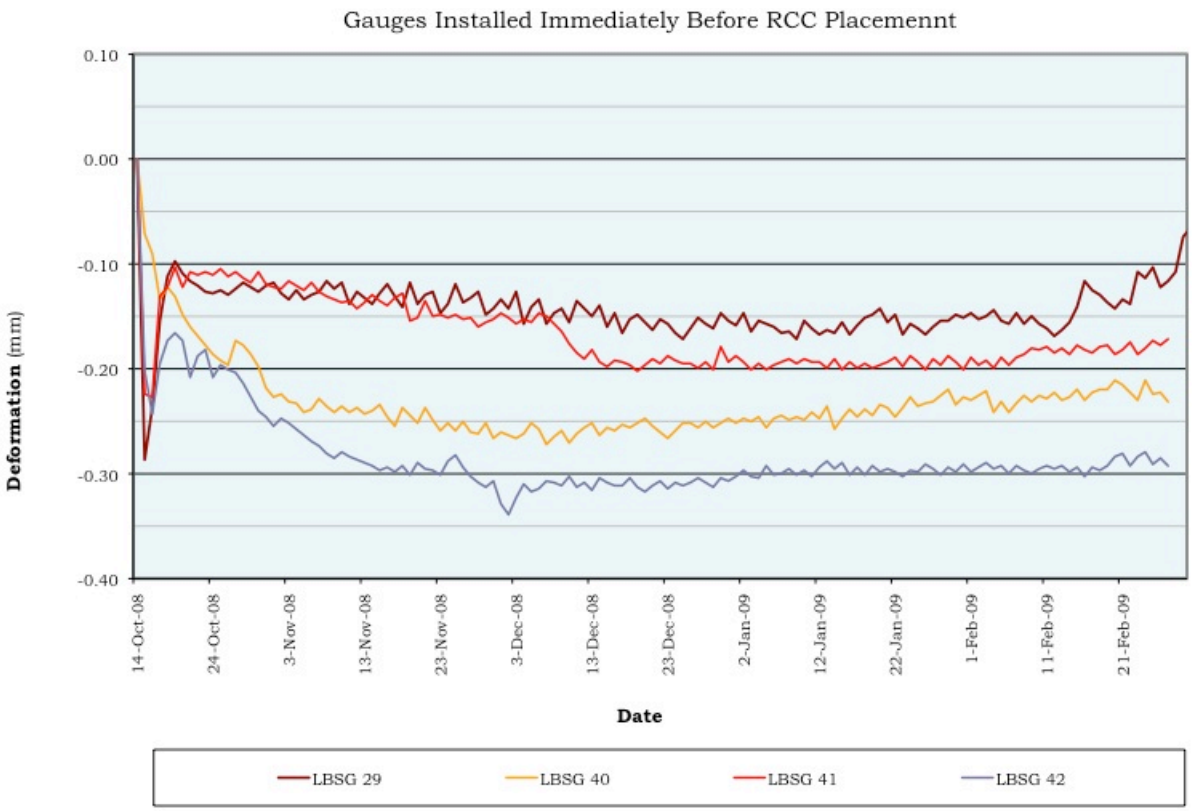

Figure 4.50: Deformations on LBSGTMs Installed Shortly Before New RCC(12)

A particular point of interest lies in the fact that the above gauges all remained in compression and behaved in a manner much more similar to that of the gauges installed at other dams where significant RCC cooling was not applied.

The deformations of all gauges at El 150 mASL have apparently arrived at a point of greater stability/finality than have the gauges at El 135 mASL, despite the older age of the concrete in the latter location. While the gauges on the abutments indicate no real joint opening in this area, the total maximum displacements/joint openings across the other induced joints sum to approximately 3.25 mm.

4.6.7. DISCUSSION OF FINDINGS

4.6.7.1. General

While some of the LBSGTM gauges indicated the development of cracks exceeding 1 mm, no signs of the same effects have become evident on the surface of the dam. If these readings were a real reflection of the general development of RCC shrinkage, this would have been expected to have been manifested in significant cracks at the induced joints on the dam surface. It is of course possible that such surface cracking will become apparent during the next cool period in December/January.

The low tensile strength across the joints was demonstrated in most instances by a gradual opening deformation being registered on the LBSGTM gauges. On only four gauges at El 135 mASL and one at El 150 mASL was the rapid development of a "crack" clearly evident.

The "expansion" measured on the majority of the LBSGTMs can only relate to the shrinkage of RCC blocks (between induced joints) away from each other. If the gauges were measuring general shrinkage strain in the RCC, they would contract, as opposed to expand, while if the gauges were subject to a swelling associated with temperature rise, thy would either contract across the more compressible induced joint, or remain unchanged, with the expansion strain being converted to restrained compressive stress. With an induced joint spacing of just 15 m, this implies that a relatively high level of confidence can be ascribed to the fact that all of the RCC shrinkage is measured on the installed gauges.

It is very significant to note that significant opening of a crack (> 0.5 mm) was indicated at El 135 mASL on induced joint Nos 4, 6, 8, 10, 11, 12, 13, 15, 17, 18 and 19 and at El 150 mASL only really on induced joint No 7. It is, however, equally significant to note that the gauges that were not installed into an environment of divergent temperatures behaved quite differently and in a similar manner to the instruments at the other dams that form part of this study.

4.6.7.2. Discussion

In the core zone of the RCC at El 150 mASL, it is apparent that the temperature is still being fairly constantly maintained at the peak hydration temperature. The exceptions to this observation are the areas at each end of the dam, where the cooler adjacent foundation has started to bring the temperatures down by as much as 3°C. On the LBSGTMs close to the foundations, this temperature reduction is starting to give rise to slight reduction in compressive strain.

As mentioned under 4.6.3 above, a specific behaviour pattern was observed wherever the temperature of the RCC into which the LBSGTMs were installed was substantially below that on the artificially cooled RCC placed immediately above. This situation was further exacerbated in most instances by the fact that the subsequent temperatures experienced in these gauges never exceeded the original "zero" temperature of the gauge. In relation to this apparent pattern, it is considered important to understand that it is very much the behaviour of the RCC in the layer beneath that is being monitored in this instance, as opposed to the fresh RCC that is placed above.

On the gauges where foundation restraint and temperature influence were not significant, it is clear that the gauges returned to their "zero" expansion at a lower temperature than that at which "zeroed". The reason for this observation cannot be determined with certainty. Should creep have occurred in the cooled RCC, the "zero" expansion should only have been reached at a temperature above, rather

than below, the "zero" temperature. It is accordingly considered that this effect arises as a result of micro adjustments in the green concrete, as a consequence of the fact that the cooling happened very rapidly, over a period of between 1 and 3 days, while the re-warming took place over a period of around a month.

It is also considered important to note that the apparent process of slow expansion that continued after the maximum hydration temperature was reached does not demonstrate any abrupt change when the state of zero deformation is reached. If the gauge and its surrounding concrete was rapidly cooled and consequently shrank, it would be expected that it would expand easily with increasing temperature until its original volume state was reached, after which the expansion forces would be resisted by the compressive strength of the concrete and expansion would abruptly diminish. The fact that the expansion appears to be gradually and very slowly diminishing is consequently considered to be a sign either of the fact that the induced joint is opening, or it is a consequence of the fact that the temperature experienced never reaches the "zero" temperature of the gauge and the surrounding RCC at the time the new RCC was placed above.

In all instances where the "zero" temperatures of the gauges were not significantly above the temperature of the new RCC, or when an obvious cracking occurs on the induced joint, no ongoing expansion is evident and the behaviour is as expected. However, it is important to take cognizance of the fact that the gauges in question were also located close to the foundation, where the restraint against movement will be greatest.

4.6.7.3. Quantitative Evaluation

General

Should RCC have behaved like conventional concrete, it would have demonstrated a combined shrinkage and creep of around 200 microstrain over a period of probably around 6 months. With no cracking at the induced joints, this would have been manifested on the LBSGTMs as an expansion of approximately 0.14 mm. If all of the movements were concentrated at the induced joints, the gauges would have indicated a net expansion of 3 mm across each of the induced joints.

LBSGTMs at EL 135 mASL

The measured total maximum expansion across all the gauges sums to 11.5 mm, implying an average opening of approximately 0.6 mm per induced joint, which translates into an average shrinking strain of approximately 43 microstrain. Three of the gauges indicated some ongoing crack development in March 2009; two very minor, one quite significant. If we assume a further 0.5 mm for the former and 0.2 mm each for the latter two, total shrinkage strain would still be less than 50 microstrain.

LBSGTMs at El 150 mASL

It is further important to note that the apparent expansion indicated on the LBSGTM gauges at El 150 mASL cannot be representative of the behaviour of the RCC between the induced joints. If this was the case, it would imply that the dam is expanding between its abutments by 165 microstrain and that the dam has increased in length by approximately 50 mm. Should it be possible to make any interpretation of the indicated expansions, it would be necessary to assume a worst-case scenario of the dam shrinking, due to autogenous/drying shrinkage and/or creep, and the induced joints accordingly opening to accommodate this process. This is considered to be a conservative assumption at best and unrealistic at worst as a consequence of two factors; namely, the fact that this behaviour is not evident at all on the gauges where the substantial temperature differences were not noted and secondly because, it appears that some slippage has occurred between the gauge and the green adjacent concrete during the process of rapid cooling when the cold new RCC was placed on top.

Reviewing this, possibly unrealistic, worst-case scenario would indicate a cumulative joint opening of approximately 3 mm across the central 19 blocks of the dam wall, which translates into a shrinkage strain of approximately 11 microstrain. If this shrinkage strain is a reality, it would probably represent a creep, as the temperature was maintained at its peak within the core of the dam over the applicable period. It is, however, possible that some form of drying shrinkage is occurring as the aggregates release the significant quantity of moisture absorbed during mixing of the RCC.

Summary

Although a similar shrinkage is apparently demonstrated at both LBSGTM installation levels, the extent of shrinkage is quite different. While it might be to be expected that the shrinkage would be greater at the gauges installed earliest, in the evaluation the shrinkage appeared to have in fact fully stabilised at the gauges at El 150 mASL, despite the fact that the temperatures were starting to drop by March 2009, but not completely at the gauges at El 135 mASL. This suggests that the cause of the shrinkage must, at least partly, be caused by some variation in materials characteristics.

4.6.7.4. Behaviour Hypothesis

Taking cognizance of the above discussion, it is considered that the behaviour of the LBSGTMs installed in Wadi Dayqah Dam relates primarily to two significant factors; firstly, the complex temperature/strain field that was set up between the placed and new RCC as a result of the significant RCC cooling applicable and secondly, some autogenous/drying shrinkage of the RCC.

It is considered most likely that the instrument readings, for the gauges away from foundation restraint, are reflecting the following behaviour scenario:

- The LBSGTMs were installed in placed RCC, where the temperature had already risen to its hydration peak. Zero strain was accordingly linked to the peak hydration temperature, while the RCC whose behaviour the gauge was intended to measure experienced zero stress at a substantially lower temperature;
- The temperature of the gauge and the surrounding RCC was dropped by between 5 and 12°C by the influence of the cooler RCC above. The gauge and the RCC across the joint shrank by between 200 and 400 microstrain, with particularly intense shrinkage occurring at the gauge due to its location immediately above a crack inducer.
- As the temperature of the RCC above rose, the RCC below acted as a partial restraint against the thermal expansion of the RCC above and it accordingly experienced expansion forces that would again have been exaggerated at the gauge by the tensile weakness in the induced joint below.
- Once the RCC above and below had reached their peak hydration temperatures, no further movement on the LBSGTMs would have been observed until the temperatures started dropping, unless some shrinkage/compression creep occurred. In view of the measured expansion while the peak temperatures were sustained, it is evident that a certain amount of creep/shrinkage in the Wadi Dayqah RCC has occurred.

4.6.7.5. Summary

Because the LBSGTMs were installed in RCC at it maximum hydration temperature, the measured shrinkage/creep could be observed. Should the gauges have been installed in the RCC at its placement temperature, constrained compression of the gauges would have masked the shrinkage until the temperature had dropped well below the peak hydration temperature. Considering the temperature flows and the consequential restraining and expanding forces, it is not considered possible that any real conclusions can be drawn in respect of the early shrinkage/creep behaviour of the RCC at Wadi Dayqah. It is considered, however, on the basis of these effects that assuming that all of the measured expansion strain can be ascribed to shrinkage/creep of the RCC under thermal expansion would be rather conservative.

It must also be borne in mind that the Wadi Dayqah RCC was a lean mix material with relatively low strength, a high w/c ratio and a high sand/aggregate ratio. Furthermore, the mix contained a very high percentage of non-cementitious fines. Considering the fineness of the aggregate/materials used, the high w/c ratio that might have resulted in excess water (not being used in hydration) being lost to

drying shrinkage, the high aggregate moisture absorption and the use of a partially crushed gravel aggregate, for which the paste/aggregate bond may not have been particularly strong, the Wadi Dayqah Dam RCC is likely to have been more susceptible to shrinkage and creep than other, higher strength RCCs investigated as part of this study. In an exposed environment, a conventional structural concrete using fine limestone filler might indicate an autogenous and drying shrinkage of around 450 x 10^{-6}[14]. Accordingly, while the origin of the measured deformations cannot be ascertained with any certainty, even in the worst-case scenario of all of the measured deformations being attributable to autogenous/drying shrinkage/creep, the maximum measured shrinkage is almost certainly substantially less than would be the case for a conventional concrete using a limestone filler in the core of a dam.

The De Mist Kraal weir in South Africa was constructed with a low cement content RCC mix[15], but high quality aggregates and this structure exhibited no detectable cracking of any significance. It is accordingly considered that the observed behaviour of the Wadi Dayqah Dam RCC is significantly more likely to relate to the aggregate quality and the high fines content than the low cement content.

4.6.7.6. Reliability & Consistency

The temperature readings at Wadi Dayqah Dam are consistent and comply with expectations. Consequently, a high degree of reliability can be ascribed to this data and a high level of confidence can be placed in the temperature distributions and the ongoing cooling process. The deformation readings from the LBSGTMs on the other hand present the opposite scenario. The pattern of behaviour is not generally consistent with that evident at any other dam for which the author has data and the indicated behaviour is quite different at each of the two elevations at which the gauges were installed.

Together with the possibility of poor aggregate performance, the complexity of the temperature flows and the respective constraining forces and the consequential data uncertainties realistically imply that any meaningful quantitative analysis of the gauge measurements is not possible.

4.6.7.7. Value of Results

The data from Wadi Dayqah Dam is of significant value, as it suggests that RCC is not immune to shrinkage/creep, confirming the findings of others in respect of lean RCC. While only qualitative analysis is realistically possible, it remains of value to observe that even in the case of an RCC mix that is relatively susceptible to shrinkage, the total creep/shrinkage strain remains very significantly less than that assumed in terms of traditional RCC materials models.

4.6.8. CONCLUSIONS

4.6.8.1. General

On the basis of an analysis of the temperature and deformation data measured for Wadi Dayqah Dam, it can be stated that some shrinkage in the RCC was evident, although it cannot be known with any certainty how much was due to autogenous shrinkage, drying shrinkage or creep. As a consequence of the continued development of shrinkage once the RCC was experiencing tension, it is considered most likely that its primary origin lies in autogenous or drying shrinkage, as opposed to creep under stress. However, the total early shrinkage was less than 50 microstrain and substantially less than would be assumed on the basis of a traditional RCC materials model. The Wadi Dayqah Dam RCC contained a high proportion of fine aggregates, a high content of non-cementitious fines and a high w/cement ratio. The aggregate quality, shape and surface texture may also not have been ideal, while the high moisture absorption of the aggregates may indicate a tendency for drying shrinkage. It is considered that these factors are the primary reason for the expansion observed on the gauges.

The findings for Wadi Dayqah Dam further demonstrate that some additional care must be taken in determining appropriate aggregates for RCC in the case of dam designs that are susceptible to materials shrinkage. Verification of appropriate materials should accordingly be demonstrated by installing temperature and strain gauges into the Full Scale Trials, or earlier in a relatively large mass of RCC.

On the basis of the findings of this Chapter, it is also suggested that very careful attention be given to the method of installation of strain gauges and LBSGTMs, particularly in the case of significantly cooled RCC. In such instances, it would be useful to position strain gauges away from the induced joint in both the receiving RCC layer and the newly placed RCC.

4.6.8.2. Implications for a New Understanding of the Early Behaviour of RCC

The implications of the findings of the Wadi Dayqah Dam instrumentation data, in respect of understanding the early behaviour of RCC, can be summarised as follows:

- The fact that shrinkage can be determined through very obviously different behaviour patterns at Wadi Dayqah serves to further validate the lack of evidence of shrinkage at the other dams investigated as part of this study.
- Aggregate quality and behaviour and the RCC mix composition must be given careful attention, as these can impact the drying shrinkage behaviour of RCC.
- Even with relatively poor materials, a high sand content and a high content of non-cementitious fines, the applicable shrinkage remains less than that assumed for a traditional RCC materials behaviour model.

- It is considered good practice to verify the early shrinkage behaviour of the proposed RCC by installing temperature and strain gauges in the RCC of the Full Scale Trial.
- The shrinkage evident in the lean RCC of Wadi Dayqah Dam is in accordance with the findings of other testing on lean mix RCC described in literature. This is not seen as detracting from the indicated behaviour for the high-paste RCC of the other dams addressed herein, but rather to further emphasise the distinction in early behaviour between high-paste RCC and lean RCC.
- In the case of an RCC arch dam for which materials shrinkage might be problematic, additional laboratory and practical testing of the RCC will be required.

4.6.8.3. Summary

The instrumentation data from Wadi Dayqah Dam provide a picture of early RCC behaviour for a quite different concrete mix, compared to Wolwedans, Knellpoort and Çine Dams. While the findings of the data evaluation highlight the caution necessary when considering the early behaviour of RCC, it further validates all other indications that the traditional model for RCC behaviour is not valid.

4.7. CHANGUINOLA 1 DAM

4.7.1. GENERAL

The general arrangements of Changuinola 1 Dam and the layout of the instrumentation installed are described in Chapter 2.

The instrumentation to be installed in Changuinola 1 is comprehensive. At the time of completing this Thesis, only the first level of instruments had been installed and only a little over 1 month of data was available, providing little information of significance at this stage. A strain gauge was, however, installed in the first RCC placed to the right side of the diversion culvert during December 2009 and this has provided data of some interest, which will be addressed in this Chapter. Furthermore, a comprehensive thermal analysis was completed for Changuinola 1, as described briefly in Chapter 5, and the associated modelling was useful in being able to simulate and confirm RCC behaviour.

4.7.2. INSTRUMENTATION

The strain gauge was installed directly into a trench cut into the RCC during the course of placement and the instrument was orientated in an upstream-downstream direction, perpendicular to the axis of the dam. The gauge is located approximately 2 m above the foundation and placement proceeded to a depth of approximately 6 m above the gauge without significant interruption. After a delay of

approximately 9 weeks, placement resumed and a further 11 m of RCC was placed above the gauge.

4.7.3. MATERIALS PROPERTIES

Laboratory testing indicated the following materials properties for the Changuinola 1 Dam RCC.

Thermal Diffusivity	1.6 m/°C
Coefficient of Thermal Expansion	8.8 x 10^{-6}/°C
Density	2475 kg/m^3
Compressive Strength at	
7 days	11.7 MPa
28 days	16.07 MPa
90 days	26.7 MPa
365 days	36.2 MPa

4.7.4. INSTRUMENT DATA

Figures 4.51 and **4.52** below indicate the temperature and strain history recorded between placement and July 2010.

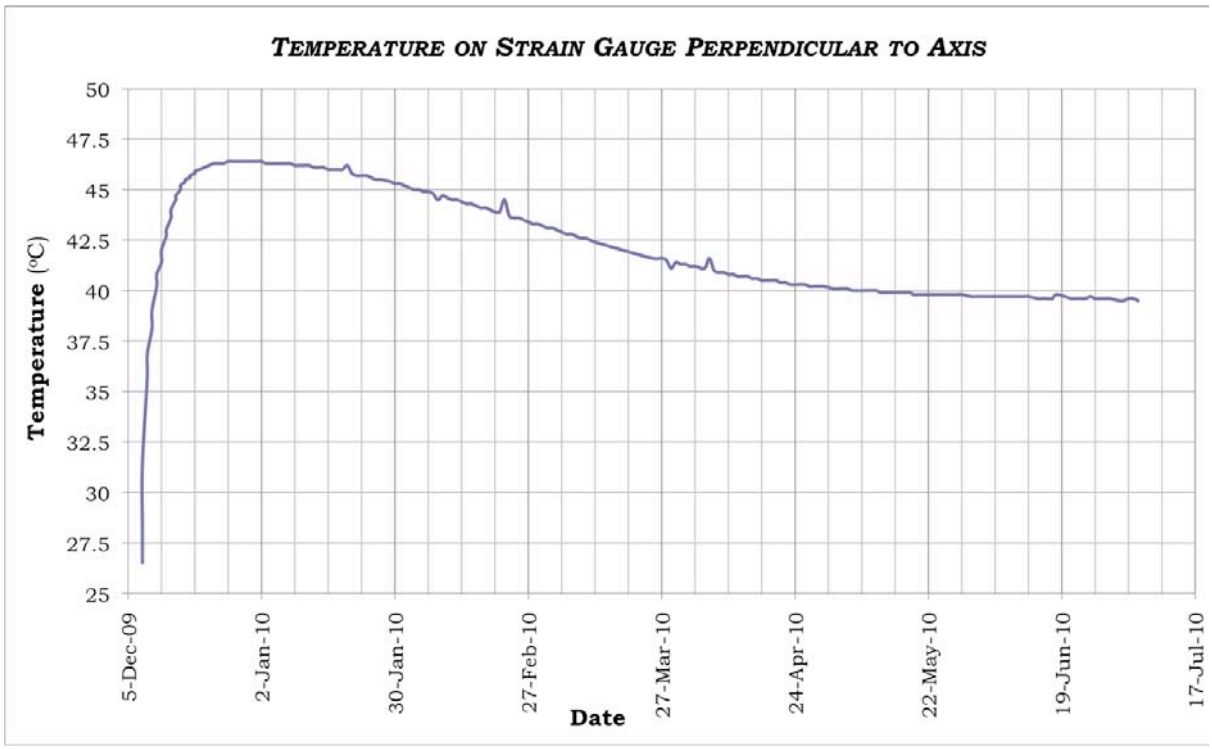

Figure 4.51: Temperature on Strain Gauge(16)

The measured temperature rise of approximately 20°C is essentially equivalent to the expected adiabatic hydration temperature rise, which is indicative of the significant level of thermal insulation provided to the gauge. The gradual (6°C) temperature drop between early January and March was halted when the impact of the RCC placed above took effect.

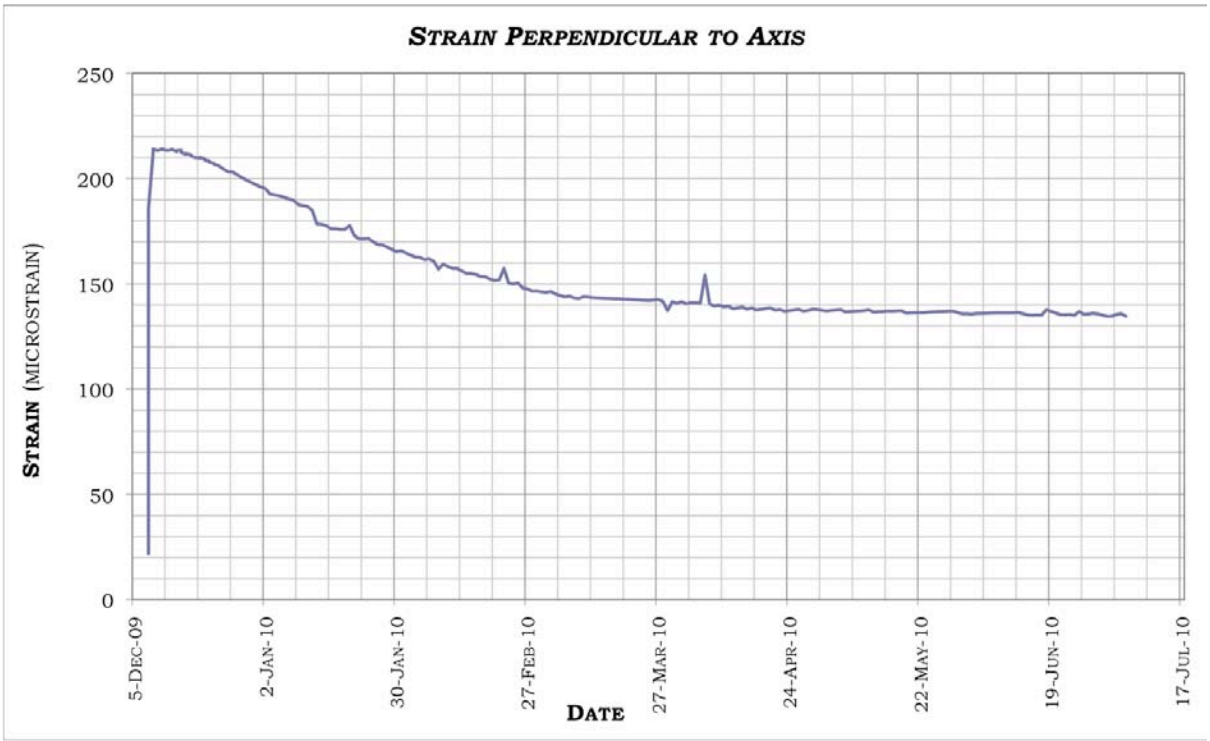

Figure 4.52: Strain Measured Perpendicular to Dam Axis(16)

A maximum expansion of 194 microstrain was developed, suggesting an effective coefficient of thermal expansion of 9.75 x 10^{-6}/°C. After the indicated 6°C temperature drop, the net expansion measured 113 microstrain for a temperature increase of 13°C, suggesting an effective thermal expansion of 8.7 x 10^{-6}/°C, which is essentially the equivalent value indicated through laboratory testing.

4.7.5. DISCUSSION

It is considered particularly interesting to note that the behaviour observed on the first strain gauge installed in Changuinola 1 Dam, orientated perpendicular to the dam axis, demonstrated the same behaviour as the gauges similarly installed in Çine Dam. The data suggests an initial over-expansion of some 12% with a subsequent relaxation to finally indicate a net RCC expansion equivalent to the temperature increase x the coefficient of thermal expansion. This confirms the indications from Çine Dam that high-paste RCC expands essentially linear-elastically under a temperature rise and that the internal restraint that would cause

part, or all of this expansion to be transformed into constrained compression and subsequently creep in CVC would not seem to be evident in high-paste RCC.

It is also significant that, whereas the strain gauges at Çine Dam were installed into the surface of a cold joint in the RCC placement, the gauge at Changuinola Dam was installed in RCC during ongoing placement. This is considered of particular importance, as it substantially eliminates any possible ambiguity that the expansion recorded at Çine might have related to the behaviour of the RCC in the cooled surface of a cold joint.

4.8. DISCUSSION AND CONCLUSIONS

4.8.1. CONCLUSIONS

Instrumentation specifically designed to measure temperature, strain and induced joint opening in RCC at Wolwedans, Knellpoort and Çine dams has repeatedly demonstrated a relatively linear relationship between temperature and strain, suggesting that the "zero stress", or T3 temperature is substantially closer to the "built in", or T1 placement temperature, than the maximum hydration, or T2 temperature, as commonly accepted for conventional mass concrete in dams. With no measurable shrinkage/creep experienced during thermal expansion and minor relaxation creep/shrinkage under thermal expansion representing the only apparent non-linearity in early RCC behaviour, the long-term structural temperature drop applicable in the case of large RCC dams is in fact significantly less than would otherwise be considered.

With thermal considerations being fundamental for RCC dams, the data presented in this Chapter has demonstrated that high-paste RCC does not exhibit shrinkage and particularly creep during the hydration heating and dissipation cycle to the same extent as CVC.

It is also considered important to take cognisance of the fact that all four of the RCC mixes for which the RCC behaviour was better than anticipated were high-paste RCC containing high proportions of fly ash.

While the evident early behaviour at Wadi Dayqah Dam was the exception, in demonstrating some definite non-linearity in temperature-strain behaviour, this confirms the finding from laboratory testing described in literature, which indicates similar, or greater creep in lean RCC, to CVC in dams. It is accordingly apparent that the key to the improved early RCC behaviour lies in the high-paste mix and the associated compaction.

4.8.2. DISCUSSION

The findings of the instrumentation data studies presented herein are of key importance for the design and analysis of significant high-paste RCC dams and of particular criticality in relation to the design and construction of RCC arch dams. For example, in the case of Çine Dam, it is unlikely that any structural temperature drop will ever be experienced within the lower body of the structure, even though a

conventional evaluation would suggest an applicable temperature drop of between 5 and 8°C. Furthermore, the practical implications for large RCC arch/gravity dams are significant. While conventional analysis might suggest that it would be possible to complete at least a first grouting of the induced joints on a large, naturally cooled RCC arch/gravity dam after perhaps 2 to 3 years, in reality the necessary delay might be substantially longer, an eventuality that would be difficult to manage.

Measurement of elastic thermal expansion, or a relatively linear temperature-strain relationship in the RCC in a direction perpendicular to the axis at Changuinola 1 Dam is considered particularly important, as this verifies the similar observations made at Çine Dam. Furthermore, in a constrained mass, with significant internal and foundation restraint, such expansion would not be expected and this is considered particularly important, as it probably represents the key to the difference in the behaviour of a high-paste RCC, compared to CVC.

It is important to bear in mind that, apart from Changuinola 1, the total hydration temperature rise applicable in the cases considered in this study is relatively low, particularly in relation to conventional vibrated mass concrete. For a higher hydration temperature rise, greater related expansion strain and higher associated stress levels can be anticipated and these may give rise to the introduction of more significant levels of creep.

4.8.3. ONGOING INVESTIGATIONS

The study presented in this Chapter forms the foundation of the programme of research and investigation subsequently addressed.

In this Chapter, the fact that high-paste RCC behaves differently to CVC, or to the manner traditionally assumed for design, is demonstrated. However, many questions remain and these cannot be answered without quantitative analysis. Consequently, the performance of Wolwedans Dam is explored in greater detail in Chapter 5, while early indications of the RCC behaviour at Changuinola 1 Dam are also discussed.

4.9. REFERENCES

[1] Oosthuizen C. *Behaviour of Roller Compacted Concrete in Arch/Gravity Dams.* Proceedings. International Workshop on Dam Safety Evaluation. Grindelwald, Switzerland. April 1993.

[2] Oosthuizen C. *Performance of Roller Compacted Concrete in Arch/Gravity Dams.* Proceedings. 2nd International Symposium on Roller Compacted Concrete Dams. Santander, Spain. pp 1053-1067. 1995.

[3] Shaw QHW. *An Investigation into the Thermal Behaviour of RCC in Large Dams.* Proceedings. 5th International Symposium on Roller Compacted Concrete Dams. Guiyang, China. pp 271-282. 2007.

[4] United States Army Corps of Engineers. *Thermal Studies of Mass Concrete Structures.* Engineering Technical Letter, ETL 1110-2-542. Washington. May 1997.

[5] Özkar Construction Internal Report. *Instrumentation Readings. Quality Control Unit.* Özkar Construction, Ankara, Turkey. October 2005 – February 2008.

[6] Geoconsult. Gibb. ARQ. *Çine RCC Dam. Phase 2 Design Report.* Vol. 4 of 4. Drawings. Özkar Construction. Ankara, Turkey. January 2000.

[7] Turanli L. *Determination of Thermal Diffusivity and Creep for Concrete Core Specimens Taken from Çine Dam.* Middle Eastern Technical University. Report Code No. 2001-03-03-2-0033. Ankara, Turkey. September 2001.

[8] Shaw QHW. ARQ (PTY) Ltd. *Çine Dam. Design Thermal Analysis Report.* Özkar Construction Internal Report No. 1596-8539. Ankara, Turkey. September 2005.

[9] Greyling R & Shaw QHW. ARQ (PTY) Ltd. *Çine Dam. Supplementary Thermal Analysis Report.* Özkar Construction Internal Report No. 1596-10288. Ankara, Turkey. June 2008.

[10] United States Army Corps of Engineers. *Arch Dam Design.* Engineering Manual, EM 1110-2-2201. USACE. Washington. May 1994.

[11] Wadi Dayqah Dam JV. *Wadi Dayqah Dam. Drawings for Construction.* Sultanate of Oman. M.R.M.E.W.R. Muscat, Oman. August 2006.

[12] Richards, M. *Instrumentation Readings, Data and Information. Wadi Dayqah Dam Joint Venture.* Quriyat, Oman. March & August 2009.

[13] Vinci & CCC Construction JV. Wadi Dayqah Dam. *Quality Control Records*. Quriyat, Oman. February 2008.

[14] Neville, AM. *Properties of Concrete.* Chapter 9. Fourth Edition. Pearson Prentice Hall. London. 2002.

[15] Hollingworth F, Druyts FHWM & Maartens WW. *Some South African Experiences in the Design and Construction of Rollcrete Dams.* Proceedings. 17th ICOLD Congress. Q62. R3. San Francisco. pp 33-51. 1988.

[16] CCWJV. *Instrumentation Readings, Data and Information. Changuinola 1 Dam.* Changuinola, Panama. January to July 2010.